

CONTROLLED RELEASE OF Ag⁺ FROM SILVER NANOPARTICLES DEPOSITED INTO
POLYELECTROLYTE MULTILAYERS AND THEIR ANTIBACTERIAL AND
ANTICANCER ACTIVITIES

Miss Sirorat Wacharanad

A Dissertation Submitted in Partial Fulfillment of the Requirements
for the Degree of Doctor of Philosophy Program in Nanoscience and Technology
(Interdisciplinary Program)
Graduate School
Chulalongkorn University
Academic Year 2012

Copyright of Chulalongkorn University

บทคัดย่อและแฟ้มข้อมูลฉบับเต็มของวิทยานิพนธ์ตั้งแต่ปีการศึกษา 2554 ที่ให้บริการในคลังปัญญาจุฬาฯ (CUIR)

เป็นแฟ้มข้อมูลของนิสิตเจ้าของวิทยานิพนธ์ที่ส่งผ่านทางบัณฑิตวิทยาลัย

The abstract and full text of theses from the academic year 2011 in Chulalongkorn University Intellectual Repository (CUIR)

are the thesis authors' files submitted through the Graduate School.

การควบคุมการปล่อยออกของเงินจากอนุภาคเงินนาโนที่สะสมเป็นฟิล์มบางพอลิอิเล็กโทรไลต์
หลายชั้นและฤทธิ์ต้านแบคทีเรียและต้านมะเร็ง

นางสาวศิริรัช วัชรานถ

วิทยานิพนธ์นี้เป็นส่วนหนึ่งของการศึกษาตามหลักสูตรปริญญาวิทยาศาสตรดุษฎีบัณฑิต
สาขาวิชาวิทยาศาสตร์นาโนและเทคโนโลยี (สหสาขาวิชา)
บัณฑิตวิทยาลัย จุฬาลงกรณ์มหาวิทยาลัย
ปีการศึกษา 2555
ลิขสิทธิ์ของจุฬาลงกรณ์มหาวิทยาลัย

ศิริรัช วัชรานาถ : การควบคุมการปล่อยไอออนของเงินจากอนุภาคเงินนาโนที่สะสมเป็นฟิล์มบางพอลิอิเล็กโทรไลต์หลายชั้นและฤทธิ์ต้านแบคทีเรียและต้านมะเร็ง (CONTROLLED RELEASE OF Ag⁺ FROM SILVER NANOPARTICLES DEPOSITED INTO POLYELECTROLYTE MULTILAYERS AND THEIR ANTIBACTERIAL AND ANTICANCER ACTIVITIES) อ.ที่ปรึกษาวิทยานิพนธ์หลัก : อ.ดร. สดพาน ที่ คูบาส, 128 หน้า.

อนุภาคเงินนาโนถูกสังเคราะห์โดยมีกรดฟอลิก, พอลิสไตรีน ซัลโฟนิค แอซิด โค มาเลอิก แอซิด และ อัลจินิก แอซิด เป็นตัวปกคลุม ซึ่งมีความเข้มข้นตั้งแต่ 0.1 ถึง 5 มิลลิโมล จากนั้นทำการวิเคราะห์ด้วยยูวี วิส สเปกโตรโฟโตมิเตอร์พบว่ามีค่าดูดกลืนแสงที่ 400 นาโนเมตร อนุภาคเงินนาโนเหล่านี้จะถูกสร้างเป็นแผ่นฟิล์มบางหลายชั้นบนกระจกใสและไหมเย็บแผล ซึ่งพบว่าถ้าความเข้มข้นของตัวปกคลุมน้อยจะสร้างฟิล์มบางได้หนาแน่นกว่าความเข้มข้นของตัวปกคลุมมาก จากนั้นนำกระจกใสและไหมเย็บแผลที่เคลือบด้วยฟิล์มบางหลายชั้นของอนุภาคเงินนาโนมาทดสอบการปลดปล่อยของเงินไอออนและการหลุดลอกของฟิล์มบางโดยการจุ่มลงในสารละลายที่มีค่าพีเอชที่ 7.4 และ 5.5 ผลการทดลองพบว่าทั้งแผ่นฟิล์มบนกระจกใสและไหมเย็บแผลจะมีการหลุดลอกและปลดปล่อยเงินไอออนได้ดีในสารละลายพีเอช 5.5 และอนุภาคเงินนาโนที่มีตัวปกคลุมน้อยมีแนวโน้มในการปลดปล่อยเงินไอออนมากกว่าอนุภาคเงินนาโนที่มีตัวปกคลุมมาก

เมื่อทำการทดสอบความเป็นพิษของอนุภาคเงินนาโนต่อเซลล์มะเร็งและเซลล์ปกติโดยการวิเคราะห์ด้วย MTT assay รวมถึงการต้านเชื้อแบคทีเรียโดยวิธีมาตรฐาน (ASTM E2149-10) พบว่าอนุภาคเงินนาโนที่ปกคลุมด้วย PSSMA และ อัลจินิก แอซิด ไม่เป็นพิษต่อเซลล์มะเร็ง ส่วนอนุภาคเงินนาโนที่ปกคลุมด้วยฟอลิก แอซิด ที่ความเข้มข้นสูงจะเป็นพิษต่อเซลล์มะเร็ง อย่างไรก็ตามอนุภาคเงินไม่เป็นที่พิษต่อเซลล์ปกติของปอด แม้จะเพิ่มความเข้มข้นมากถึง 53.5 ไมโครกรัมต่อมิลลิตรก็ตาม สำหรับคุณสมบัติการต้านแบคทีเรียของอนุภาคเงินนาโนพบว่าสามารถต้านเชื้อแบคทีเรียประเภท E. coli ได้เกือบ 100 เปอร์เซ็นต์ แต่สามารถต้านเชื้อ S. aureus ได้น้อยกว่า E. coli ซึ่งประสิทธิภาพในการต้านแบคทีเรียจะขึ้นกับค่าความเข้มข้นและชนิดของตัวปกคลุม

สาขาวิชา.....วิทยาศาสตร์นาโนและเทคโนโลยี.....ลายมือชื่อนิสิต.....
ปีการศึกษา 2555.....ลายมือชื่อ อ.ที่ปรึกษาวิทยานิพนธ์หลัก.....

5187824720 : MAJOR NANOSCIENCE AND TECHNOLOGY

KEYWORDS : SILVER NANOPARTICLES /SUTURE MATERIAL / LAYER BY LAYER

SIRORAT WACHARANAD : CONTROLLED RELEASE OF Ag⁺ FROM SILVER NANOPARTICLES DEPOSITED INTO POLYELECTROLYTE MULTILAYERS AND THEIR ANTIBACTERIAL AND ANTICANCER ACTIVITIES.
ADVISOR : STEPHAN T DUBAS, Ph.D., 128 pp.

Silver nanoparticles capped with a different stabilizing agent including Folic acid(FA), Poly(4-styrenesulfonic acid-co-maleic acid) sodium salt (PSSMA), Alginate acid (AL) were prepared. Concentration of stabilizing agent was varied from 0.1 to 5 mM. These silver nanoparticles solutions were characterized by UV-Vis spectroscopy and showed the LSPR around 400 nm. Then SNP was formed layer by layer with PDADMAC via polyelectrolyte multilayers technique on glass slide and polyamide suture material. It was found that in low capping agent of SNP was formed more close packing than high capping agent. Then both coated glass slide and suture material were studied the pattern of silver ion leaching from polyelectrolyte multilayer thin film in phosphate buffer (pH 7.4) and acetic-acetate buffer (pH 5.5). The result of this study was shown that the silver ion could release from thin film in pH 5.5 more than pH 7.4 and in low capping agent had trend to release silver ion more than high capping agent. Finally, SNP solution was characterized their anticancer and antibacterial activity via MTT assay and standard method of antibacterial test(ASTM E2149-10) sequentially. All condition of SNP was exposed to MCF-7, BT474, ChaGo and Jurkat cell which was a various type of cancer cell and analyzed in IC₅₀, it was performed that SNP-AL and SNP-PSSMA were not toxic and destroy cancer cell. However, SNP-FA could kill cancer cell when increasing concentration of folic acid. It was different to Jurkat cell that all condition of SNP were more toxic than other cell. All conditions of SNP could not toxic to WI-38 cell, so this SNP was not toxic to healthy cell. For their antibacterial activity, all condition of SNP could reduce E. coli nearly 100%. However, SNP with all capping agent could reduce S. aureus less than E. coli depend on the concentration and type of capping agent.

Field of Study : Nanoscience and Technology Student's Signature

Academic Year : 2012 Advisor's Signature

ACKNOWLEDGEMENTS

I would like to express my deepest gratitude to Dr. Stephan Thierry Dubas; my advisor for his kind advisor, his consultant and helpful in my work and dissertation.

I would like to thanks committee: Associate Professor Dr. Vudhichai Parasuk, Dr. Ratthapol Rangkupan, Assistant Professor Dr. Warangkana varisnoyjaroen, Associate Professor Nalena praphiruksit for their comment to my dissertation.

I would like to acknowledge the the 90th Anniversary of Chulalongkorn University Fund (Ratchadaphiseksomphot Endowment Fund), the Center for Innovative Nanoscience and Nanotechnology (CIN grant 2555), NSTDA through Nanotec grant: p-11-00990 and nanoscience and technology program for enhancing and providing financial support.

Finally, I would like to thanks my family for great encouragement and their love to me all the time. This is an importance force which is support me to success in this work.

CONTENTS

	Page
ABSTRACT (THAI).....	iv
ABSTRACT (ENGLISH).....	v
ACKNOWLEDGEMENTS.....	vi
CONTENTS.....	vii
LIST OF TABLES.....	xii
LIST OF FIGURES.....	xiii
LIST OF ABBREVIATIONS.....	xix
CHAPTER	
I INTRODUCTION.....	1
II LITERATURE REVIEW.....	3
2.1 Silver nanoparticles.....	3
2.1.1 Silver nanoparticles preparation.....	3
2.1.2 Stabilizing agent.....	4
2.1.2.1 Folic acid.....	4
2.1.2.2 Alginate.....	4
2.1.2.3 PSSMA.....	5
2.1.3 Anticancer property.....	6
2.1.3.1 Size.....	7
2.1.3.2 Surface.....	7
2.1.3.3 Ligand.....	7
2.1.4 Antibacterial property.....	8
2.2 Folic-folate receptor.....	9
2.3 Polyelectrolyte multilayers technique.....	10
2.3.1 Material use to form PEMs.....	12
2.3.1.1 Polyelectrolytes.....	12
2.3.1.2 Protein and enzyme.....	15

CHAPTER	Page
2.3.1.3 Conducting polymer.....	15
2.3.1.4 Nanoparticles.....	15
2.3.1.5 Supramolecules.....	15
2.3.2 Building of PEMs.....	16
2.3.2.1 Behavior of polyelectrolyte in solution.....	16
2.3.2.2 Polyelectrolyte adsorption.....	17
2.3.2.3 Overcompensation.....	18
2.3.2.4 Polyelectrolyte multilayer formation (layer- by- layer)....	19
2.3.3 Major parameters controlled the growth of PEM.....	20
2.3.3.1 Number of layer.....	20
2.3.3.2 Salt concentration (ionic strength).....	22
2.3.3.3 pH-controlled polyelectrolyte multilayer growth.....	23
2.3.4 Minor parameter controlled the growth of PEM.....	24
2.3.4.1 Dip time and polymer concentration.....	24
2.3.4.2 Temperature.....	26
2.3.2.3 Solvent.....	28
2.3.5 Permeability properties of the PEMs.....	29
2.3.5.1 Parameters controlling the permeability of PEMs.....	29
2.3.5.1.1 The effect of Swelling and ionic strength.....	29
2.3.5.1.2 The effect of film thickness.....	31
2.3.6 Degradation of PEM.....	33
2.3.6.1 The effect of pH.....	34
2.3.6.2 The effect of crosslinking.....	35
2.4 MTT assays.....	35
2.5 Antibacterial test.....	36
2.6 Scanning electron microscopy.....	37
2.7 Atomic adsorption spectroscopy.....	38
2.8 Atomic force microscopy.....	39
2.9 UV-vis spectroscopy.....	40

CHAPTER	Page
III METHODOLOGY	41
3.1 Chemical agents.....	41
3.1.1 Silver nitrate.....	41
3.1.2 Stabilizing agent.....	41
3.1.3 Reducing agent.....	41
3.1.4 Primer.....	41
3.2 Silver nanoparticles preparation.....	43
3.3 Polyelectrolyte monolayer and multilayer thin film formation.....	44
3.3.1 Monolayer thin film formation.....	44
3.3.2 Study effect of salt to monolayer adsorption.....	45
3.3.3 Study the effect of dilution.....	45
3.3.4 Multilayers formation.....	45
3.4 Study silver ion leaching from PEM.....	47
3.4.1 Silver ion leaching from SNP film on glass slide.....	47
3.4.2 Silver ion leaching from SNP coated on suture material.....	47
3.5 anticancer and antibacterial test.....	48
3.5.1 Cytotoxicity test.....	48
3.5.2 Antibacterial test.....	48
IV RESULTS	50
4.1 Chapter planning.....	50
4.2 Silver nanoparticles preparation and their parameters.....	51
4.2.1 Study the effect of concentration of stabilizing agent.....	51
4.2.2 Particles size and morphology by AFM.....	54
4.2.2.1 Silver nanoparticles capped with folic acid.....	54
4.2.2.2 Silver nanoparticles capped with PSSMA.....	55
4.2.4.3 Silver nanoparticles capped alginic acid.....	56

CHAPTER	Page
4.3 Layer - by-layer deposition of SNP.....	58
4.3.1 Monolayer adsorption.....	58
4.3.1.1 Effect of type and concentration of capping agent.....	58
4.3.1.2 Effect of concentration of salt to monolayer adsorption.....	61
4.3.1.3 Effect of dilution to monolayer adsorption.....	68
4.3.2 Polyelectrolytes multilayer thin film (PEM).....	70
4.3.2.1 PEM on glass slide.....	70
4.3.2.1.1 Effect of type of capping agent	70
4.3.2.1.2 Effect of number of layer.....	71
4.3.2.2 PEM on suture material.....	75
4.3.2.2.1 Effect of type and concentration of capping agent.....	76
4.3.2.2.2 Effect of high temperature to PEM on suture material.	81
4.4 silver ion leaching from PEM.....	84
4.4.1. Silver ion leaching from PEM coated on glass slide.....	84
4.4.1.2 Thickness of PEM film before and after release measure by AFM.....	89
4.4.2 Silver ion leaching from PEM coated on suture material(AAS).....	90
4.5 Anticancer and antibacterial testing.....	97
4.5.1 Anticancer test.....	97
4.5.1.1 Effect of SNP to BT474.....	98
4.5.1.2 Effect of SNP to MCF-7.....	100
4.5.1.3 Effect of SNP to Jurkat cell	101
4.5.1.4 Cytotoxicity of SNP to Chago cell (lung undifferentiated human) and WI-38VA-13 subline 2RA (fibroblast human lung cell).....	103
4.5.2 Antibacterial test.....	106
V CONCLUSIONS.....	111

	Page
REFERENCES	113
APPENDICES	124
BIOGRAPHY	128

LIST OF TABLES

	Page
Table 2.1 Anionic polyelectrolyte and their structure.....	13
Table 2.2 Cationic polyelectrolyte and their structure.....	14
Table 3.1 The proportion of silver nitrate, sodium borohydride and capping agent which had to mix follow by each condition. Total volume was 100 ml and final concentration of silver nitrate and sodium borohydride were 1 and 10 mM sequentially. For capping agent, the final concentration were 0.1, 0.5, 1 and 5 mM.....	44
Table 4.1 The particles size of SNP (all conditions) measured by AFM	58
Table 4.2 The percent of film degradable from the glass slide after releasing in buffer pH 5.5 and 7.4 at 28 day.....	88
Table 4.3 The thickness of SNP multilayer thin film was measured by AFM analysis. Compare between multilayer thin film of PDADMAC/SNP 20 layer, PDADMAC/SNP 20 layer released in buffer pH 5.5 for 28 day and PDADMAC/SNP 20 layer released in buffer pH 7.4 for 28 day.....	89
Table 4.4 The concentration of silver ion was coated on suture material in different in type and capping concentration.....	91
Table 4.5 Cytotoxicity of SNP to breast cancer cell (BT474).....	99
Table 4.6 Cytotoxicity of SNP to breast cancer cell (MCF-7) and Vero cell.....	101
Table 4.7 Cytotoxicity of SNP to Jurkat cell.....	102
Table 4.8 Cytotoxicity of SNP to Chargo cell (lung cancer cell) and Wi-38 (fibroblast human lung cell).....	104
Table 4.9 Antibacterial test to staphylococcus aureus (S. aureus) and Escherichia coli (E. coli).....	106

LIST OF FIGURES

Figure	Page
2.1	Synthesis silver nanoparticles via wet chemical process..... 3
2.2	Chemical Structure of folic acid..... 4
2.3	Chemical structure of alginate..... 5
2.4	Chemical structure of PSSMA..... 6
2.5	Diagram show silver nanoparticles specific targeting to cancer cell..... 10
2.6	Schematic representation of Polyelectrolyte multilayer formation process..... 11
2.7	Represent of behavior of polyelectrolyte in solution (a) the absence of salt in solution (b) the presence of salt in solution..... 16
2.8	Schematic representation polyelectrolyte chain, when (a) no salt concentration in polyelectrolyte and (b) the presence of salt that this counterion cloud have removed electric field line..... 17
2.9	Demonstrate the surface charge reversal of PDADMA and PSS multilayer with 0.5 M NaCl using capillaries electrophoresis..... 19
2.10	Thickness as a function of the number of layers for a PSS/PDADMAC multilayer deposited on silicon wafer from 1M NaCl. Polymer concentration 1mM ; 5 min deposition time. Sample was either dried between layers (squares) or left in contact with solution (triangles)..... 21
2.11	Layered structure of LbL Chitosan/poly (acrylic acid) film as from the QCM technique. The first layer has a lower mass if compared to the average mass deposited mass per layer. The linearity arise only after three layer are formed..... 21
2.12	Film thickness vs salt concentration for multilayer with 10 layer pairs each..... 22
2.13	Schematic representation of the molecular organization of PAA/PAH multilayer film assembled with the dipping solution at different pH levels..... 24
2.14	Thickness vs deposition time for each layer for 10 layer pair of PSS/PDADMAC deposition..... 25
2.15	Thickness vs polymer concentration of PSS/PDADMAC for 5 layer pairs..... 26

Figure	Page	
2.16	Thickness of hand-dipped(PDDA/PSS) film 10 layers deposited at different temperatures in the presence of 1M NaCl.....	26
2.17	Film thickness (nm) of PDDA/PSS film 5 layers deposited under different conditions. Left two columns compare film deposited at 23 °C (white) and 70 °C (shaded) in the absence or presence of 1M NaCl. Right two columns compare the effect of heating only the PDDA or the PSS to 70 °C while the other polymer is deposited at 23 °C.....	27
2.18	Illustrate thickness vs wt % ethanol for a 10-layer-pair multilayer of PSS/PDADMA from water/ethanol mixtures with 0.1 M NaCl.....	28
2.19	Thickness as a function of NaCl concentration for three multilayers: (a) PAA/PDADMA ; (b) PSS/PDADMA ; (c) PSS/PAH.....	30
2.20	Permeability of PEM capsules as a function of ionic strength at pH 7 (circles) and pH 8 (triangles).....	31
2.21	Fluorescein permeability coefficient as a function of layer number.....	32
2.22	Changes in the average pore diameters of multilayer in the pore of Track-etched Polycarbonate membrane (TEPC) estimated from SEM images as a function of the number of bilayers.....	32
2.23	The fluorescent intensity of films as a function of pepsin treatment time. (a) show degradation of film as function of time (b) show IDM release profile from micro capsule (L is layer number and T is deposition temperature).....	33
2.24	Permeability of MF- derived capsules for FITC-dextran (molecular weight 77kDa. open at pH 3.5 and closed at pH 10 states of (PSS/PAH) ₄ hollow capsule.....	35
3.1	Structure of capping agents and polyelectrolyte.....	42
3.2	The schematic of silver nanoparticles preparation.....	43
3.3	Schematic representation of Polyelectrolyte multilayers formation process between PDADMAC and SNP.....	46
4.1	Diagram of section of experiment.....	50

Figure	Page
4.2	(a) Calibration curve of folic acid in phosphate buffer solution (pH 7), (b) The maximum localized surface plasmon resonance absorbance peaks of various concentration of folic acid were displayed at 280 nm..... 52
4.4	Diagram of primer formation 53
4.3	The localized surface plasmon resonance absorbance peak of silver nanoparticales capped with (a) FA (SNP-FA), (b) PSSMA(SNP-PSSMA) and (c) AL (SNP-AL) with a various concentration. The picture showed SNP-FA solution with a different concentration of capping agent..... 54
4.5	AFM image of SNP-FA with a various concentration of stabilizing agent..... 55
4.6	AFM image of SNP-PSSMA with a various concentration of stabilizing agent..... 56
4.7	AFM image of SNP-FA with a various concentration of stabilizing agent..... 57
4.8	The plot of lambda max of plasmon absorbance value as the function of time of SNP-FA monolayer adsorption..... 60
4.9	The plot of lambda max of plasmon absorbance value as the function of time of SNP-PSSMA monolayer adsorption..... 60
4.10	The plot of lambda max of plasmon absorbance value as the function of time of SNP-AL monolayer adsorption..... 61
4.11	The plot of maximum absorbance value of SNP-FA 1:5, SNP-FA 1:1 and SNP-FA 1:0.1 as a function of concentration of salt at 18 hour..... 62
4.12	The kinetic adsorption of (a) SNP-FA 1:5, (b) SNP-FA 1:1 and (c) SNP-FA 1:0.1 on the substrate when varied concentration of salt from 0 to 100 mM..... 63
4.13	The plot of maximum absorbance value of SNP-PSSMA 1:5, SNP-PSSMA 1:1 and SNP-PSSMA 1:0.1 as a function of concentration of salt at 18 hour..... 64
4.14	The kinetic adsorption of (a) SNP-PSSMA 1:5, (b) SNP-PSSMA 1:1 and (c) SNP-PSSMA 1:0.1 on the substrate when varied concentration of salt from 0 to 100 mM..... 65
4.15	The plot of maximum absorbance value of SNP-AL 1:5, SNP-AL 1:1 and SNP-AL 1:0.1 as a function of concentration of salt at 18 hour..... 66

Figure	Page
4.16 The kinetic adsorption of (a) SNP-AL 1:5, (b) SNP-AL 1:1 and (c) SNP- 1:0.1 on the substrate when varied concentration of salt from 0 to 100 mM.....	67
4.17 The plasmon absorbance of SNP-FA monolayer adsorption when was diluted 2,10 and 100 times.....	68
4.18 The plasmon absorbance of SNP-PSSMA monolayer adsorption when was diluted 2,10 and 100 times.....	69
4.19 The plasmon absorbance of SNP-AL monolayer adsorption when was diluted 2,10 and 100 times.....	69
4.20 The plasmon absorbance peak of SNP/PDADMAC multilayer thin film at 20 layers. Each of SNP was varied the concentration of capping agent (0.1,0.5, 1 and 5 mM).....	71
4.21 UV-Vis absorbance values of PDADMAC and SNP-FA multilayer thin film on glass slides as a function of the number of layers of silver nanoparticles deposited. The nanoparticles were prepared with various concentrations of sodium alginate (0.1 mM= ◆, 0.5 mM=■, 1 mM= ▲, 5 mM=●) and the different color of PDAD-MAC/SNP-FA film at 20 layers.....	72
4.22 UV-Vis absorbance values of PDADMAC and SNP-PSSMA multilayer thin film on glass slides as a function of the number of layers of silver nanoparticles deposited. The nanoparticles were prepared with various concentrations of sodium alginate (0.1 mM= ◆, 0.5 mM=■, 1 mM= ▲, 5 mM=●) and the different color of PDAD-MAC /SNP-PSSMA film at 20 layers.....	73
4.23 UV-Vis absorbance values of PDADMAC and SNP-AL multilayer thin film on glass slides as a function of the number of layers of silver nanoparticles deposited. The nanoparticles were prepared with various concentrations of sodium alginate (0.1 mM = ◆, 0.5 mM=■, 1 mM= ▲, 5 mM=●) and the different color of PDAD-MAC/SNP-FA film at 20 layer.....	74

Figure	Page	
4.24	PEM of PDADMAC and SNP coated on polyamide suture material. (a) PDADMAC /SNP-FA 20 layers, (b) PDADMAC/SNP-PSSMA 20 layers and (c) PDADMAC/SNP-AL 20 layers.....	75
4.25	SEM image of polyamide suture material with no SNP coated on the surface.....	76
4.26	SEM image of PDADMAC/SNP-FA was coated layer-by-layer on suture material with a various concentration of folic acid (0.1, 0.5, 1 and 5mM).....	78
4.27	SEM image of PDADMAC/SNP-PSSMA was coated layer-by-layer on suture material with a various concentration of folic acid (0.1, 0.5, 1 and 5mM).....	79
4.28	SEM image of PDADMAC/SNP-AL was coated layer-by-layer on suture material with a various concentration of folic acid (0.1, 0.5, 1 and 5mM).....	80
4.29	SEM image of PDADMAC/SNP-FA film with a various concentration of capping agent was coated on suture material after autoclave at 121 °C.....	81
4.30	SEM image of PDADMAC/SNP-PSSMA film with a various concentration of capping agent was coated on suture material after autoclave at 121 °C.....	82
4.31	SEM image of PDADMAC/SNP-FA film with a various concentration of capping agent was coated on suture material after autoclave at 121 °C.....	83
4.32	The plot of the absorbance value of PDADMAC/SNP-FA as a function of time when dipped in buffer solution pH 5.5 and 7.4(0.1 mM= ◆, 0.5 mM=■, 1 mM=▲, 5 mM=●).....	86
4.33	The plot of the absorbance value of PDADMAC/SNP-PSSMA as a function of time when dipped in buffer solution pH 5.5 and 7.4(0.1 mM= ◆, 0.5 mM=■, 1 mM=▲, 5 mM=●).....	87
4.34	The plot of the absorbance value of PDADMAC/SNP-AL as a function of time when dipped in buffer solution pH 5.5 and 7.4(0.1 mM= ◆, 0.5 mM=■, 1 mM=▲, 5 mM=●).....	88
4.35	The plot of the concentration of silver ion released from PDADMAC/SNP-FA which coated on suture material as a function of time when dipped in buffer solution pH 5.5 and 7.4(0.1 mM= ◆, 0.5 mM=■, 1 mM=▲, 5 mM=●).....	92

Figure	Page
4.36 The percent of silver ion release form PDADMAC/SNP-FA film on suture material after dipped in buffer solution until 28 days.....	93
4.37 The plot of the concentration of silver ion released from PDADMAC/SNP-PSSMA which coated on suture material as a function of time when dipped in buffer solution pH 5.5 and 7.4(0.1 mM= ◆, 0.5 mM= ■, 1 mM= ▲, 5 mM= ●).....	94
4.38 The percent of silver ion release form PDADMAC/SNP-FA film on suture material after dipped in buffer solution until 28 days.....	95
4.39 The plot of the concentration of silver ion released from PDADMAC/SNP-AL which coated on suture material as a function of time when dipped in buffer solution pH 5.5 and 7.4(0.1 mM= ◆, 0.5 mM= ■, 1 mM= ▲, 5 mM= ●).....	96
4.40 The percent of silver ion release form PDADMAC/SNP-AL film on suture material after dipped in buffer solution until 28 days.....	97

LIST OF ABBREVIATIONS

SNP	:	Silver nanoparticles
PEM	:	Polyelectrolyte Multilayer Thin Films
PDADMAC	:	Poly(diallyldimethylammonium chloride)
PSS	:	Poly(sodium 4- styrene sulfonate)
SNP-FA	:	Silver nanoparticles capped with folic acid
SNP-AL	:	Silver nanoparticles capped with Alginic acid
SNP-PSSMA	:	Silver nanoparticles capped with Poly(4-styrenesulfonic acid- co-maleic acid)
mM	:	milli Molar
nm	:	nanometer

CHAPTER I

INTRODUCTION

Because of their small size, nanoparticles having sizes ranging from 1 to 100 nm exhibit amazing optical and physical properties that are very different from their bulk counterpart. These special properties found in silver nanoparticles, gold nanoparticles or carbon nanotubes for example can be used in many areas of research and industry especially in pharmaceutical and electronic. Recently, silver nanoparticles have been considered to be an interesting alternative to the over-used antibiotics in various fields including medical, drug delivery system, textile coating, water treatment, food packaging and biosensor. Silver nanoparticles prepared through chemical reduction were capped with polyelectrolytes which provide water dispersability.

In this work, silver nanoparticles were used toward two distinct applications for antibacterial coating on surgical suture and as anti-cancer targeted drug delivery. In the first application the nanoparticles were coated using the layer-by-layer approach on suture material to prevent the development of bacterial colony. In the second application silver nanoparticles were modified with Folic acid which is a well known targeting agent for cancer cells such as breast, lung, ovary and brain cancer cell.

The nanoparticles were synthesized by chemical reduction of silver salt by sodium borohydride and in the presence of either folic acid, alginate or PSSMA which were used as stabilizing agent. Folic acid is vitamin B9 was chosen because it can target the folate receptor on the surface of cancer cell as a drug delivery system. Alginate is natural agent which is derived from algae which has a good biocompatibility and can be used as stabilizing agent in silver nanoparticle preparation. The last capping agent was PSSMA which is a co-polyelectrolyte of sulfonic and maleic and present better pH stability.

The research work presented here follows the timeline of the project and starts with the synthesis of the silver nanoparticles and finish with the anti-bacterials and anti-cancer testing. It unfolds with increasing complexity and focus on the first part on the synthesis and characterization of the nanoparticles using the three different capping agent. Optical properties and plasmonic characterization were used with atomic force microscopy measurements to

confirm the morphology of the nanoparticles. The nanoparticles were then used to form monolayer and multilayers on glass slides while the main parameters used in the deposition process were studied. These included the capping concentration, the dipping time, the number of layers and the ionic strength of the dipping solutions. The third part of the research was dedicated to the coating of the surgical sutures with the silver nanoparticles. The leaching of toxic silver ions from the suture was studied using Uv-Vis spectroscopy, AFM and Atomic adsorption because it is an important factor in the antibacterial activity. finally the anti-bacterial activity to bacterial and the cytotoxicity cancer cells was evaluated.

CHAPTER II

BACKGROUND AND THEORY

2.1 Silver nanoparticles

Silver nanoparticles have been the subject of research in recent years because they show unique physical, chemical and biological properties compared to bulk silver. Due to their size and shape-dependent properties, silver nanoparticles have been used in many applications for instance anti-bacterial agents in health industry, medical device (such as bone cement, surgical instrument, surgical mask and wound dressing), food storage, textile coating [1], biosensor [2-4] and home appliances to water treatment [5] and biological label.

2.1.1 silver nanoparticles preparation

Silver nanoparticles can be synthesized by physical process such as laser ablation evaporation [1] or by chemical process in which silver ions are reduced by reducing agent and form a small cluster or aggregates shown as figure 1. The reducing agent most commonly used include hydrazine, citrate, sodium borohydride or natural agent such as polysaccharides, plants extract and micro-organism [1]. In the chemical process a stabilizing agent is used to protect the nanoparticles by binding onto nanoparticles surface preventing their agglomeration. Example of the stabilizing agent are polymer such as poly(vinylpyrrolidone) (PVP), poly(ethylene glycol) (PEG), polymethylmethacrylate (PMMA) or polyelectrolytes such as alginic acid and gelatin [1].

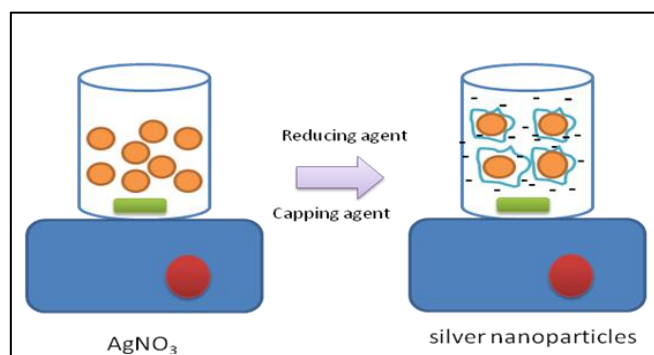


Figure 2.1 Synthesis silver nanoparticles via wet chemical process.

2.1.2 Stabilizing agent

2.1.2.1 Folic acid

folic acid is essential for biosynthesis so they are usually used as a supplementation in pills and food essential for proliferation and maintenance of all cells. Naturally occurring Folate is most abundant in dark green leafy vegetables, orange juice, legumes (e.g. black beans, kidney beans), nuts, asparagus, and strawberries[6]. Folic acid has a high affinity to cell surface folate receptors. Moreover it is nonimmunogenic, highly stable and inexpensive[7]. Thus it promotes the internalization of nanoparticles or other agents through cell membrane specific to folate receptor on cancer cell surface by endocytosis pathway [8-10]. So folic – folate receptor are applied to used in drug delivery specific to cancer cell [11].

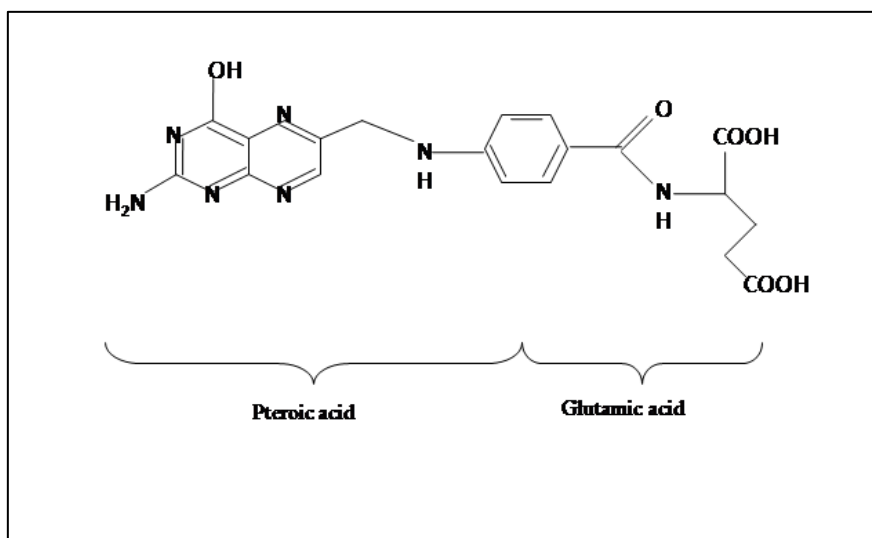


Figure 2.2 Chemical structure of folic acid

2.1.2.2 Alginate

Alginate is anionic polysaccharides which is the cell wall of brown algae. The properties of alginate are very interesting such as natural polyelectrolytes made this alginate is biocompatible, non-toxic, biodegradable and inexpensive[12, 13]. Alginate compose of two type including mannuronic acid or M block and guluronic acid or G block. M block forms 1-4

linkages pattern which shows in linear and flexible form. For G block form rise to 1-4 linkages which show the steric hindrance around the carboxyl group. So the pattern of G block shows rigid and folds structure[12, 13]. pKa of alginate is 1.5-3.5 which can dissolve completely and show negatively charge. Alginate can form hydrogel due to divalent cation(Ca^{2+}) which can crosslink between functional group of alginate chain. Moreover alginate also have carboxylic group (COO^-) lead to adjust surface charge of alginate by controlling pH value. This importance property of alginate promotes them to use in many fields especially in modification surface of material or chemical.

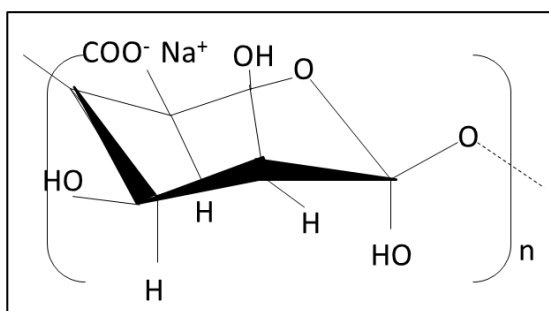


Figure 2.3 Chemical structure of alginate

2.1.2.3 PSSMA

Poly(4-styrenesulfonic acid-co-maleic acid) sodium salt or PSSMA is weak polyelectrolytes which contain both strongly negative charge group (sulfonate) and weakly negative charge group (carboxylate)[14]. This unique characteristic make this PSSMA become adjustable polyelectrolytes. PSSMA can be adjusted charge group and stability by control pH value. Generally, sulfonate group can be form electrostatic bond which enhance multilayer film stable and carboxylate group can be from bond in control pH condition [15-17]. The structure of PSSMA is shown in figure 2.4

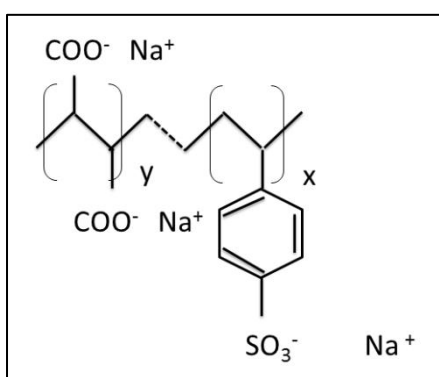


Figure 2.4 chemical structure of PSSMA

The property of PSSMA which can be control the surface charge by changing pH value used to develop this multilayer thin film of PSSMA for biomaterial or drug releasing[15].

2.1.3 Anticancer property

In recent years, nanoparticles is applied to use in medical field such as antibacterial agent, anticancer agent, drug carrier and imaging for detect the disease. Due to the special in structure and size of these nanoparticles can improve in diagnosis and therapy process. Silver nanoparticles are well known for anticancer agent. Silver nanoparticles was prepare by Sriram et al for Dalton's lymphoma ascites (DLA) cell therapy. They found that silver nanoparticles can decrease DLA cell in mice and promote survival in mice that was lymphoma disease[18] . There are two mechanisms of anticancer agents which could disrupt cancer cell. First, silver nanoparticles will interfere normal cellular function and cell membrane leading to induce apoptosis signaling gene of cell and programmed cell death[19, 20]. Second, silver nanoparticles have influence to mitochondria in cell by inhibiting mitochondrial respiration chain. Then ATP level will be decreased and increase reactive oxygen species(ROS) in cell leading to cancer cell death[19, 21]. Parameters which influence to anticancer property of silver nanoparticles consist of three importance factors include size, surface area and ligand.

2.1.3.1 Size

silver nanoparticles should be 10-100 nm which can promote anticancer property. For 10 nm, because of the kidney has the threshold first pass elimination around 10 nm. So for avoiding of silver nanoparticle is removed from the body, their size is should not less than 10 nm[ref 9, sil can]. For the upper value, in tumor normally has enhanced permeability and retention effect or EPR effect which their vascular is leakage especially for macromolecule. Therefor size of silver nanoparticles around 100 nm can leak out of the vessel and pass through the tumor cell. Moreover, the pore size of vessel wall of normal human cell is around 1-2 nm[22, 23]. It can be confirm that silver nanoparticles which contained size sround 10 – 100 nm cannot destroy the normal cell.

2.1.3.2 Surface

The unique characterization of silver nanoparticles is high surface area due to small size of particles. These improve the interaction to other cell or cell membrane. Normally the wall of vessel and cell membrane contain a negative surface charge including the tumor cell. Therefore if silver nanoparticles have slightly negative and positive charge, they can go through the tumor cell due to less in repulsive force between negative surface charges. Moreover in larger positive and negative charge of silver nanoparticles is removed by macrophage out of the body. So silver nanoparticle should be small in 10-100 nm for increase surface area and interaction and contain slightly in positive or negative charge for decrease in repulsive force between silver nanoparticles and tumor cell and easy to across to tumor cell[23].

2.1.3.3 Ligand

Silver nanoparticles are internalized in to cell by three pathways that are fluid- phase endocytosis, phagocytosis and receptor mediated endocytosis. Normally silver nanoparticles have limited access to the cell by endocytosis, so surface modified with ligand was developed to efficiently internalized to target cell via receptor mediated endocytosis pathway[8, 11, 24]. ligand is the agent which used to modify surface of drug or chemical agent for improve their affinity to target surface. The samples of ligand are aptamer, peptides, hormones, antibodies, protein and

vitamins [9, 25, 26]. Liong et al prepared iron oxide nanocrystals were encapsulated with mesoporous silica which loaded anticancer drug inside porous. Then their surface was modified with phosphonate and folic acid which high affinity to receptor on the cancer cell. They found that these modified agent increase the uptake into cancer cell due to it coated with folic acid that was specific attach to folate receptor on surface the cancer cell. Moreover, iron oxide also improve the ability of these particles for image. So this versatile agent can be used for therapeutic and diagnosis also[11]. Saad et al form three patterns of nanocarrier including linear polymer, dendrimer and liposome, then their surface were coated with LHRH peptide which targeted to receptor of on the cancer cell. It was found that all nanocarriers that coated with LHRH peptide increase intracellular uptake into cancer cell and anticancer ability more than uncoated LHRH peptide significantly. And the potential of this ligand is more impact to cancer cell than the structure of nanocarriers [27]. From these review is illustrate that specific ligand can improve the affinity of nanoparticles targeted to cancer cell.

2.1.4 Antibacterial property

The dominant property of silver nanoparticles is antibacterial property. Mechanism of bactericidal has many hypothesis, normally was due to both silver ion and silver nanoparticles. First, silver nanoparticles can bind to the sulfur-containing protein on the cell wall of bacteria, then permeability of cell membrane is increase and cell die. Second, silver ion can promote intracellular reactive oxygen species (ROS) in bacteria cell which increase cell death. Third, silver ion can enter to the bacterial cell wall and a bacterium is destructed. Moreover, silver nanoparticles which size is less than 10 nm can increase pore of bacterial cell wall, then the cytoplasm is leak out resulting to cell death [28]. Because of their toxicity, silver nanoparticles were applied to use and study in many fields. Feng Zhang et al synthesized silver nanoparticles by mixing silver nitrate with aminoterminated hyperbranched polymer and stirred until silver nanoparticles were formed. Then silver nanoparticles were coated on cotton textile for increase their antibacterial property. They found that the cotton textile could decrease both *Escherichia coli* and *Staphylococcus aureus* more than 99 % [29]. Moreover silver nanoparticles were used in

water treatment product such as Prashant Jain and T. Pradeep used silver nanoparticles coated on polyurethane foam which use for drinking water filter. After used this foam was test with *Escherichia coli* and found that no bacterium occur[30]. It meant that silver nanoparticles could be used as antibacterial agent and applied to use in many fields. There are many factors effect to antibacterial property of silver nanoparticles such as size, shape, concentration, type of stabilizing agent and time to expose. Sukdeb Pal and et al found that shape of silver nanoparticles had impacted to antibacterial property by a basal plane is toxic to bacterial cell more than spherical and rod shape [31]. Panacek et al found that a very low of concentration of silver which around 1.69 ug/ml could antibacterial completely [32]. Size of silver nanoparticles varied from 1 to 100 nm, size less than 15 nm was potentially to antibacterial more than larger size[33].

2.2 Folic-folate receptor

There are many agents which contain specific target property to receptor on surface of cancer cell. The samples of these agents are galactose-based ligand which target to the asialoglycoprotein receptor(ASGPR) usually occur on hepatocytes for treatment in primary liver cancer cell[22], retroviral vectors which can target to human breast cancer cells [34] and folic acid which contain high affinity to folate receptor. Folic acid is vitamin B 9 which essential for biosynthesis so they are usually used as a supplementation in pills and food essential for proliferation and maintenance of all cells. Naturally occurring Folic acid is most abundant in dark green leafy vegetables, orange juice, legumes (e.g. black beans, kidney beans), nuts, asparagus, and strawberries[6]. Folate receptor (FR) is known as the high affinity membrane folate-binding protein. It compose of glycosylphosphatidylinositol(GPI)-link membrane glycoprotein with molecular weight of 38-40 kDa. Two membrane-bound isoforms of FR are designated α and β . FR can bind with folic acid with high affinity [35, 36]. FR, most of type α , are frequently presence on a variety of human cancers including breast, ovaries, endometrium, kidneys, colon, brain, and myeloid cells of hematopoietic origin[7-9, 24, 35, 36]. Although FR type β has been found in normal cell but it lack affinity for folic acid. Due to folic acid has a high affinity to cell surface folate receptors, nonimmunogenic, highly stable and inexpensive, so many researches

used this folic acid to modified surface of chemical agent and drug for improve the ability to attach to folate receptor on cancer cell. The figure 2.5 show the diagram of silver nanoparticles modified surface with folic acid and can specific attach to folate receptor on surface of cancer cell.

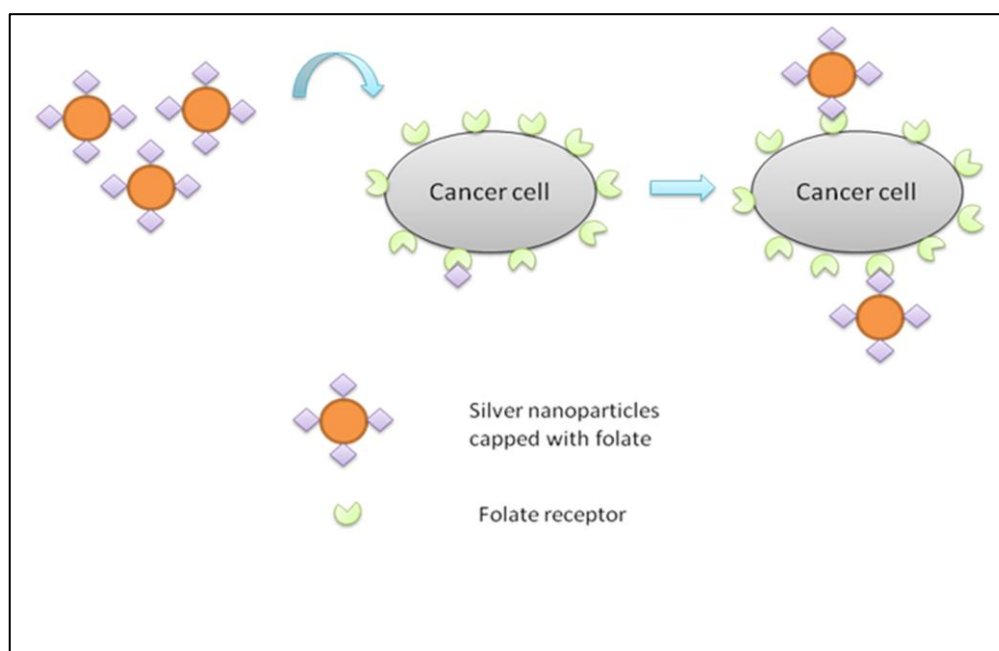


Figure 2.5 Diagram show silver nanoparticles specific targeting to cancer cell.

2.3 Polyelectrolyte multilayers technique

Polyelectrolyte multilayers (PEMs) have been proposed to modify the surface of materials by sequential adsorption of positively and negatively charge polyelectrolyte on various substrates. Basic method for the preparation of polyelectrolyte multilayers was demonstrated in 1991 by Decher and Hong [37] and developed continuously then the self-assembled polyelectrolyte multilayers have proven to be versatile materials. Moreover, this methodology is easy to prepare in the lab because it is simply based on a dipping of a substrate in various solutions of polyelectrolytes. This technique also has a low cost because as the price of polymer and equipment is low. A variety of substrate can be coated by polyelectrolyte

multilayer thin film for instance glass slide, silicon wafer, gold, aluminum, stainless steel, wood and fiber[37, 38]. Regarding the type of polyelectrolyte used in the assembly for example polymers(both synthetic and biopolymers), proteins, nanoparticles, clay, minerals, dendrimers, metal colloids [39, 40], dye and even modified carbon nanotubes. All of these advantages made polyelectrolyte multilayers very interesting to study both in basic knowledge of formation as well as their properties usage to create innovative material in various fields including medicine, dentistry, engineering and industry.

The process of construction PEMs start from, the substrate is first immersed into the polyelectrolyte which have opposite charge from the substrate. It will compensate by positive and negative charge between polyelectrolyte and surface called intrinsic compensation which found a strong inversion of the charge. Then the substrate is rinsed during PEMs formation in each layer in order to remove the excess polyelectrolyte. After that the substrate is dip into oppositely charged polyelectrolytes and rinsed again. The formation of PEMs is illustrated in figure 2.6. The cycle of immersion between positive and negative charged species is repeated until the desired number of layers is obtained.

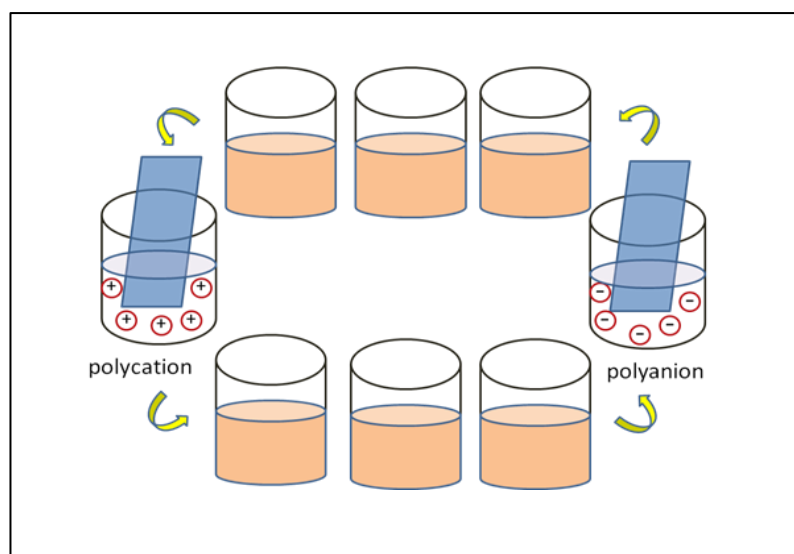


Figure 2.6 Schematic representation of Polyelectrolyte multilayer formation process.

Nanoparticles which can act as both polyelectrolytes and substrate in PEMs process are synthesized into small size that have diameter 1-100 nm and high surface area. When used to be assembled, they have to be applied with polyelectrolyte which enhance in adsorption on the substrate. In this work, suture material both absorbable and non-absorbable type will be modified surface with nanoparticles by layer by layer technique [41]. This process will promote suture material become to bioactive suture for releasing nanoparticles or drug into target areas after surgery [42-46]. On the other hand nanoparticles can be used as the substrate by forming the layer by layer on particles surface. This pattern mostly applied to use in drug delivery system by loading drug on multilayer that coated on particles surface and deliver internalized cell for treatment [47].

2.3.1 Material use to form PEMs

2.3.1.1 Polyelectrolytes

Polyelectrolytes are usually used to form polyelectrolyte multilayer thin film. Polyelectrolytes are the polymer system consisting of a macroion that have anionic or cationic groups and low-molecular counterion used for electroneutrality [48]. These macromolecular structure by covalently attaching a number of ionic groups to the polymer backbone, forming with linear or branched macromolecules soluble in aqueous medium. Polyelectrolyte can be classified by many groups for example anionic/cationic, synthetic/natural and strong/weak polyelectrolyte. Anionic/cationic polyelectrolyte are the most commonly divided into weak and strong acid and basic groups. Examples of polyelectrolyte classification show in table 2.1 and 2.2.

Table 2.1: Anionic polyelectrolyte and their structure [48, 49].

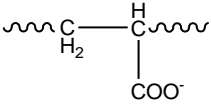
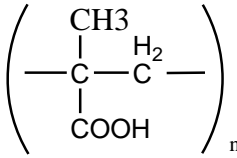
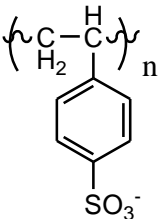
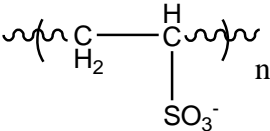
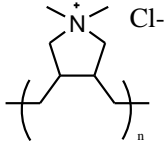
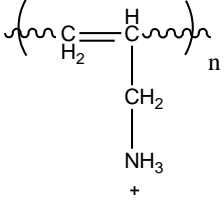
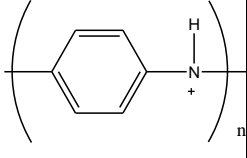
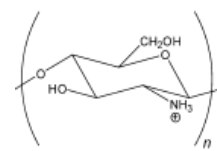
Anion	Structure	Strong/weak
Poly(acrylic acid)	 $\sim\text{C}_{\text{H}_2}-\underset{\text{COO}^-}{\overset{\text{H}}{\text{C}}}\sim$	weak
Poly(methacrylic acid)	 $\left(\begin{array}{c} \text{CH}_3 \\ \\ \text{---C---C---} \\ \quad \\ \text{COOH} \quad \text{H}_2 \end{array} \right)_n$	weak
Poly(styrenesulfonic acid)	 $\left(\begin{array}{c} \text{H} \\ \\ \text{---C---C---} \\ \quad \\ \text{H}_2 \quad \text{C}_6\text{H}_4 \\ \\ \text{SO}_3^- \end{array} \right)_n$	strong
Poly(vinyl sulfonic acid)	 $\left(\begin{array}{c} \text{H} \\ \\ \text{---C---C---} \\ \quad \\ \text{H}_2 \quad \text{SO}_3^- \end{array} \right)_n$	strong

Table 2.2 Cationic polyelectrolyte and their structure [48-51]

cation	structure	strong/weak
Poly(diallyldimethyl-ammonium chloride)		strong
Poly(allylamine hydrochloride)		weak
Poly(aniline)		weak
Chitosan		weak

A special classes of polyelectrolyte called polyampholytes present both anionic and cationic groups covalently bound to the macro molecule are usually in nature by proteins, but it can made a various of synthetic polyampholytes like maleic acid – diallylamine copolymer.

2.3.1.2 Protein and enzyme

Protein or enzyme composed of polypeptide contains amino acid groups such as aspartic acid and glutamic acid. These can be assembled layer-by-layer through electrostatic interaction and hydrogen bond [39]. Examples of proteins used to form PEMs include lysozyme, Histone f3, Myoglobin and Hemoglobin [52].

2.3.1.3 Conducting polymer

Conducting polymers are most commonly based on pyrrole, thiophene or aniline monomer. Advantages of these polymers are low power consumption because they require low power transfer via them and induced to start the mechanism of application. Moreover they are inherently compliant structure, light weight, simple construction, simple operation principle not requiring advanced electronics and noiseless operation. These conducting polymers are noiseless operation because they are prepared by dissolve in aqueous media and applied into many applications [53]. Conducting polymer can be applied to build sensor, artificial muscle and microchip.

2.3.1.4 Nanoparticles

Nanoparticles are synthesized into small size that has diameter 1-100 nm and high surface area. When used to be assembled, they had to be applied with polyelectrolyte which enhance in adsorption on the substrate. These particles possess optical, electric and magnetic properties usually used in optic, electronic and sensor field. Example of these nanoparticles are silver, gold, CdS, ZnS and TiO₂ [52, 54].

2.3.1.5 Supramolecules

There are many supramolecules that can be constructed into multilayer thin film such as dye and dendrimer. Ionic dye that are most commonly used are divided into two

groups: cationic dyes for example Methylene blue and Acridine orange and anionic dyes for example Methyl orange, Ethyl orange, methyl red and 1-aniline-8-naphthalene sulfonic acid[48]. Dendrimer is a class of polymer that have a highly branched dendritic structure and contained unique properties such as high density of active groups, good structure homogeneity, intense internal porosity and good biocompatibility. Their application are sensor, catalyst and gene delivery agents [39].

2.3.2 Building of PEMs

2.3.2.1 Behavior of polyelectrolyte in solution

Polyelectrolyte solution can be prepared by dissolve them in aqueous medium, they are ionized and transformed into charged chain by electrostatic interaction. Usually, the characteristic of polyelectrolytes chain is stretched chain because of the repulsive interaction of cationic or anionic groups within polyelectrolyte chain as shown in figure 2.7a. The behavior of single polyelectrolyte chain was considered in aqueous solutions, the chain has weak interaction with one another and can be mentioned as isolated chain dispersed in solution. When added salt in solution, polyelectrolyte chain become to flexible chain and exhibit more loop chain. This characteristic occur from attaching of salt ion to chain lead to decrease repulsive interaction intrapolyelectrolyte chain. This condition was shown in figure 2.7b.

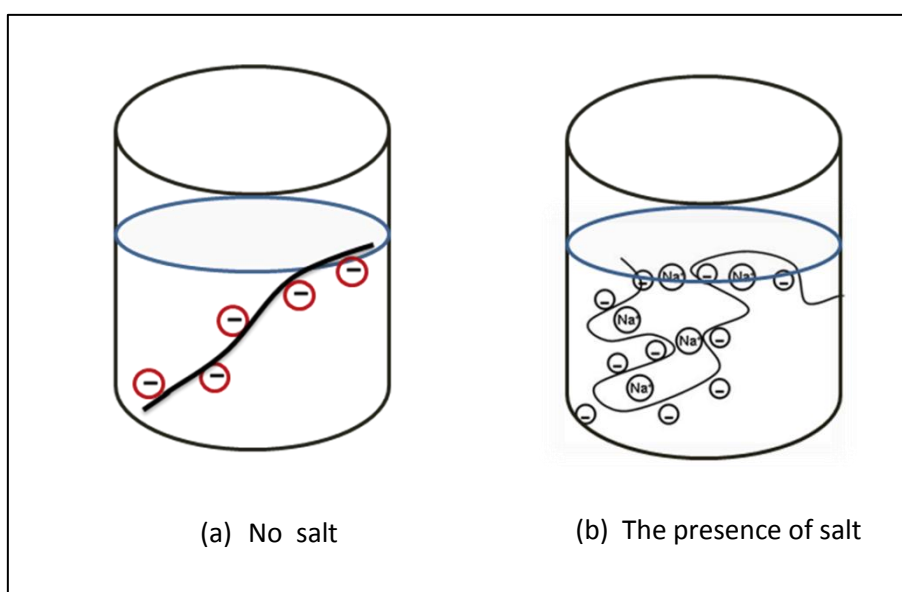
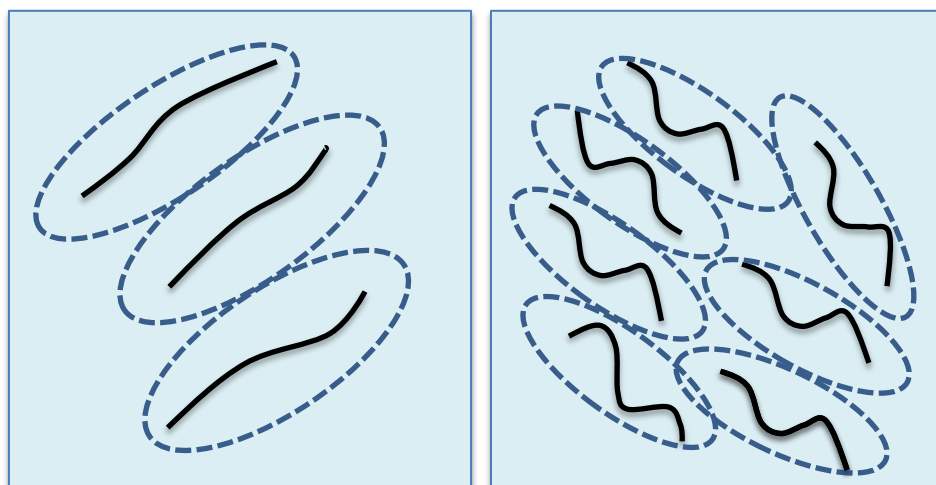


Figure 2.7 Represent of behavior of polyelectrolyte in solution (a) the absence of salt in solution (b) the presence of salt in solution.

2.3.2.2 Polyelectrolyte adsorption

For monolayer polyelectrolyte adsorption, in the absence of salt, is thin and low in overcompensation surface charge resulting to minimal polymer build up. The trend of monolayer adsorption as function of time, it can be observe that the higher coverage is in the early stage and then approach to constant line. When compared with added salt condition, the adsorbed layer is a significantly higher coverage on the surface, this is due to the salt ion help to decrease repulsive interaction and the Bjerrum length which facilitate the attachment on the surface. When determine in relation between salt concentration and thickness, increase in salt concentration directly increases the thickness of PEMs[55].

When adding salt into the solution, free ion from the salt reduces the coulomb interaction. This condition enhances collapse of polyelectrolyte chain show in figure 2. If increasing amount of salt into the solution, the potential energy between chains will approach to zero. This characteristic is called “Debye screening length (K^{-1})” [52, 56]



(a) No salt

(b) The presence of salt

Figure 2.8 Schematic representation polyelectrolyte chain, when (a) no salt concentration in polyelectrolyte and (b) the presence of salt that this counterion cloud have removed electric field line.

The conformation of polyelectrolytes adsorbed on the surface can be explained in two conditions. First is formed by stretched chain and second is formed by flexible or loop chain. For the stretched chain adsorbed on the surface, the conformation of PEMs are condense and thin layer. The conformation of PEMs which formed by the flexible chain are more loop and loose structure lead to increase thickness of PEMs.

2.3.2.3 Overcompensation

The key in polyelectrolyte adsorption can be explained by the overcompensation process. In the presence of adding polyelectrolyte of one type, overcompensation occur near the surface and give the excess surface charge reversal required for the opposite charge on the next layer. The sign of the surface charge and theirs reversal are shown by electroosmotic flow experiment on capillaries coated with multilayer [52]. The direction of electroosmotic flow is depend on sign of the wall charge like figure 3. This flow is reversal every new charge density present to the solution of interface. Overcompensation at the surface increase the degree of freedom. When compare in the bulk that a lot of steric repulsive interaction between polymer segment, it can found that adding salt enhance to increase long length of excess charge and increase in thickness of PEM directly. The characteristic of PEM formation measure by zeta potential of PAH/PSS on magnetic liposome as a function of number of layer show reversal of charge when addition new layer [57].

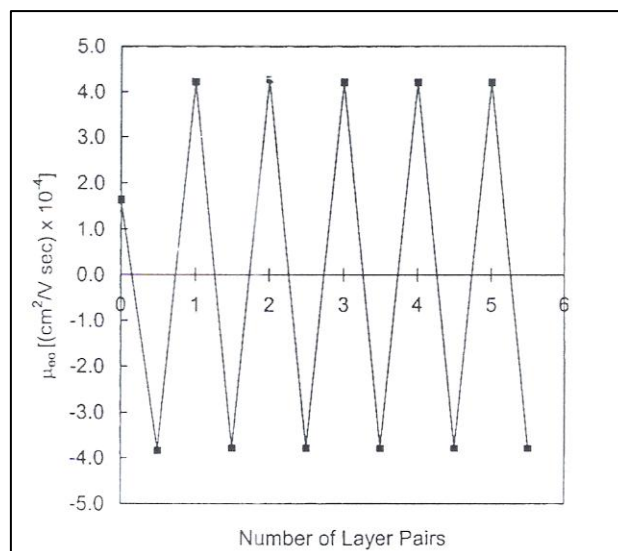


Figure 2.9 Demonstrate the surface charge reversal of PDADMA and PSS multilayer with 0.5 M NaCl. using capillaries electrophoresis [52].

2.3.2.4 Polyelectrolyte multilayer formation (layer- by- layer)

The process of polyelectrolyte multilayer formation start from preparation polyelectrolyte in solution form, this step mention on dissociation into polyelectrolyte depend on each properties of chemical and pK_a . If the chemical agents can dissociate completely, it increase amount of polyelectrolyte adsorption on the surface. The substrate is first immersed into the polyelectrolyte which have opposite charge from the substrate. It will compensate by positive and negative charge between polyelectrolyte and surface called intrinsic compensation which found a strong inversion of the charge. In few first layer of thin film require a strong adsorption for anchoring the polyelectrolyte on the surface. The various of strong polyelectrolyte can be used as the primer to form a stronger anchor adsorption [48] such as PDADMAC/PEI and PDADMAC/PSS. Usually, the primer base is formed about 3-5 layers then opposite charge is followed onto the primer base layer which is called first layer of PEMs. The substrate is rinsed during PEMs formation in each layer in order to remove the excess polyelectrolyte. Rinsing step is very importance to PEMs construction because it can affect to PEMs surface morphology. Moreover, the rinsing agent must be used as distilled water or buffer solution that have the same pH environment with

polyelectrolyte. The formation of PEMs is illustrated in figure 2.6 The sample two-step of immersion between positive and negative charge are repeated until the desired number of layer will be obtained.

Recently, polyelectrolyte multilayers have been developed into sprayed-assembled polyelectrolyte multilayer which use polyelectrolyte solution spray on the substrate as follow by spraying with distill water [52, 58]. Moreover, the inkjet-printer was applied to inkjet-printed thin film in order to print polyelectrolyte onto the substrate which can create feature size as small as 200 μm [52, 59]. Polyelectrolyte stamping technique was also used to stamp PEMs which have advantages over other techniques such as possible to pattern in any shape [52].

2.3.3 Major parameters controlled the growth of PEM

2.3.3.1 Number of layer

When considering the thickness as a function of the number of layer, increasing the number of layer, the thickness is increase follow by these layers correspond to the experiment of Stephan T. dubas et al [55] show formation of polyelectrolyte multilayer thin film with PSS/PDADMAC that have concentration 1 mM contain with 1 M of NaCl deposit on silicon wafer like figure 2.11.

In Mass deposition per layer of polyelectrolyte multilayer thin film by Quartz crystal microbalance (QCM) show in figure 2.12. When increase number of bilayer of PAA/chitosan, the deposit mass is increase follow the number of bilayer by the adsorbed mass changes linearly only after the deposition of three bilayers. For that reasons the first layers are usually thinner than the other layer is contained a lower amount of adsorb polyelectrolyte due to the lower electrical charge of the surface in relation to the polyelectrolyte chains. After the first few layers, a stationary regimen

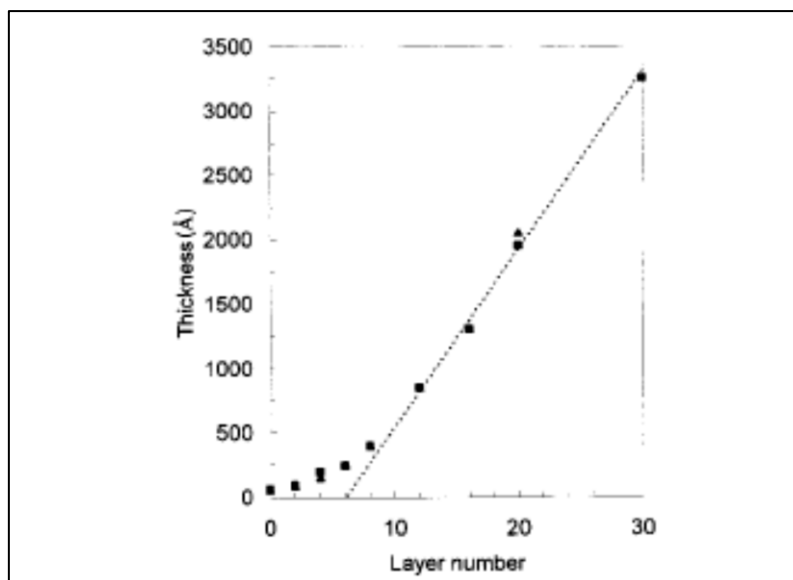


Figure 2.10 Thickness as a function of the number of layers for a PSS/PDADMAC multilayer deposited on silicon wafer from 1M NaCl. Polymer concentration 1mM ; 5 min deposition time. Sample was either dried between layers (squares) or left in contact with solution (triangles) [55]

is reached and the properties of the films are independent of the feature of surface [60]. This result was agree with Limsavarn L. and co worker who prepare that the formation silver nanoparticles thin film by PEMs method can be provide a linear relationship between absorbance at maximum wavelength as a function of the number of layers [54].

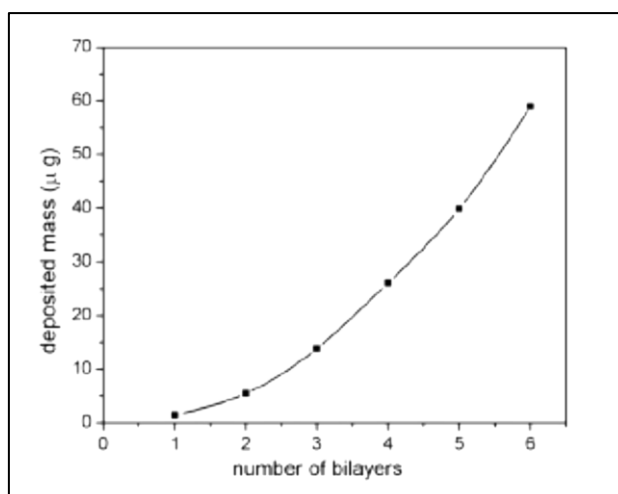


Figure 2.11 Layered structure of LbL Chitosan/poly (acrylic acid) film as from the QCM technique. The first layer has a lower mass if compared to the average mass deposited mass per layer. The linearity arise only after three layer are formed [37].

2.3.3.2 Salt concentration (ionic strength)

Adjustment ionic strength of dipping solution means adding salt into the solution for change ionic strength for control the growth of PEMs. The effect of salt concentration to polyelectrolyte system is related to electrostatic theory[52]. When adding salt into the solution, induce more adsorption of polyelectrolyte on the surface. This changed ionic strength affected PEMs thickness that show linear dependence on salt concentration between 0.01 M and 2 M was shown in figure 7[55] When adding salt, the charged polymer segments was completed salt ion for charged surface site by electrostatic mechanism called external compensation. In figure 2.13 show high slope in early stage and then slope was decrease in late stage. This can be explained that at low salt concentration polyelectrolyte segment are very efficient at seeking out surface charge lead to increase swelling of PEMs. At high salt concentration, salt ion is sufficient to all the polyelectrolyte chain from the surface. Then desorption of polyelectrolyte segments is occurred lead to decrease in thickness of the PEMs and decrease in slope at the late stage.

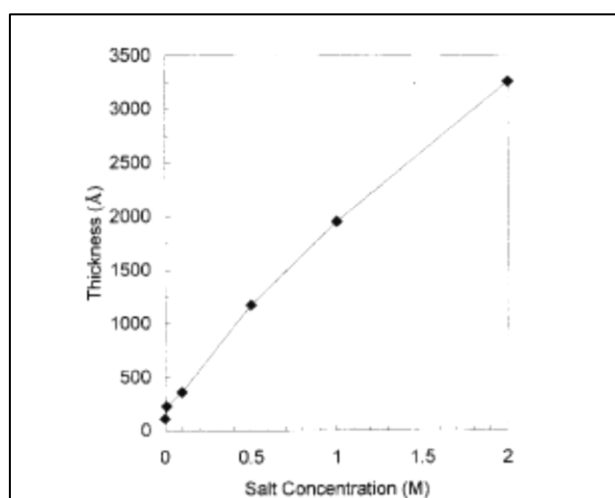


Figure 2.12 Film thickness vs salt concentration for multilayer with 10 layer pairs each[55].

For the influence of salt type on polymer adsorption a stronger binding salt ion would be functionally equivalent to adding more salt and a less solvated. The stronger binding ion would decrease the solvation energy of solution polymer that would drive the polymer to the interface [55].

2.3.3.3 pH-controlled polyelectrolyte multilayer growth

The pH of polyelectrolyte solution has influenced to weak polyelectrolyte adsorption because it relate to degree of ionization. However, for strong polyelectrolyte such as polystyrenesulfonic acid and polyvinylsulfonic acid, pH adjustment is not influence to polyelectrolyte adsorption because it can be ionized form in every pH value. Each of weak polyelectrolyte have different pH value that suitable for ionize in solution. When preparing the polyelectrolyte solution, the solution should adjust pH value follow by pKa of each polymer to enhance complete ionization in solution be as solution at acidic pH condition, PAA decrease in ionization resulting to low charge density of PAA. When solution pH is increased, PAH will decrease in ionization resulting to low charge density of PAH and their ammonium groups become to deprotonated as shown in figure 2.14. pH of solution is sensitive to ionization and charge density of polyelectrolyte. If polyelectrolyte can be increasingly ionized, charge density is directly increased. Therefore, the influence of ionization or charge density to polyelectrolyte multilayer growth trend to linear relationship. In case of completely ionized polyelectrolyte, the charge density increase facilitate to form a good adsorption in multilayer thin film. Thus, different pH value of polyelectrolyte solution provide different degree of ionization. When polyelectrolyte adsorb on the substrate, the film form in different structure as shown in figure 2.14. Three different multilayer system of PAA/PAH that exhibit particular patterns was shown in figure 2.14.

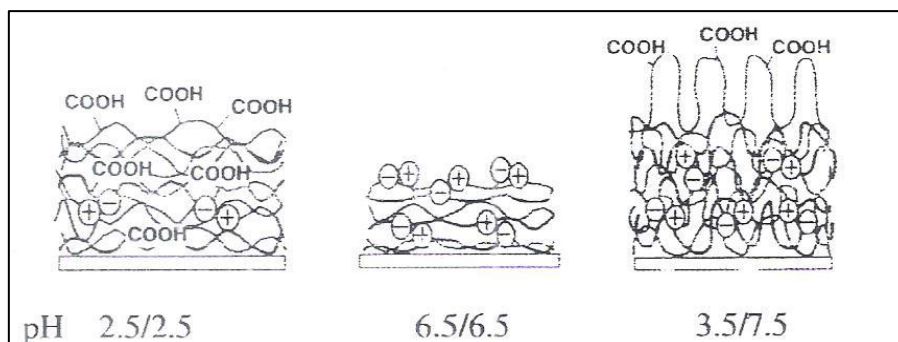


Figure 2.13 Schematic representation of the molecular organization of PAA/PAH multilayer film assembled with the dipping solution at different pH levels [52].

When the substrate was immersed in PAA/PAH solution which contained pH value 2.5, low degree of ionization of PAA whereas fully degree of ionization of PAH resulting to form a non stoichiometric pairing. This film is swell with a relatively low ionic crosslink density. When the substrate was immersed in neutral pH, polyelectrolyte solution that both of polymers are completely ionization. This condition create equal amount of PAA and PAH resulting to form highly ionic crosslinked density within multilayer film. In the third condition, solution pH of PAA/PAH is 3.5 and 7.5 respectively. Both PAA and PAH chain are low degree of ionization adsorb onto the substrate with the loop conformation [52]. This result relate to Yoo et al [49] who report the thickness as a function of number deposited bilayer of PAH/PAA by varying pH solution. This result also showed that the thickness deposition can be varied from 30-70 Å by varying pH in range 2.5-4.5 pH range. Linear and reproducible deposition of polyelectrolyte on the surface can be formed under condition that PAA chains contain a very low degree of ionization.

2.3.4 Minor parameter controlled the growth of PEM

2.3.4.1 Dip time and polymer concentration

Before determining in dip time and polymer concentration for construction PEMs, we should understand the mechanism of monolayer formation including two steps. The first step is diffusion

of ion to the surface and the second step is binding to the surface. The deposition time per layer refers to these two steps. The relationship between deposition time as a function of thickness in monolayer adsorption of PSS/PDADMAC as shown in figure 2.15. The high slope in the early stage was observed at first few minutes which represent to high flux on the surface. The number of equivalent monolayer is higher in fast few minutes represent to the high flux on the surface.

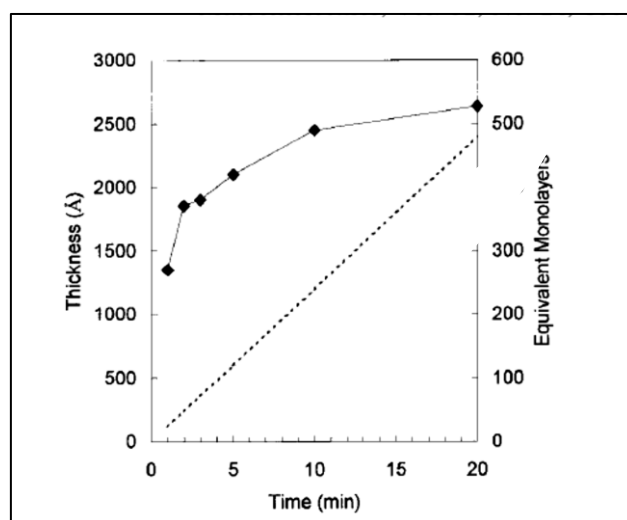


Figure 2.14 Thickness vs deposition time for each layer for 10 layer pair of PSS/PDADMAC deposition [55].

Correspond to the variation of polymer concentration leading to increase the thickness of PEMs in the early stage and then approach to constant curve was shown in figure 2.16. It can be explained that PEMs contains a wide range of the time required to form a layer. This formation of monolayer is limited by mass transport of polymer to the surface and solution mass transport is a function of the solution concentration and hydrodynamics which should be specified in layer formation time of each polymer. The polymer concentration affected to adsorption only the early stage because is limited by the number of charge on the former layer. Even through this solution is added more the concentration, It has no effect on adsorption. This occur from the polymer are

adsorbed to the surface sufficiently and the like-charged electrostatic barrier can prevent the approach of additional polymer. The result is shown in constant curve [55].

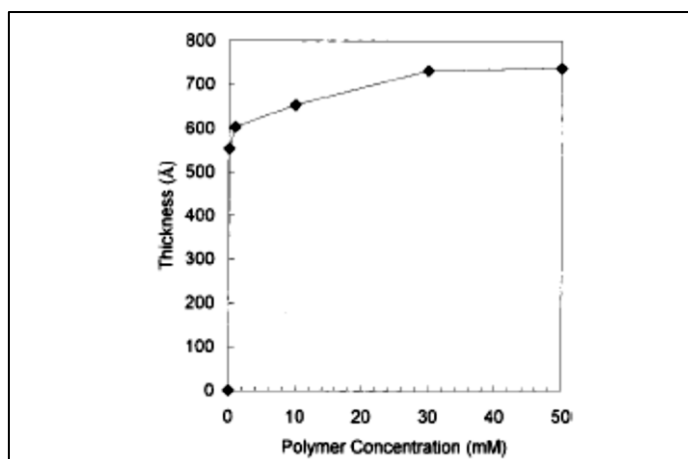


Figure 2.15 Thickness vs polymer concentration of PSS/PDADMAC for 5 layer pairs [55].

2.3.4.2 Temperature

Temperature is one of parameter that can control PEMs growth. Formation of PEM by dipping in solution by hand use PDADMAC/PSS 1mM with 1M NaCl and vary temperature from 10 – 70 °C. The thickness increase in linear relation with respect to temperature can be observed as illustrated in figure 2.17.

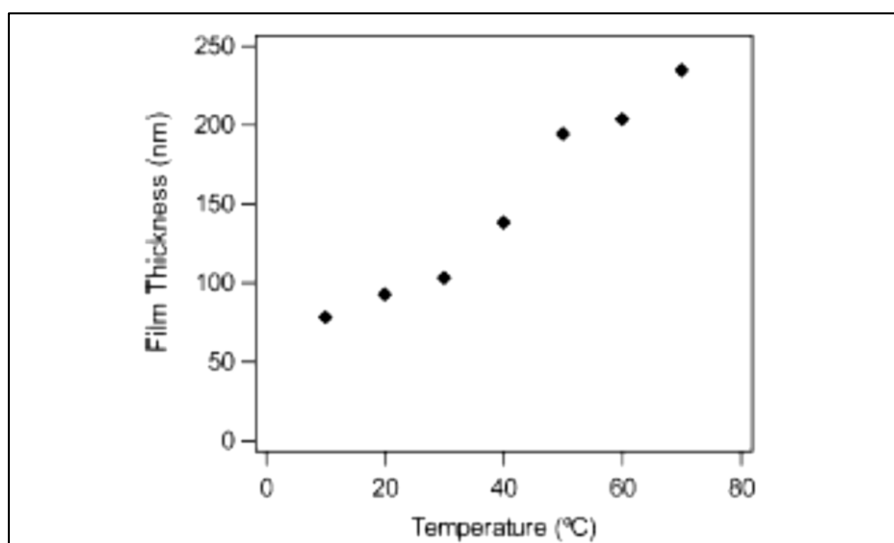


Figure 2.16 Thickness of hand-dipped(PDDA/PSS) film 10 layers deposited at different temperatures in the presence of 1M NaCl [61].

To investigate the relationship between temperature and thickness when PEMs was formed and without salt, The result was shown in figure 2.19. When the temperature increased the thickness of PEMs was increased. The difference in the result when increasing temperature with salt is show higher in the thickness[61].

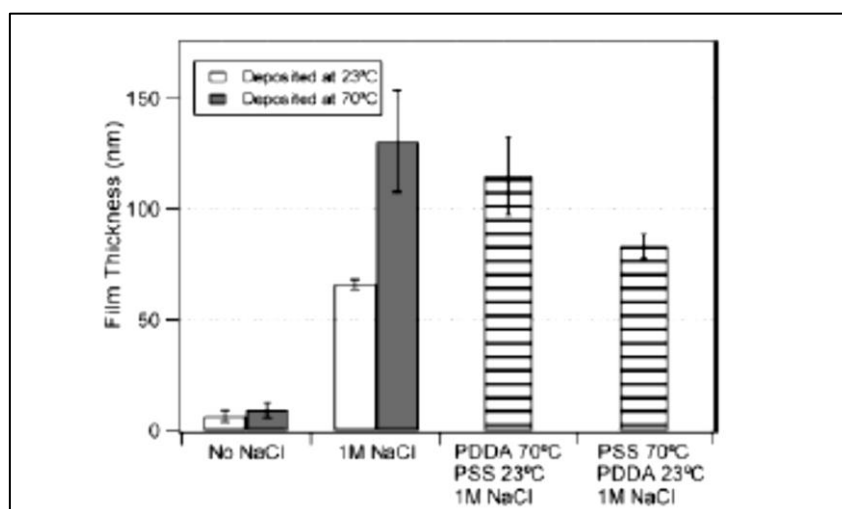


Figure 2.17 Film thickness (nm) of PDDA/PSS film 5 layers deposited under different conditions. Left two columns compare film deposited at 23 °C (white) and 70 °C (shaded) in the absence or presence of 1M NaCl. Right two columns compare the effect of heating only the PDDA or the PSS to 70 °C while the other polymer is deposited at 23 °C [61].

The effect of temperature on the thickness of film when adding salt is explained clearly that adding salt in solution affect to the thickness of film by increasing film swelling because of the screening of electrostatic force together. Therefore, the dissociation of polycation and polyanion binding site and fluidity in the film were increased at high temperature, localized dissociation was promoted and conformational dynamic was also increase. So both salt and heat lead to increase loop and tail of polyelectrolyte chains and increase the thickness of PEM film.

2.3.2.3 Solvent

Polyelectrolytes which are poor solubility in solvent let to increase adsorption on the substrate. Oppositely, if polyelectrolytes are highly soluble in solvent enhance to decrease in adsorption on the substrate. The solvent which is lower in dielectric constant resulting to increase in the electrostatic interaction follow by equation (1), this enhance to adsorption of polyelectrolyte. Dielectric constant in solvent can be adjusted by adding small amount of ethanol in water [62]. This was shown in figure 14. When the ratio of ethanol in water was varied, the thickness of PEMs is increase until 40% ethanol and then it became precipitate. This shows that solvent composition offers another degree of ionization, influencing to control multilayer formation[55]. Furthermore, Lesser solvation of polymer would decrease intrapolymer segment repulsion and aggregate on the surface. Selection the solvent for PEMs formation should be low in dielectric constant and more hydrophilic to increase electrostatic interaction.

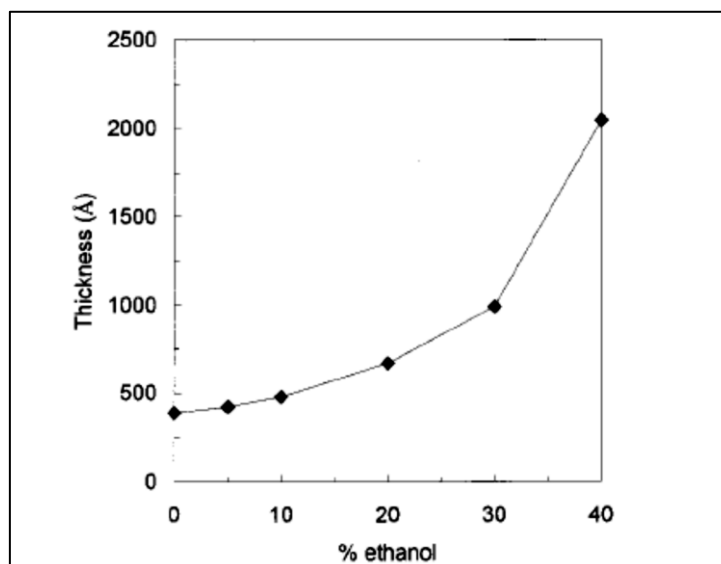


Figure 2.18 Illustrate thickness vs wt % ethanol for a 10-layer-pair multilayer of PSS/PDADMA from water/ethanol mixtures with 0.1 M NaCl [55].

2.3.5 Permeability properties of the PEMs.

When the parameters controlling the growth of PEMs were varied, the property of thin film can be controlled to provide high permeable, semi-permeable and nearly impermeable film. This property related to control release molecule pass through the film. The film that contain high permeable enhance to high rate of releasing. Permeability of the PEM film can be controlled by pH, ionic strength [63], thickness [64] and crosslinking polymer [65, 66]. Adjustment of these parameters effect of the backbone interaction between polyelectrolyte molecule in PEM leading to alter the layer structure and permeability. Other parameters are number of layers, multilayer porosity and the size of permeable compound.

2.3.5.1 Parameters controlling the permeability of PEMs

2.3.5.1.1 The effect of Swelling and ionic strength

PEMs can be controlled in swelling characteristic by salt. Dubas and schlenoff [63] studied the swelling of film from observed for three conditions of polyelectrolytes: PAA/PDADMA, PSS/PAA and PSS/PDADMA. They found that Swelling curve can be reproducible until salt concentration reach to 2 M for PSS/PDADMAC and 0.3 M for PAA/PDADMAC and after this point, the film started swelling as illustrated in figure 2.21. These difference occur the reflection of relative degree of association with opposite charged segments. Polymer pair which form more hydrophobic complexes are expected to attach strongly with aqueous solution and less prone to swell by salt.

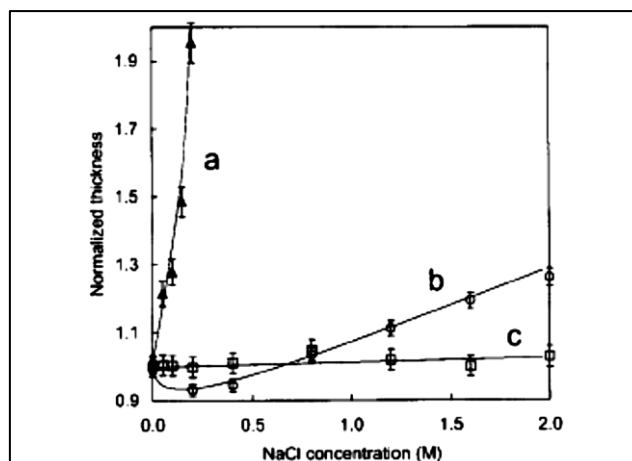


Figure 2.19 Thickness as a function of NaCl concentration for three multilayers: (a) PAA/PDADMA ; (b) PSS/PDADMA ; (c) PSS/PAH [67].

Similarly to Borke and Barrett [68] determine the effect of ionic strength on the swelling of PAH/HA film. They found that the degree of film swelling is related to the total number of layers, solution pH, ionic strength and cross-linking because all of these factors contribute to the structure of the film matrix which will be explained later part of this review.

Ionic strength is used to control permeability of PEM both low molecular compound and macromolecule [69]. Salt concentration cause a greater degree of swelling leading to change in film morphology, enhance film permeability and ease in transportation of counterion within the film [70]. The effect of salt ion is decrease of number of contacts between opposite charged would and leading to loosening of the layer structure and enhance permeability [63]. Salt concentration have influenced to thin film in extrinsic compensate resulting to increase swelling of the film [71].

Antipov et al [63] investigated the influence of ionic strength on permeability of PSS/PAH layer by used fluorescein as release agent and found that the permeability coefficient has strong nonlinear dependence on salt concentration as shown in figure 2.21.

It can be concluded that swelling of PEM film facilitate the release of molecule by transporting counterion into film for screen the electrostatic interaction and by create voids and pores that the molecule can travel through this film[72].

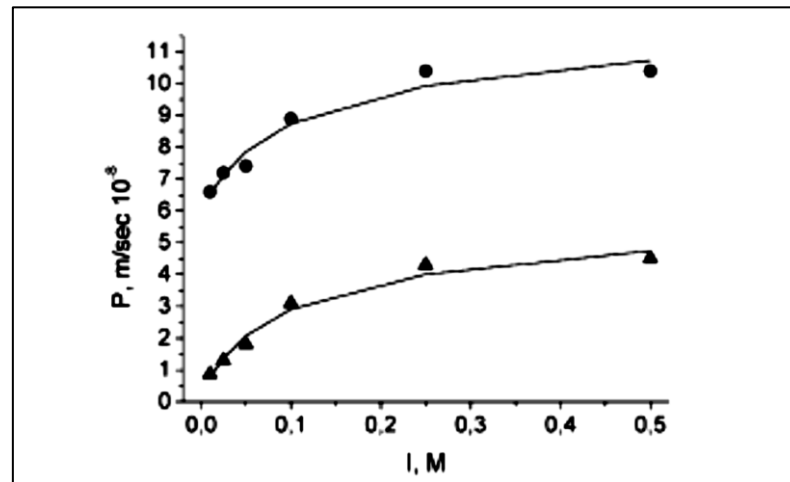


Figure 2.20 Permeability of PEM capsules as a function of ionic strength at pH 7 (circles) and pH 8 (triangles) [63].

2.3.5.1.2 The effect of film thickness

The permeability of multilayers is decrease when increasing the number of layers [65]. In the behavior of the permeability coefficient as function of thickness, the number of layer was varied up to 18 layers are of PSS/PAH film, resulting to decrease significantly in permeability coefficient as shown in figure 18. This result relate to diffusion model of fluorescein through PEM that diffusion coefficient is inversely to the number of layer [73].

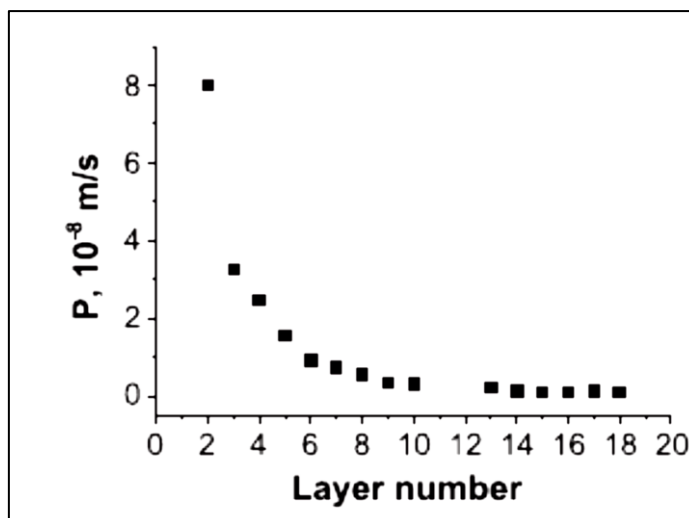


Figure 2.21 Fluorescein permeability coefficient as a function of layer number [64].

This effect can be confirmed by Lee et al [74], they found that the growth of PAH/PSS multilayers in cylindrical pore of Track-Etched Polycarbonate membranes (TEPC) at pH 9.3. In addition they found that the diameter of pores decrease when the number of layer increase as shown in figure 2.24 and without found that clogging the pores when increase layer up to 24.5 bilayers. Because the conformation of the polyelectrolyte chains was most likely not affected by the curvature of the pores since the size of pores in this study is much larger than the radius of gyration (10 nm) of polyelectrolytes used in this study.

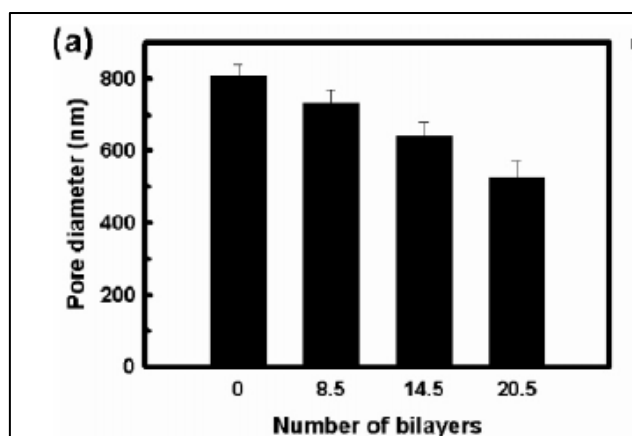


Figure 2.22 Changes in the average pore diameters of multilayer in the pore of Track-etched Polycarbonate membrane (TEPC) estimated from SEM images as a function of the number of bilayers[74].

2.3.6 Degradation of PEM

Degradation of PEMs is related to permeability in the term of thickness of film. There are two model of degradation in PEMs including hydrolytically degradation that the film erode by immerge in buffer solution and the enzymatic degradation that the thickness of film is decreased by enzymatic interact with this PEM. Degradation of PEMs can be measured by film thickness as a function of time after expose in buffer solution or enzymatic. Wang et al [75] measured desorption of multilayer films of FITC-Alginate /Chitosan by pepsin. This film was partially dissolved into pepsin solution, leading to decrease in fluorescence intensity of film when the time increased like figure 20. Similar to Ren et al [76] detect in degradation of poly-L-lysine /DNA films in a α – chymotrypsin solution that linearly decrease of thickness as a function of time. For hydrolytically degradation, Wood et al [77] found that the PEMs is swelling in early step and decrease continuously. This is directly proportional to the releasing of agents from PEM. The stability of the film can be controlled by adding crosslinking agent in order to that reduce the desorption and drug release rate [78]. This property can be applied to use in control release of drug by controlling film thickness, composition of film and crosslinking [75-77].

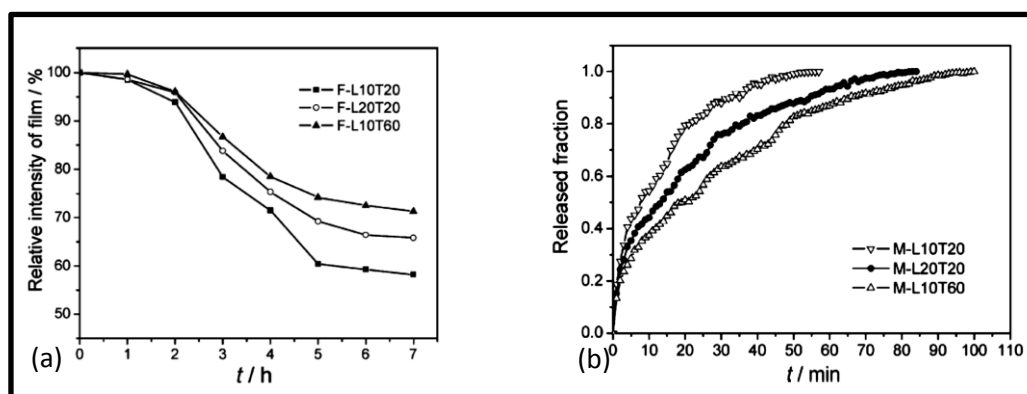


Figure 2.23 The fluorescent intensity of films as a function of pepsin treatment time. (a) show degradation of film as function of time (b) show IDM release profile from microcapsule (L is layer number and T is deposition temperature) [75]

2.3.6.1 The effect of pH

Permeation of the PEMs can be controlled by adjustment of the pH value. This adjustment enhance to change the conformation of the PEMs lead to form condense or loose structure of the film. This influence to permeable and drug release pass through PEMs [69, 72-74, 79]. The PAH/PSS film 18.5 bilayers were deposited on 800 mm. pore of Track-Etched Polycarbonate membrane at pH 2.5 to 10.5 adjusted by water for 3 min after the pH 10.5, the pore of this membrane was decreased until pH 5. Then the pH was adjusted lower than 5 leading to the pore effective close. For the membrane was prepared at pH 2.5, the pore still open. After pH 9, the pore was closed and the flux was extremely low follow by the pore size [74]. While Zhao Q. and Li B. [79] found that adjustment pH value of capsule created which from PLL/CS multilayer can control the release of BSA. The release rate of BSA was faster when the pH increase. This result are the same behavior with another case that show permeability of fluorescently labeled dextran in PSS/PAH hollow capsule. At pH 3.5, the pore of film was opened and closed at pH 10 [73] as shown in figure 21. This reversible was adjusted by change the pH suitable to each of polyelectrolyte. Adjustment proportion between negative and positive charge is effect to pore size and permeability [65]. The optimum condition for release molecule are occurred repulsive rather than attractive force between molecule and film [72].

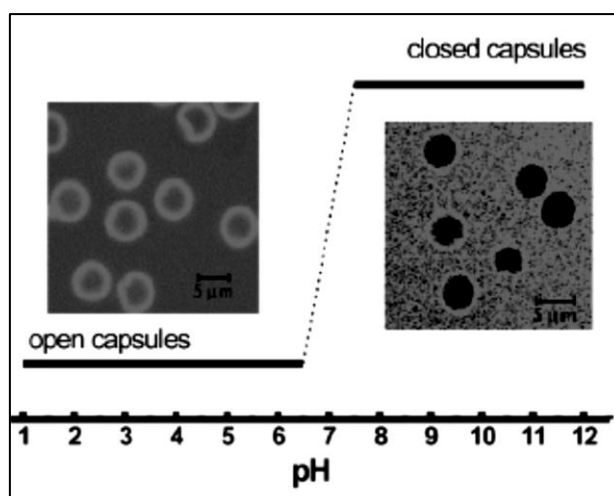


Figure 2.24 Permeability of MF- derived capsules for FITC-dextran (molecular weight 77kDa. open at pH 3.5 and closed at pH 10 states of (PSS/PAH)₄ hollow capsule [73].

2.3.6.2 The effect of crosslinking

The crosslinking of the PEMs structure not only provide stability at film [65] but also influence to their permeability. Ye S. et al [66] reported that when crosslink the alginate in alginate/chitosan capsule shell was crosslinked with calcium ion and loaded insulin in microcapsule, the insulin release rate was decreased. Moreover, this crosslinking step can maintain the film structure when pH value was varied.

2.4 MTT assays

The MTT assay is colorimetric assays for measuring the activity of enzymes that reduce MTT to formazan dyes, giving a purple color. MTT is 3-(4,5-Dimethylthiazol-2-yl)-2,5-diphenyltetrazolium bromide which contain a yellow tetrazole and is reduced to purple formazan in living cells. A main application use to measure the viability and the proliferation of cells. It can be used to determine cytotoxicity of medical agents and toxic materials. In this work use MTT assay to assess the effect of silver nanoparticles would stimulate or inhibit in normal human cell and cancer cell viability. Ahamed et al used MTT assays to evaluate the toxicity of polysaccharide coated on silver nanoparticles and uncoated silver nanoparticles to mouse embryonic stem (mES)

cells and mouse embryonic fibroblasts (MEF). They found that coated silver nanoparticles more destroy both mES and MEF cell than uncoated silver nanoparticles[80]. Liu et al tested cell viability via MTT assay with a various size of silver nanoparticles. They analyzed in A549, SGC-7901, HepG2 and MCF-7 cell. And they found that smaller size of silver nanoparticles had more toxicity to cell than larger size[81]. In this work three type of cell is mentioned including human breast adenocarcinoma cells (MCF-7), human breast cancer cell line (BT474), Jurkat cell which is a cancer of the blood or bone marrow called leukocytes, human lung bronchus carcinoma(ChaGo-K-1) which is derived from bronchogenic carcinoma and Caucasian fibroblast-like fetal lung cell (WI 38 cell line human).

2.5 Antibacterial test

Antibacterial test is the method use to analyze the interaction of the sample to bacterial property. There are many way to test this activity including broth dilution tests, antimicrobial gradient method, disk diffusion test and automated instrument system[82]. In broth dilution tests, the sample solution was diluted two-fold dilution such as (1, 2, 4, 8 and 16 units) in nutrient broth solution. Then they were incubated with bacterial suspension at 37 °C 24 hr. after that thae sample were characterized for visible bacterial growth by turbidity and reported in to the lowest concentration of sample that could to antibacterial growth or the minimal inhibitory concentration (MIC). The good advantage of this method is can be report in quantitative result but it has to practice in every process for prevent an error occur. The next method is disk diffusion test which is a simple and standard method. The bacterial colony was streaked on surface of Mueller-Hinton agar plate. Then sample disks are plated on agar surface and incubated 24 hr at 37 °C. The zone of growth inhibition around the sample disks is analyzed and compared with the criteria published by clinical and laboratory standard institute or the us food and drug administration (FDA). The advantage of this method is easy to test, no expensive equipment and result is easy to analyze. But it do not contain an automation of the test[82]. In this work, the combination between broth and disk diffusion test were used to test antibacterial activity. Silver nanoparticles were incubated

with bacterial colony in nutrient broth 24 hr at 37 ° C. Afterward bacteria which already exposed to SNP was streaked on agar and incubated at 37 °C for 24 hour. Colony of bacteria was counted and calculated follow as formula below

$$\% \text{ of reduction} = \frac{(A-B)*100}{A}$$

Where A was the number of bacterial colony which was not exposed to SNP (controlled sample)

B was the number of bacterial colony which was not exposed to SNP (treated sample)

2.6 Scanning electron microscopy

Scanning electron microscopy or SEM is an electron microscopy which use high energy electron shoot to the surface of sample and scan sample. After sample is scanned with high energy electron, a different signal is collect form the sample and produce an image represent the surface of sample. SEM image can give different information from sample including surface morphology, structure and phase composition. The main three signals which are usually collected form SEM are secondary electron, backscattered electron and characteristic X-ray. These signals are collected by detector that can collect the electron near the surface. Generally, secondary electron can form the SEM image, backscattered electron which is a reflecting electron from the surface use to analyze in different element in the sample and characteristic X-ray is occur when inner shell electron is remove from the sample by electron beam. Mechanism of this SEM is electron gun shoot electron go through the sample. The electron adsorb into the surface and form a tear drop shaped volume deep around 100nm to 5 µm. then the detector collect the signal and produce an 2 D SEM image. The resolution of SEM is around 1 nm. The sample can be measured in vacuum and wet condition.

The scanning electron microscopy will be used for scan the surface of polyamide suture material before and after layer by layer with PDADMAC and silver nanoparticles capped with folic acid, alginate and PSSMA. SEM can show characteristic and size of silver nanoparticles on suture material. Boccaccini et al coated bioactive glass powder on the surface of polyglactin 910 suture material for increase hydroxyapatite formation. They investigated surface of suture material by using SEM image and can confirm that have bioactive glass powder on its surface[83].

2.7 Atomic adsorption spectroscopy

Atomic adsorption spectroscopy or AAS is an instrument use to analyze the element in the sample. The element will adsorb the optical radiation by free atom in gaseous condition. Then the concentration of element is reported. This technique has the standard which used to refer the relation between the absorbance and the concentration of element. The principle of this show that when atom of element is received the energy from radiation which is given, electron will move up to the excite state in a short time. This specific radiation or wavelength is unique and can be used to indicate the element. The detector collect the absorbance of both with sample and without sample, Then the ratio between the two absorbance is calculated to concentration via the Beer-Lambert Law. This law is indicated that the absorbance is directly proportional to the thickness and concentration of the sample[84].

In this work AAS was used to analyze to concentration of silver ion which release from multilayer thin film coated on the polyamide suture material. Liu and Hurt synthesized silver nanoparticles by using citrate as stabilizing agent and reducing agent. Then studied the parameter which influence to silver ion release by using AAS to analyze[85].

2.8 Atomic force microscopy

The atomic force microscopy (AFM) is one type of scanning probe microscope or SPM and is usually used for scanning surface of material in nanoscale. It has three modes: contact mode, tapping mode and non-contact mode. AFM consists of an optical lever which is used to analyze the reflecting of a laser after it points to the cantilever of the AFM tip. This reflection is incident on the position-sensitive detector, which is composed of 4 sections. The reflection of the laser incident in different areas on the detector indicates the angle of the cantilever and the position of the laser during scanning. If the laser is out of the center, AFM will adjust the signal back to the center. The repulsive and attractive forces between the AFM tip and the surface of the sample are recorded and converted into an AFM image. The AFM tip is made from silicon and silicon nitride, which consists of a tip for contact and tapping modes. The samples that can be analyzed by AFM are insulators (polymer, glass, composite, and biomolecules) and conductive materials. AFM can measure the morphology of a sample in terms of roughness, composition, which shows in different phases. Moreover, the thickness of the sample and the size of particles can be analyzed by AFM as well.

In this experiment, AFM was used in tapping mode to characterize the morphology, thickness, and size of silver nanoparticles. Tanaka et al. studied the parameter that affects the effect of PS/PMMA thickness, including interaction and the degree of entanglement among polymer chains. They measured their thickness using AFM [86]. Hoo et al. analyzed the particle size of polystyrene nanoparticles by using dynamic light scattering (DLS) and compared it with atomic force microscopy (AFM). They found that the particle sizes measured by DLS were slightly larger than the normal value, and the result from AFM was opposite to the result from DLS [87].

2.9 UV-vis spectroscopy

UV-visible spectroscopy is a technique that uses a light source that passes through a solution or film and reports an absorbance value. This instrument measures the absorbance value of the sample in the ultraviolet and visible wavelength regions. The light source of this

instrument has to generate continuous and intensity of radiation in the selected wavelength. There are two type of light source, first it is deuterium lamp which generate the light in 185-375 nm and tungsten lamp which generate in 320-2500 nm. When light from light source spot to the monochromator used to select the wavelength and reflect the light in different angle. Then the light passes through the sample which has to prepare in quartz cuvette normal cuvette. For quartz cuvette has to use in ultraviolet wavelength. Then the light that can transmit to the sample is analyzed by detector for detect the different of light after it is adsorb by sample. The final signal is analyzed and reported.

In this experiment will use UV-VIS spectroscopy to monitor the localized surface plasmon resonance (LSPR) band of silver nanoparticles capped with a various concentration of capping agent. in both solution and thin film. Martı́nez-Castan˜o'n et al synthesized silver nanoparticles in different in size and studied their antibacterial property. After prepared silver nanoparticles, their LSPR peak was analyzed by UV-vis spectroscopy and shown around 400 nm[88].

CHAPTER III

EXPERIMENTAL METHODS

In this part, the chemical agents used in this work are described. The methods that were used for silver nanoparticles preparation and multilayer thin film formation have been illustrated. The process which was used to study of silver nanoparticles leaching from thin film in different stabilizing agents and conditions are listed. The procedures of anticancer and antibacterial test are also displayed. The methods and instruments used to characterize samples are shown in this part clearly.

3.1 Chemical agents

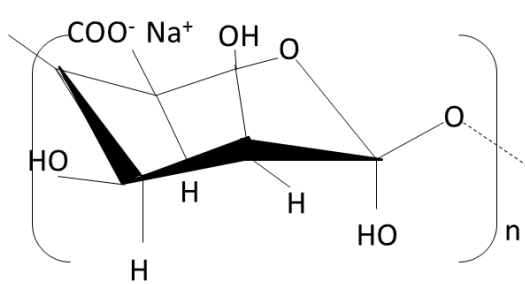
3.1.1 Silver nitrate which was used for silver nanoparticles preparation was purchased from VWR, Thailand.

3.1.2 Stabilizing agent used to protect silver nanoparticles from aggregation. This work used three capping agents which were purchased from Aldrich as below. The structure of these capping agents were illustrated in figure 3.1

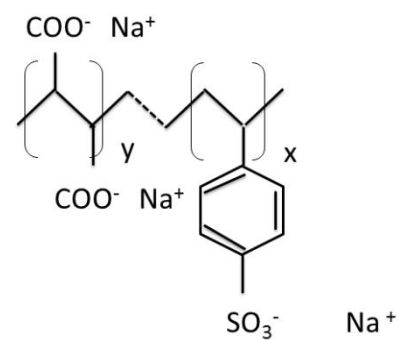
- Folic acid (FA) MW 441
- Poly(4-styrenesulfonic acid-co-maleic acid) sodium salt (PSSMA) MW 2×10^4
- Alginic acid, sodium salt (AL) MW 198

3.1.3 Reducing agent used to reduce silver ion into Ag^0 was sodium borohydride (NaBH_4) and purchased from Aldrich MW 37.83

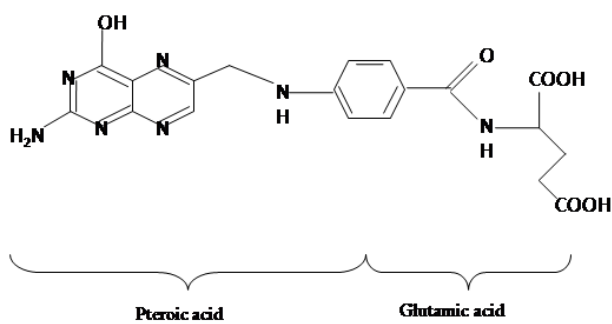
3.1.4 Primer coatings used in this work consist of Poly(diallyldimethylammonium Chloride)(PDADMAC)(MW 200,000-350,000) which was used as cationic polyelectrolyte and polystyrene - 4- sulfonic acid (PSS) MW 206 which was used as anionic polyelectrolyte. These polymers were purchased from Aldrich. Sodium chloride was purchased from Carlo Erba.



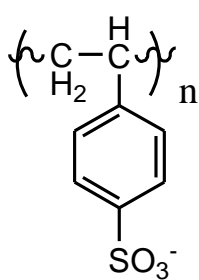
Alginic acid



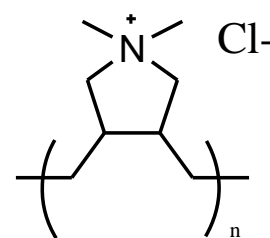
PSSMA



Folic acid



PSS



PDADMAC

Figure 3.1 structure of capping agents and polyelectrolyte

3.2 silver nanoparticles preparation

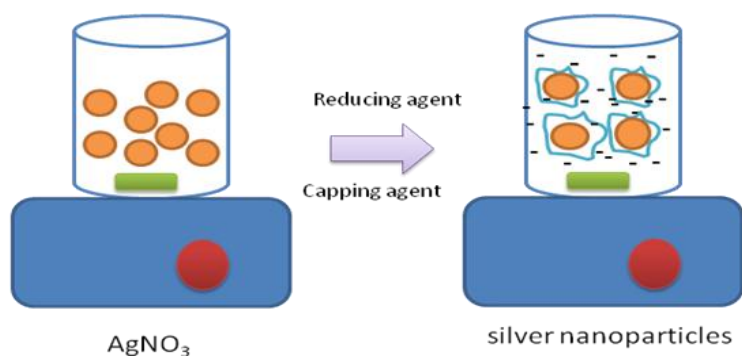


Figure 3.2 the schematic of silver nanoparticles preparation

1mM Silver nitrate solution and 10mM sodium borohydride solutions were dissolved in distilled water as stocks. A folic acid stock solution (10mM) was prepared in phosphate buffer (pH 7) to improve its dissolution. silver nitrate 1 mM and folic acid were mixed accordingly to obtain a final concentration of folic acid of 0.05, 0.1, 0.5, 1 and 5 mM. Then, the sodium borohydride 10 mM was added quickly to the folic-silver solution and stirred 10 minutes. The process of silver nanoparticles preparation was displayed in figure 3.2. Solutions were kept for 6h at room temperature and then stored at 4°C until used. The silver nitrate and sodium borohydride stock solution were prepared at 50 mM and stock solution of capping agent was prepared at 10 mM. Then mixed silver nitrate with capping agents first and stirred 10 minute. Finally, added sodium borohydride and stirred 15 minutes. The proportion of volume of all agents were illustrated in table 3.1

Table 3.1 the proportion of silver nitrate, sodium borohydride and capping agent which had to mix follow by each condition. Total volume was 100 ml and final concentration of silver nitrate and sodium borohydride were 1 and 10 mM sequentially. For capping agent, the final concentration were 0.1, 0.5, 1 and 5 mM.

Condition	Silver nitrate (ml)	Capping agent (FA,PSSMA, AL) (ml)	Sodium borohydride (ml)	DI water (ml)
SNP:capping agent 1:0.1	2	1	20	77
SNP:capping agent 1:0.5	2	5	20	73
SNP:capping agent 1:1	2	10	20	68
SNP:capping agent 1:5	2	50	20	28

Characterization: 1. SNP solution all conditions were measured the localized surface plasmon resonance absorbance peak by UV- vis spectroscopy

2. SNP solution were analyzed surface charge by Zeta potential

3.3 Polyelectrolyte monolayer and multilayer thin film formation

3.3.1 Monolayer thin film formation

Primer coating was prepared by 10 mM PDAMAC and 10 mM PSS 3 layers. 1 M Sodium chloride was added in both solutions. After dipped in each solution, primer was rinsed with distilled water. When glass slide had been adjusted surface with primer already, thin film was dried with nitrogen gas and kept in box. Then this primer was dipped in to all condition of SNP-FA, SNP-PSSMA and SNP-AL for 15 minutes.

Characterization: 1. Monolayer thin film was measured the LSPR absorbance peak by UV-vis spectroscopy

2. Monolayer of SNP was characterized with AFM in their surface morphology and size.

3.3.2 Study effect of salt to monolayer adsorption

SNP-FA, SNP-PSSMA and SNP-AL with a various concentration of capping agent were added sodium chloride (NaCl) include 1, 5, 10, 20, 50 and 100 mM. After that every solutions was studied the kinetic adsorption on the substrate by dipping the substrate in these solutions and measuring the absorbance value by UV-vis spectroscopy every 0.5, 1, 2, 3, 5, 7, 10, 15, 30, 45, 60, 120, 240 and overnight. The lambda max of absorbance peak was plot as a function of time and compared to different concentration of NaCl.

Characterization: UV-vis spectroscopy was used to measure the LPSR absorbance peak at any given time.

3.3.3 Study the effect of dilution

SNP-FA, SNP-PSSMA and SNP-AL solutions were diluted with distilled water 2, 10 and 100 times. Glass slide which already coated with primer 5 layers were dipped in SNP all conditions for overnight. After that this thin film were rinsed with distilled water, dried with nitrogen gas and kept in box.

Characterization: monolayer thin film with different dilution were measured the LPSR absorbance band by UV-vis spectroscopy. The plot of lambda max of absorbance peak was showed as a function of dilution time.

3.3.4 Multilayers formation

PDADMAC (10mM) which dissolved in distilled water with 0.1 M NaCl was used as polycations whereas a various concentration of SNP-FA, SNP-PSSMA and SNP-AL (0.1, 0.5, 1 and 5 mM) was used as polyanions. Multilayers thin film between PDADMAC and SNP were constructed on

the glass slide and polyamide suture material via polyelectrolyte multilayers technique. The substrate was dipped for 5 minutes in the PDADMAC solutions then it was rinsed in distilled water for 5 minutes. Then the substrate was dipped in SNP solution for 5 min and rinsed in distilled water 3 times. After finish this step, it contained the bi-layer of PDADMAC and SNP-FA. Then the process was continued until the 20 layers. The samples were dried with nitrogen gas and kept in a dry box.

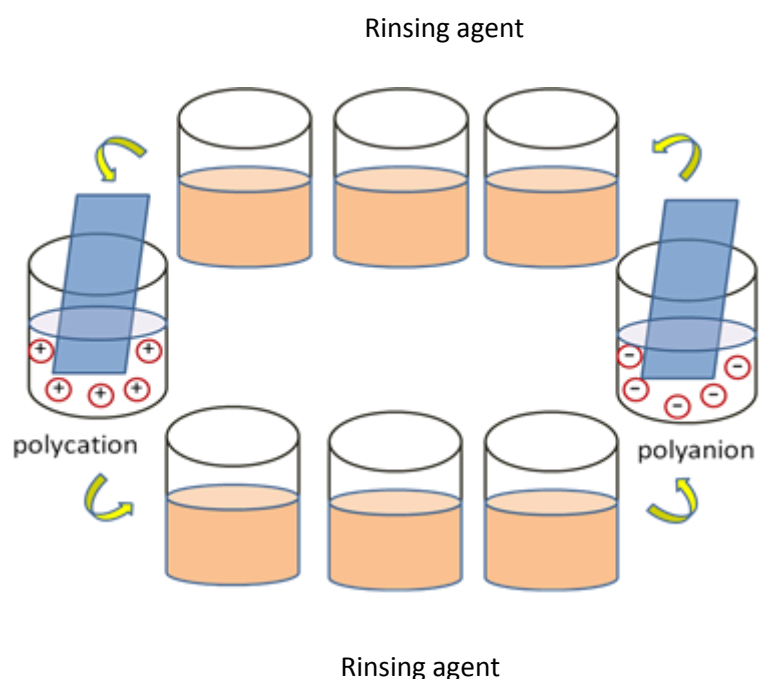


Figure 3.3 Schematic representation of Polyelectrolyte multilayers formation process between PDADMAC and SNP.

Characterization: the LPSR absorbance band was analyzed every 4 number of layers until 20 layers by UV-vis spectroscopy. Then the lambda max value of each condition was plot as a function of number of layer.

3.4 Study silver ion leaching from PEM

3.4.1 Silver ion leaching from SNP film on glass slide

PDADMAC/SNP capped with FA, PSSMA and AL were formed layer by layer on glass slide 20 layers (follow by the method in 3.3.2). Each condition of SNP had to prepare 2 samples, so the final samples were 24 samples. Buffer solution was prepared at pH 5.5 and pH 7.4 by used acetic-acetate buffer and phosphate buffer sequentially. One of sample was dipped in pH 5.5 and another was dipped in pH 7.4. Study the Silver ion leaching by analyzed the sample every 1, 3, 7, 14, 21 and 28 days.

Characterization: 1. Multilayer thin film was measured the LSPR absorbance band by UV-vis spectroscopy. The absorbance was noted before dipped in buffer solution and after dipped 1, 3, 7, 14, 21 and 28 days.

2. The thickness of films (before and after dipped 28 days) was measured by used AFM.

3.4.2 Silver ion leaching from SNP coated on suture material

This process was as the method in 3.4.1. However the substrate had been changed to polyamide suture material. The length of suture material was 2 m and dipped in pH 5.5 and 7.4. Then collected the buffer solution 6 ml every 1, 3, 7, 14, 21 and 28 days and kept in box avoiding the light.

Characterization: The solution which collected every 1, 3, 7, 14, 21 and 28 were analyzed by Atomic adsorption (AAS) for investigated the concentration of silver ion which leached from suture material.

The suture material that lapse on the glass slide were characterized the reflecting with ocean optic before and after 28 days. Moreover, the surface of suture material coated with PDADMAC/SNP was scanned with scanning electromicroscope(SEM)

3.5 anticancer and antibacterial test

3.5.1 Cytotoxicity test

BT474 which is invasive ductal breast carcinoma derived from solid[89] and MCF -7 which is human breast adenocarcinoma was used to test cytotoxicity with SNP-FA, SNP-PSSMA and SNP-AI via MTT assay. BT474 and MCF-7 cell were grown in Dulbecco's Modified Engle Medium (DMEM) mix with 10% of FBS and seed 1×10^5 cells/ml in 96 well by each well contained 100 μ l. Then they were incubated 24 h at 37 °C. Then all condition of SNP which two-fold- diluted into 53.5, 26.75, 13.38 and 6.69 μ g/ml were added into well plate in the volume 100 μ l/well. Then samples were still incubated for 24 h at 37 °C. MTT solution (3-(4,5-Dimethylthiazol-2-yl)-2,5-diphenyltetrazolium bromide) was exposed to BT474 cell and incubated for 4 h at 37 °C. After 4 h, MTT was removed. Formazan were dissolved with DMSO:25 ml of glycine and formazan crystal was changed into purple solution. Finally, formazan solutions were analyzed by Microtiter plate reader at 570 nm. Each condition was calculated to found % of cytotoxicity by this equation.

$$\% \text{ Cytotoxicity} = [(A-B)/A] \times 100$$

A = Absorbance value of control samples

B = Absorbance value of test samples

3.5.2 Antibacterial test

In this part mentioned antibacterial property of SNP-FA, SNP-PSSMA and SNP-AL with a different concentration of capping agent including 0.1, 0.5, 1 and 5 mM which was prepared follow as table 3.1. General environment such as air around us contained many bacteria which potentially infected people. These bacteria could be called airborne bacteria usually deposit on the surface of object which people can touch, transmit to other and cause to disease. The sample of airborne bacteria was staphylococcus aureus or S. aureus which was well known and cause to

infection. Escherichia coli or E.Coli is gram negative bacteria which cause to infection in gastro-intestinal system. Herein, all conditions of SNP were tested with S. aureus and E. Coli and studied in their antibacterial effect. Nutrient broth was prepared in proportion of nutrient broth powder 8 grams to distilled water 1 liter. Dissolve powder into water completely. Then nutrient broth was sterilized at 121°C 20 min by autoclave. Then nutrient agar was dissolved in distilled water 23 grams to 1 liter and boiled around 5 min for completely dissolved. Nutrient agar was sterile 121°C for 20 min and cool down. Pouring nutrient agar in culture plate and incubating plate at 45 °C until became solid.

Then SNP all conditions was added into nutrient broth which contained bacterial colony and incubated at 37 °C for 24 hours. Then SNP with bacterial colony in nutrient broth were Tenfold diluted until 10^{-7} . Afterward they are streaked on agar and incubated at 37 °C for 24 hour. Colony of bacteria was counted and calculated follow as formula below

$$\% \text{ of reduction} = \frac{(A-B)*100}{A}$$

Where A was the number of bacterial colony which was not exposed to SNP (controlled sample)

B was the number of bacterial colony which was not exposed to SNP (treated sample)

CHAPTER IV

RESULTS AND DISCUSSION

4.1 Chapter planning

In this part, the results of the experiments are exhibited and discussed followed by the section of methodology. Four main parts include the silver nanoparticles preparation (section 4.2), silver nanoparticles adsorption on the substrate both monolayer and multilayers (section 4.3), study of the factor which influenced to silver ion leaching from silver nanoparticles thin film (section 4.4) and anticancer and antibacterial of silver nanoparticles (section 4.5). The diagram of experiment was show in figure 4.1.

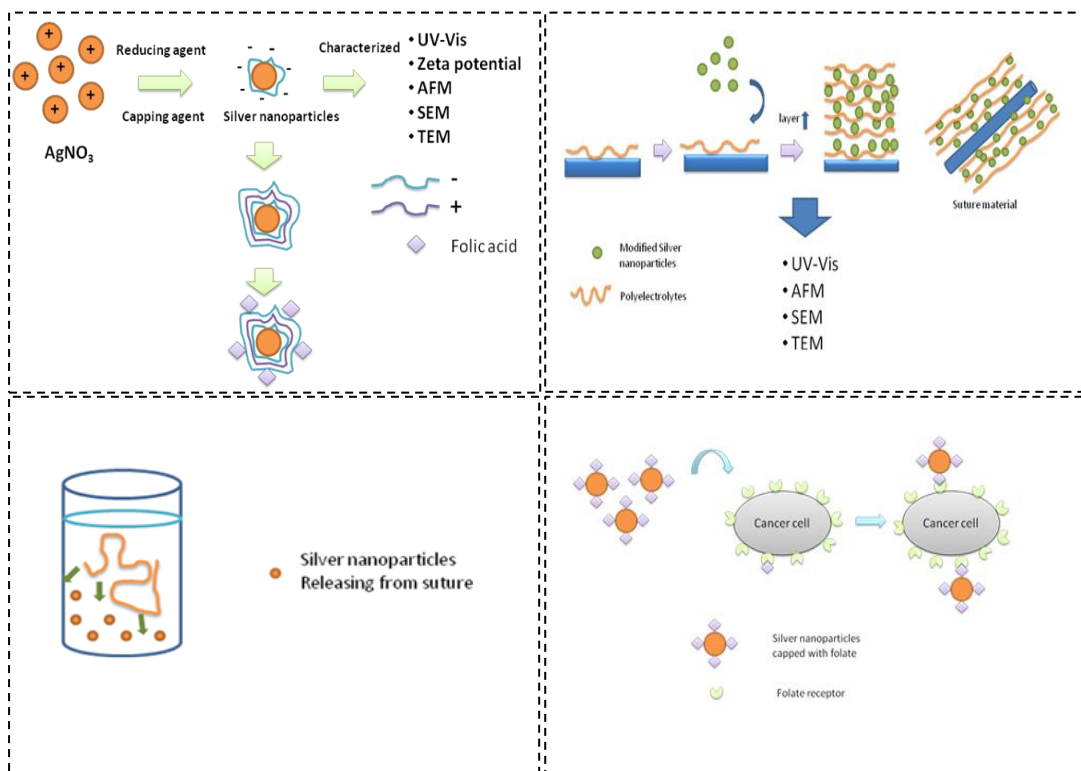


Figure 4.1 Diagram of section of experiment

4.2 Silver nanoparticles preparation and their parameters

In this part, silver nanoparticles were prepared by chemical reduction studying two parameters that are the concentration and type of stabilizing agent since they influence the property of the silver nanoparticles. The mechanism for the stabilizing process is based on the electrostatic repulsion between the surface of silver nanoparticles with anionic group from capping agent. In this work used alginate, PSSMA and folic acid were used as stabilizing agent, all containing carboxylate group which could interact with to surface of silver nanoparticles. This stabilizing agent is used to prevent the agglomeration of silver nanoparticles after reduction with sodium borohydried. Therefore it is important to study the effect of stabilizing agent on the silver nanoparticles preparation.

4.2.1 Study the effect of concentration of stabilizing agent.

The silver nanoparticles were synthesized via chemical process using sodium borohydried (NaBH_4) as reducing agent. NaBH_4 undergoes hydrolysis and release electrons and H_2 gas that can reduce silver ion to Zero valence Ag^0 . The objective was to study the effect of capping agent. The same concentration of silver nitrate(1mM) and sodium borohydried(10 mM) was used, but the concentration of stabilizing agent compose of alginate, PSSMA and folic acid were varied from 0.1 to 5 mM. After preparation, the optical property of silver nanoparticles were characterized by UV-vis spectroscopy. Their maximum localized surface plasmon resonance absorbance peaks were found at 400 nm which correspond to the surface plasmon resonance of silver nanoparticles as in figure 4.4. It can be observed that the concentration of stabilizing agent affected the positive of trend for SNP-AL and SNP-PSSMA. When the concentration of alginate and PSSMA was increased, the plasmon resonance absorbance peak was slightly higher wavelength to the increasingly polar capping which tends to increase the dielectric constant on the surrounding of the silver nanoparticles[90]. While the concentration of capping agent was effect a little in SNP-FA properties because a plasmon resonance absorbance peak of SNP-FA was

slightly red shift when increased concentration of capping agent probably because FA is a more hydrophobic molecule. The calibration curve of folic acid was shown in figure 4.2 with their LSPR peak which displayed at 280 nm. It could be observed that in the LSPR peak of high capping of SNP-FA was shown peak of folic acid which was around 280 nm, so it could be subtract this folic acid peak from SNP-FA for modifying this peak clearly.

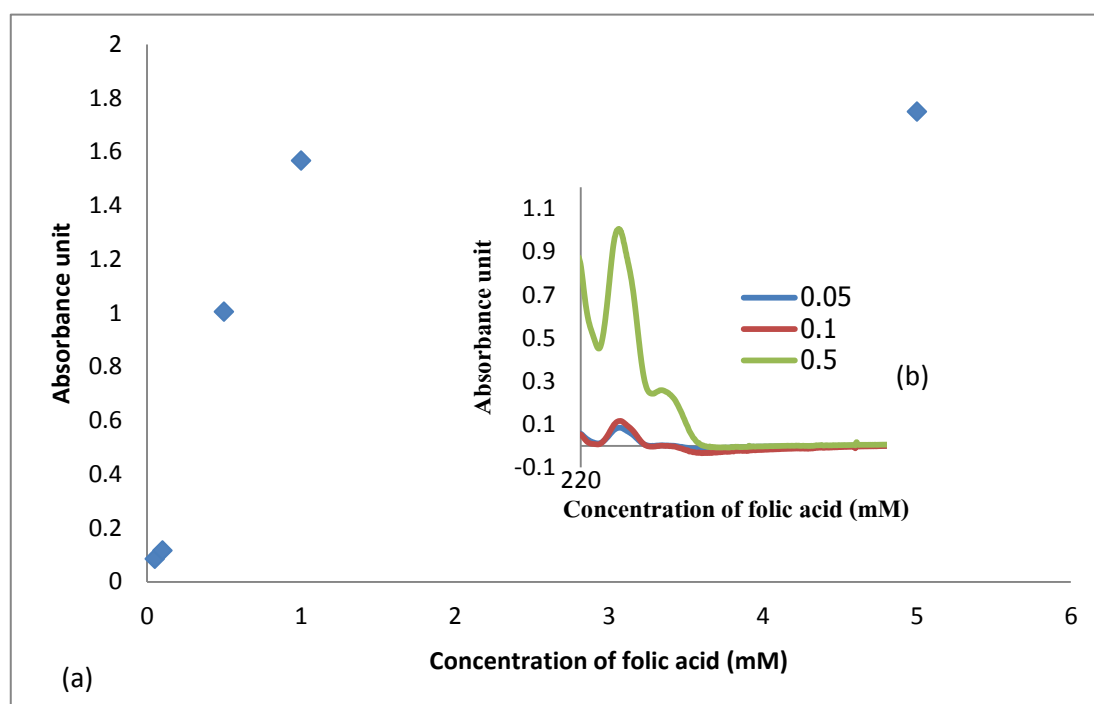


Figure 4.2 (a) Calibration curve of folic acid in phosphate buffer solution (pH 7), (b) The maximum localized surface plasmon resonance absorbance peaks of various concentration of folic acid were displayed at 280 nm.

For the picture of the silver nanoparticles solution, it can be observed that SNP-FA solution was not different in color when was varied the concentration of capping agent. In SNP-PSSMA was exactly change in color when used a different concentration of capping agent. And SNP-AL had different in 5 mM of alginate which was more yellowish. The change in absorbance is due to the concentration of SNP. The lower capping cannot prevent the aggregation of the particles and therefor lead to bigger SNP since the silver ion is fixed to 1 mM lower capping have the particles and therefore lower absorbance.

4.2.2 Particles size and morphology by AFM

4.2.2.1 Silver nanoparticles capped with folic acid

In order to study the SNP with AFM, it is necessary to immobilize the particles onto a flat substrates. Glass slide were used because they are easy to coat and cut to fill in the AFM. The SNP would not stick well on the glass slide and a cationic layer needs to be coated first. The layer-by-layer method is used to coat the glass slide base on cationic polyelectrolytes and anionic polyelectrolyte (PDADMAC and PSS) which was shown in figure 4.3.

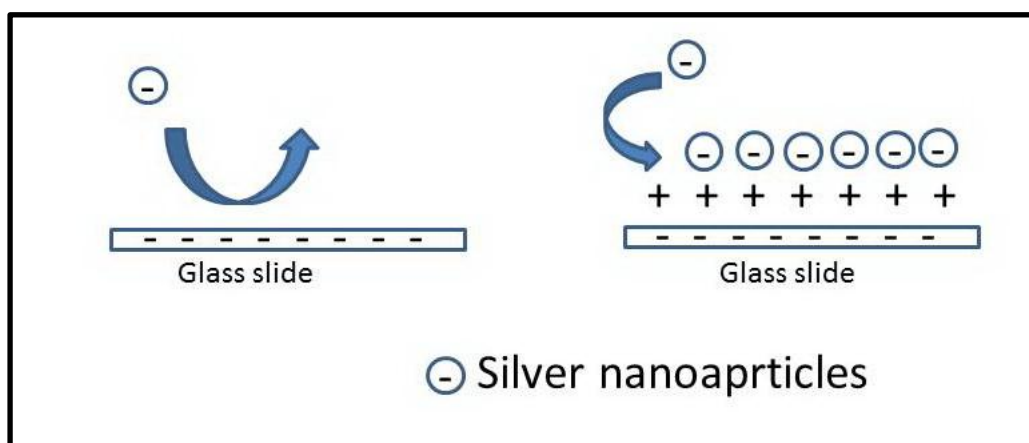


Figure 4.3 Diagram of primer formation.

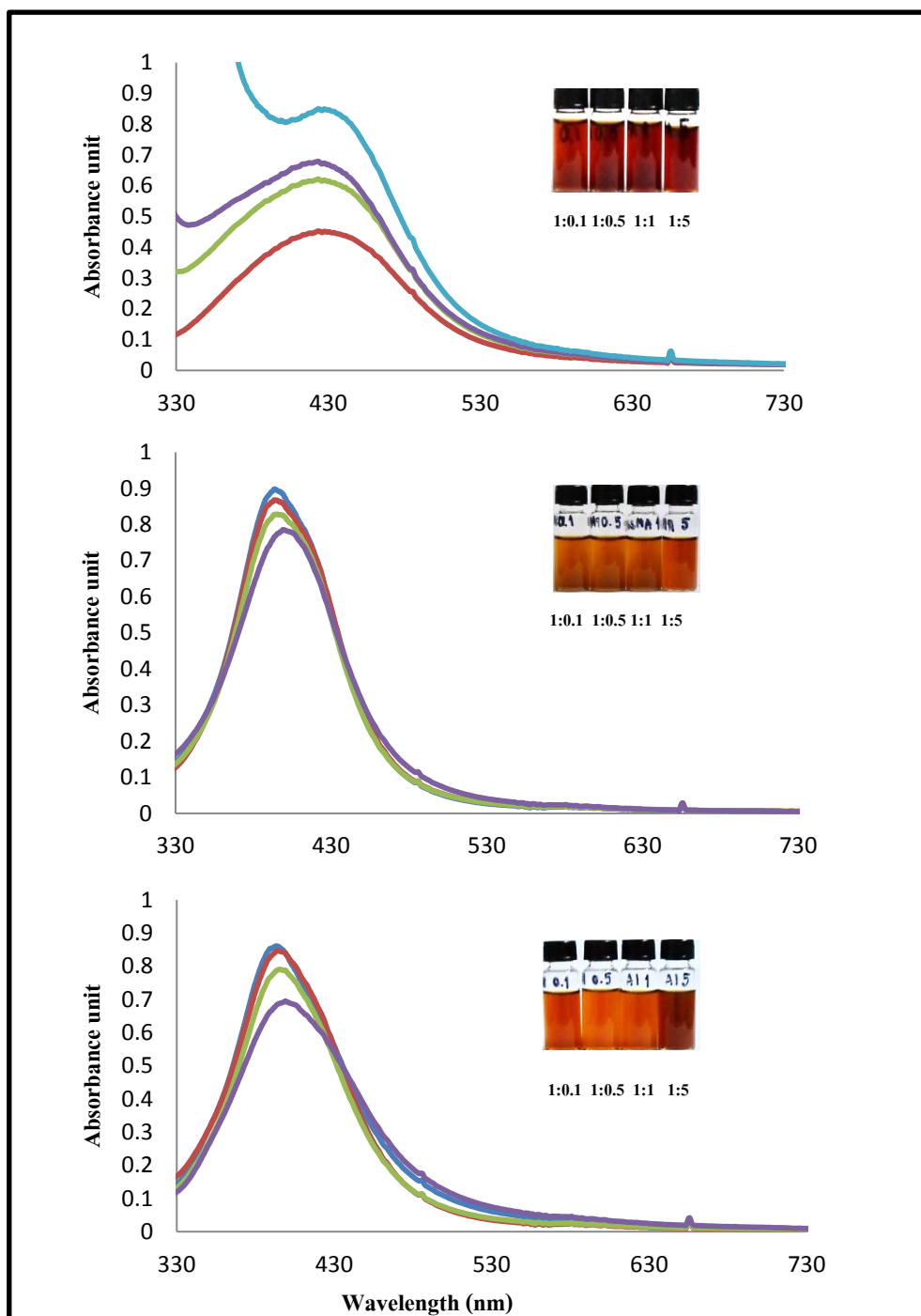


Figure 4.4 The localized surface plasmon resonance absorbance peak of silver nanoparticles capped with (a) FA(SNP-FA), (b) PSSMA(SNP-PSSMA) and (c) AL(SNP-AL) with various concentration ((0.1 mM= —, 0.5 mM= —, 1 mM= —, 5 mM= —). The picture showed SNP-AL solution with a different concentration of capping agent.

The primer coated on glass slide was dipped into SNP solution for 30 s and analyzed by AFM. The particles sized of SNP which were measured by AFM were exhibited in table 4.1. When varied capping agent of silver nanoparticles, it was found that it was less impacted to particles size of SNP-FA which was around 14.04 nm in the lowest capping agent. And other concentration of capping agent was no different in size which was around 8 nm. The figure of AFM image of SNP-FA with a various capping agent was showed in figure 4.5. When analyzed in surface roughness, it was found that 0.1 mM of FA made the surface roughness of SNP-FA film was the highest value around 3.94 nm. However the surface roughness of other concentration of capping agent was not different.

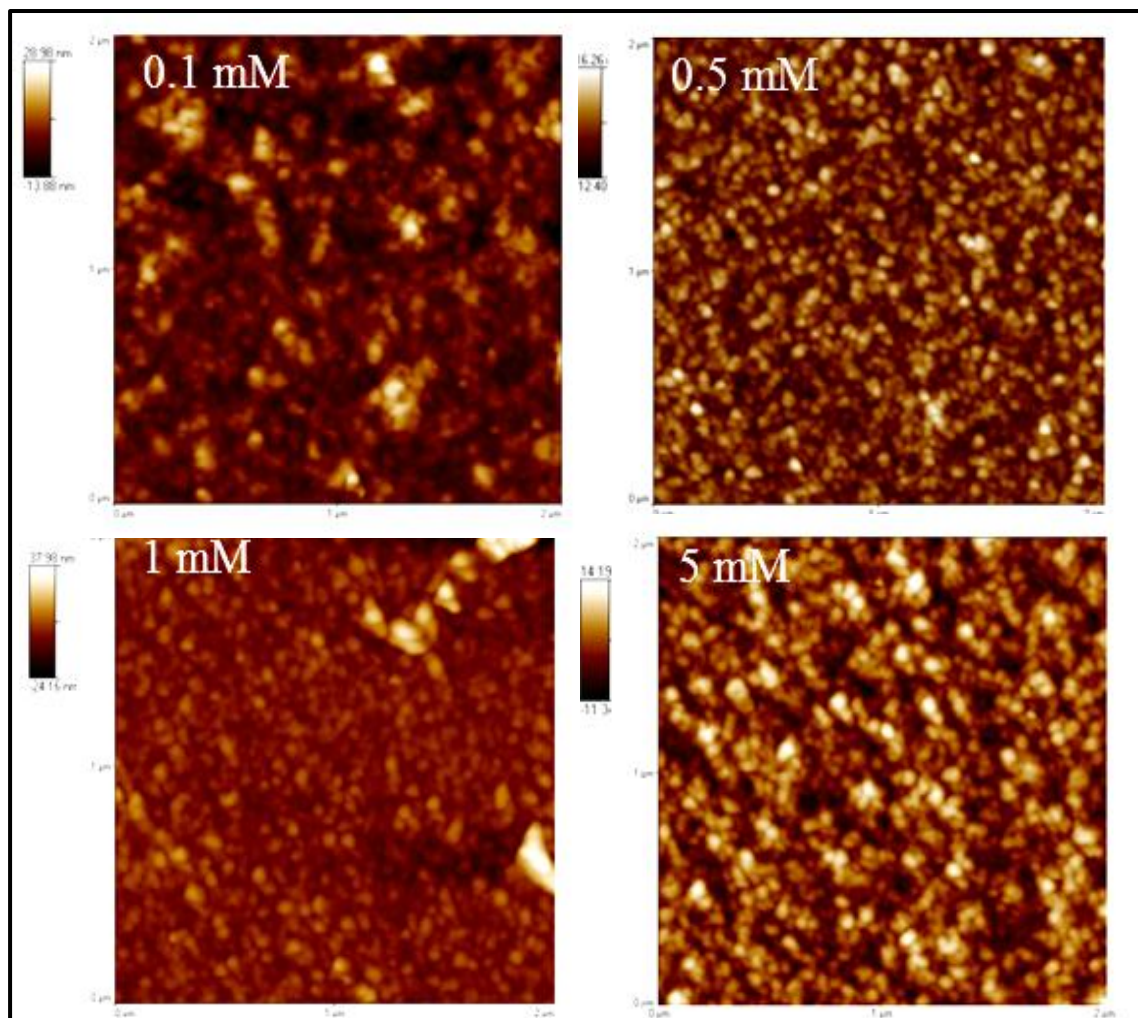


Figure 4.5 AFM image of SNP-FA with a various concentration of stabilizing agent

4.2.3.2 Silver nanoparticles capped with PSSMA

AFM image of monolayer of SNP-PSSMA were shown in figure 4.6. Particles size of lower capping of SNP-PSSMA was slightly larger than higher capping. The lowest capping agent was around 14.50 nm in size and the highest capping agent was around 8.21 nm. This was due to in low capping agent was contained low repulsive force to nearby particles, so particles was aggregated and form larger size. The surface roughness of 0.5mM SNP-PSSMA was the highest around 3.14 nm and the lowest was 1 mM SNP-PSSMA around 1.46 nm . When increased concentration of capping agent, it was high negative charge leading to particles was less in close packing. Film was formed smoother than low capping agent.

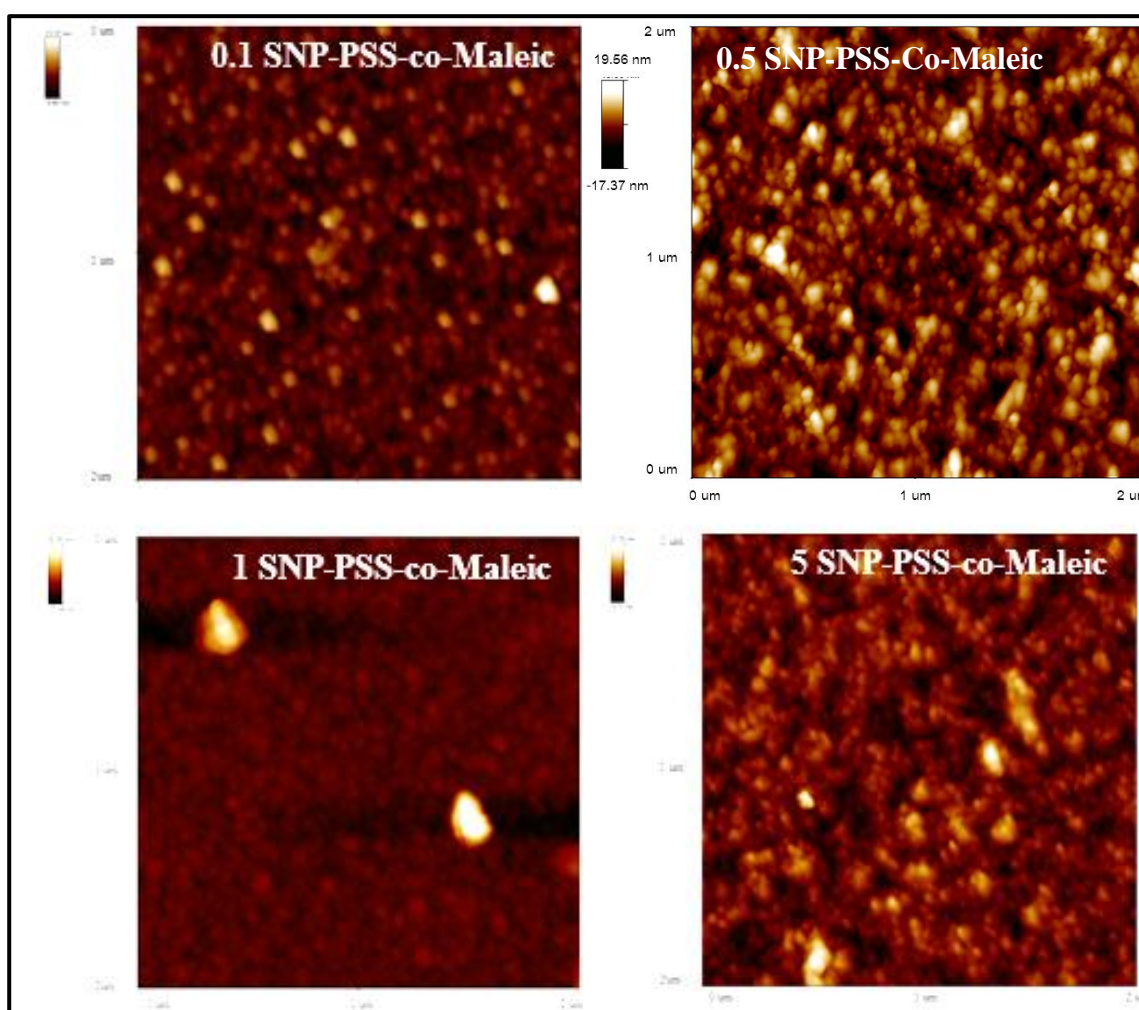


Figure 4.6 AFM image of SNP-PSSMA with a various concentration of stabilizing agent

4.2.3.3 Silver nanoparticles capped alginic acid

The monolayer of SNP-AL was exhibited in figure 4.7. From AFM image, it was analyzed in their particles size and found that particles size was increased with increasing the concentration of capping agent. Particles size of highest capping agent was around 6.98 nm and in the lowest capping agent was around 15.86 nm. This was corresponding to SNP-PSSMA. Their surface roughness was around 3.17 nm and slightly change in roughness when change in concentration of capping agent.

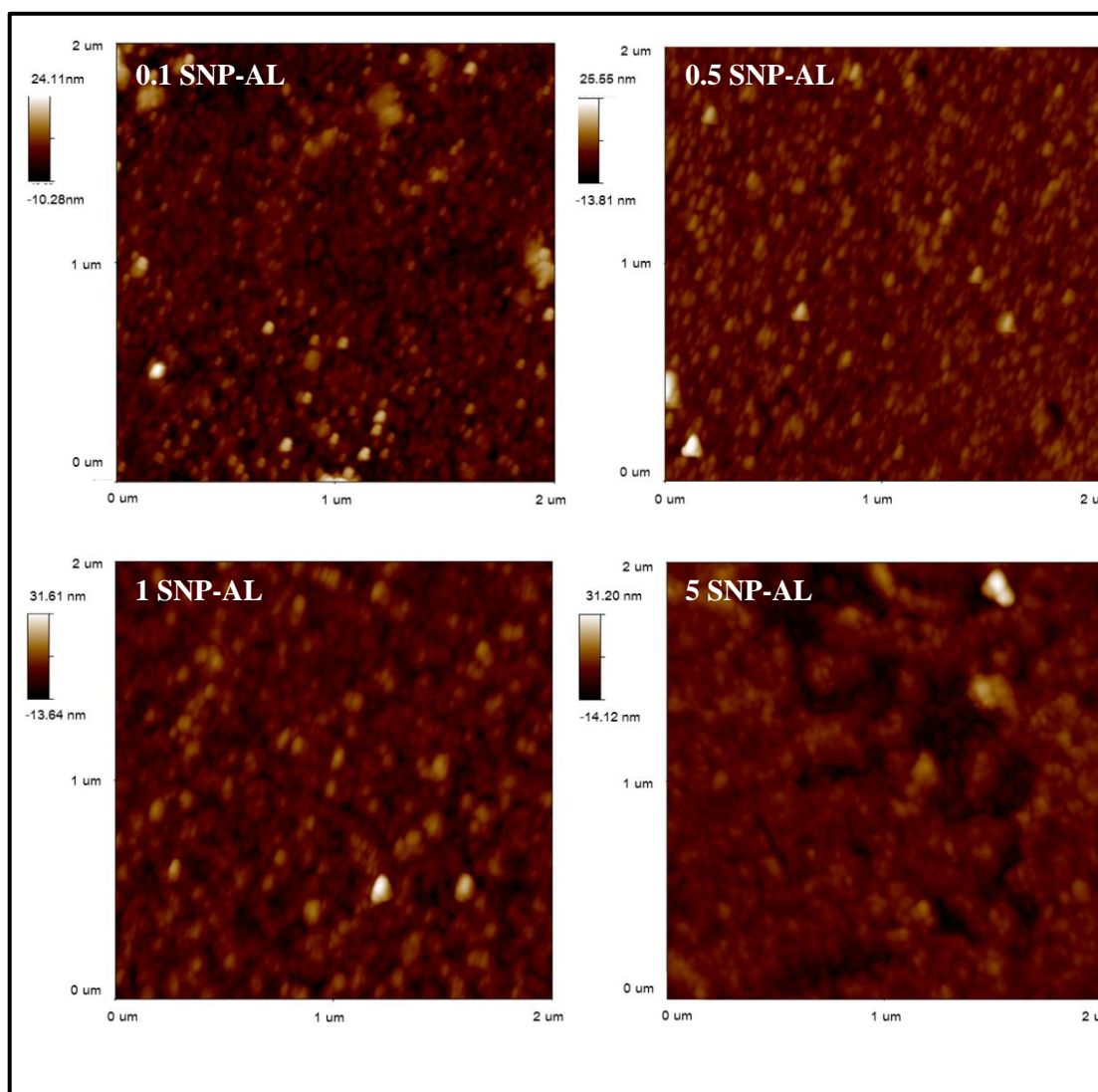


Figure 4.7 AFM image of SNP-FA with a various concentration of stabilizing agent

Table 4.1 The particles size of SNP (all conditions) measured by AFM

Condition	Thickness	Thickness	Thickness
	SNP-FA (nm)	SNP-PSSMA(nm)	SNP-AL(nm)
1:0.1	14.04 ± 1.65	14.51 ± 0.58	15.86 ± 1.07
1:0.5	9.85 ± 0.58	11.42 ± 0.92	11.46 ± 1.27
1:1	8.65 ± 0.89	10.26 ± 1.55	11.52 ± 1.29
1:5	8.23 ± 0.33	8.21 ± 0.72	6.98 ± 0.77

4.3 Layer-by-layer deposition of SNP

To understand the PEM and film formation, we lead to study the monolayer formation on glass slide and characterize by UV-Vis spectroscopy and AFM. All of SNP could be adsorbed on many substrates including glass slide, silicon wafer and fiber. In this part, glass slide and polyamide suture material were used to study the adsorption properties of SNP. For monolayer adsorption, SNP was used as negatively polyelectrolyte, so the substrate was modified surface by forming the primer which was formed layer –by-layer between positively and negatively polyelectrolyte. The top of primer was coated positively polyelectrolyte for supporting the next layer with SNP. Parameters which influenced to monolayer adsorption of SNP were studied including type and concentration of capping agent, time, concentration of sodium chloride(NaCl) and dilution. Then polyelectrolyte multilayer thin film between SNP and PDADMAC were constructed and their parameters were studied especially the number of layer and concentration of capping agent.

4.3.1 Monolayer adsorption

4.3.1.1 Effect of the concentration of capping agent

In this experiment, silver nanoparticles were prepared using a difference of capping agent (alginate, PSSMA and folic acid). The difference in property and concentration of capping agent were effect to adsorb on the substrate of SNP. The kinetic adsorption of SNP was measured via UV-vis spectrophotometer and shown in figure 4.8-4.10. It was found that SNP-FA could adsorb on the surface more than other. In figure 4, the kinetic adsorption exhibit the absorbance value was more than 0.5 in highest capping agent and the value nearly 1 in lowest capping agent. For SNP-PSSMA was the lowest in efficient to attach on the surface effect to the absorbance value in kinetic adsorption was less than 0.3 in the lowest capping agent. Therefore folic acid promoted the adsorption property of SNP on the substrate more than PSMA and alginate. When analyzed in concentration of capping agent, it was observed that the characterization of adsorption was similar of all capping agent. In high concentration of capping agent of SNP-FA, SNP-PSSMA and SNP-AL were less adsorb than lower concentration of capping agent. Oppositely, in lowest capping agent could form thin film thicker than higher capping agent. For the lowest capping agent contained low negative charge leading to form close packing on the substrate. Because of low repulsive force between particles and competition from excess of capping agent induced particles arrange on the substrate more closely and densely. When compared to high negative charge in high capping agent contained high repulsive force between particles and less particles could adsorb on the substrat[90]. It can be concluded that in the limit of time SNP-FA can be form thin film thicker and denser than other SNP.

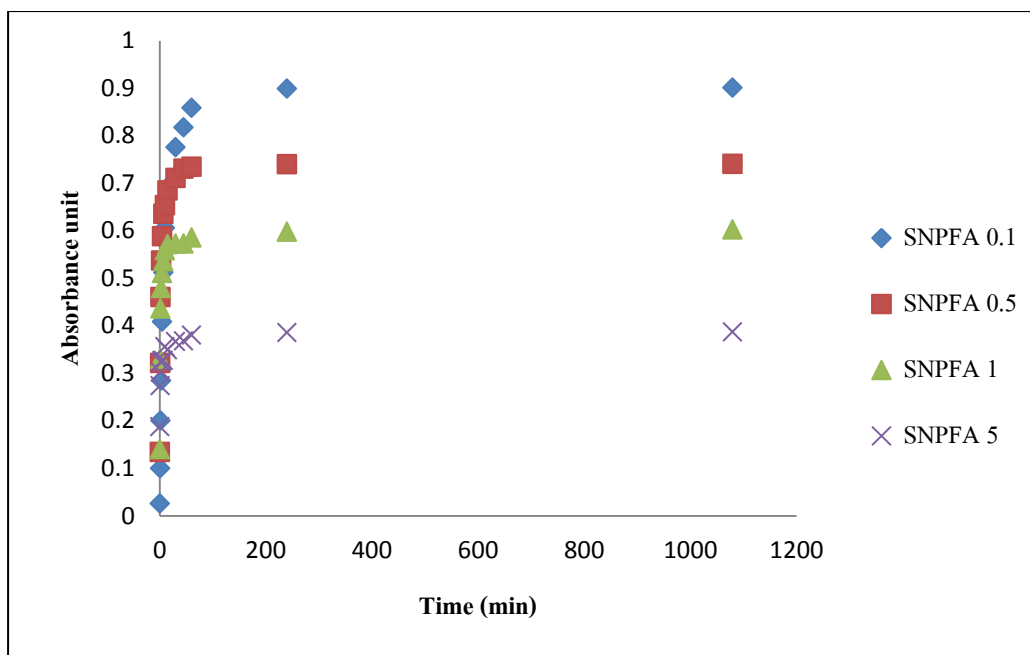


Figure 4.8 The plot of lambda max of plasmon absorbance value as the function of time of SNPFA monolayer adsorption.

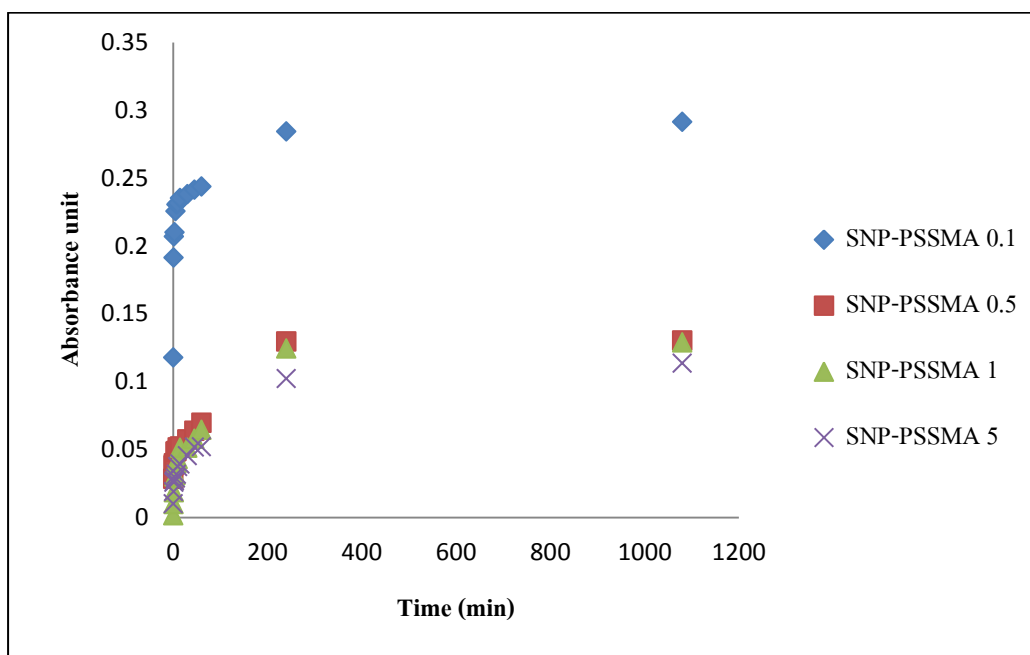


Figure 4.9 The plot of lambda max of plasmon absorbance value as the function of time of SNP-PSSMA monolayer adsorption.

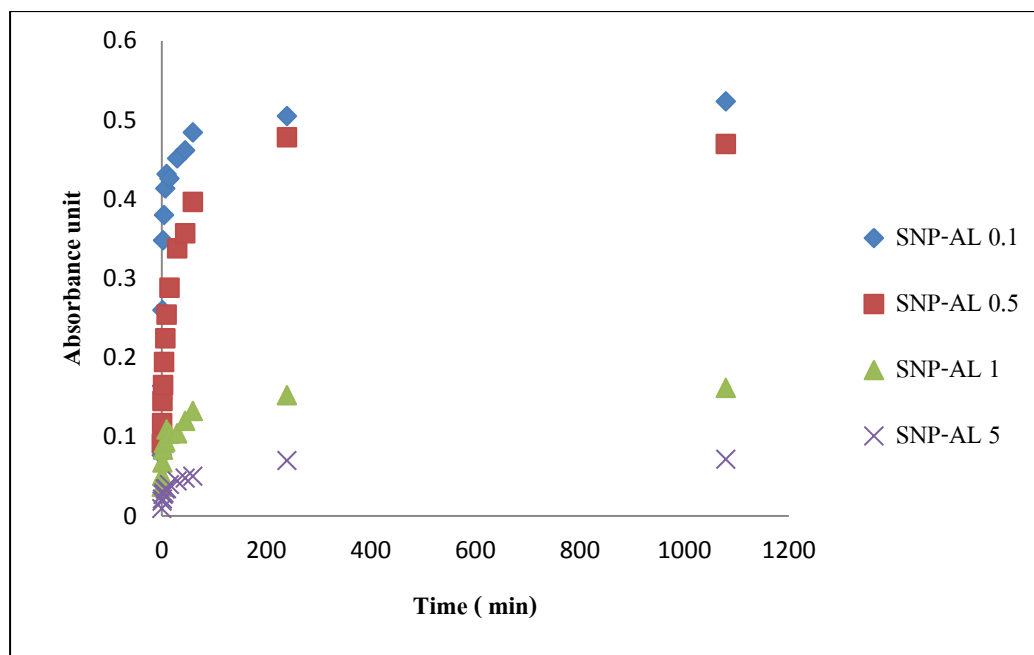


Figure 4.10 The plot of lambda max of plasmon absorbance value as the function of time of SNP-AL monolayer adsorption.

4.3.1.2 Effect of concentration of salt to monolayer adsorption

When adding sodium chloride (NaCl) in the solution, NaCl was ionized into Na^+ and Cl^- . Ion can screen the charges on the surface of the particles which results in an decrease the repulsion which induced the packing of particles. This effect of salt promoted the adsorption of particles due to low repulsive force between particles and close pack of particles. However adding salt more than equilibrium concentration, surface charge was change into zero and positive charge leading to precipitate. After solution precipitate, the particles cannot adsorb on the surface and low efficient to form film.[52, 91]

In this work, salt was used to study in term of ability to adsorption and stability of SNP in all capping agent and concentration. Effect of salt to SNP-FA was shown in figure 4.11 and 4.12. After adding various concentration of salt in SNP-FA 5:1, 1:1 and 0.1:1, these solutions were

coated as monolayer on glass slide and then measured absorbance by UV-vis spectrophotometer as a function of time. It was found that the absorbance value of SNP-FA was highly increased in early time, then It was constant after 60 minutes all conditions. When considered of each concentration of capping agent, the absorbance value of monolayer SNP-FA film decreased after adding salt 1mM. It meant that salt could not improve the adsorption property of SNP-FA in high, medium capping agent especially in low capping agent. Because SNP-FA had low surface charge and low stability, so adding salt induced precipitate of SNP-FA by Na^+ was neutralized negative charge on the surface of SNP-FA which was important repulsive force to made SNP-FA disperse in solution and not aggregation.

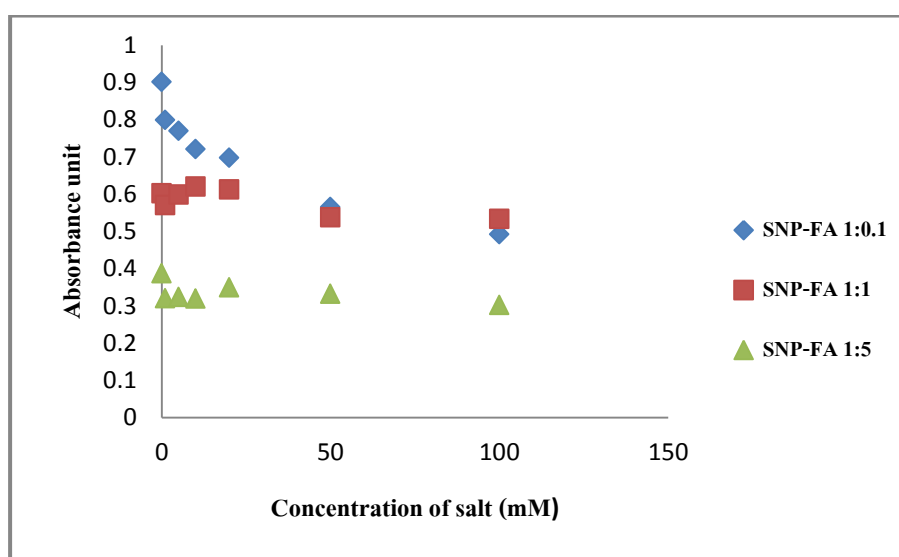


Figure 4.11 The plot of maximum absorbance value of SNP-FA 1:5, SNP-FA 1:1 and SNP-FA 1:0.1 as a function of concentration of salt at 18 hour.

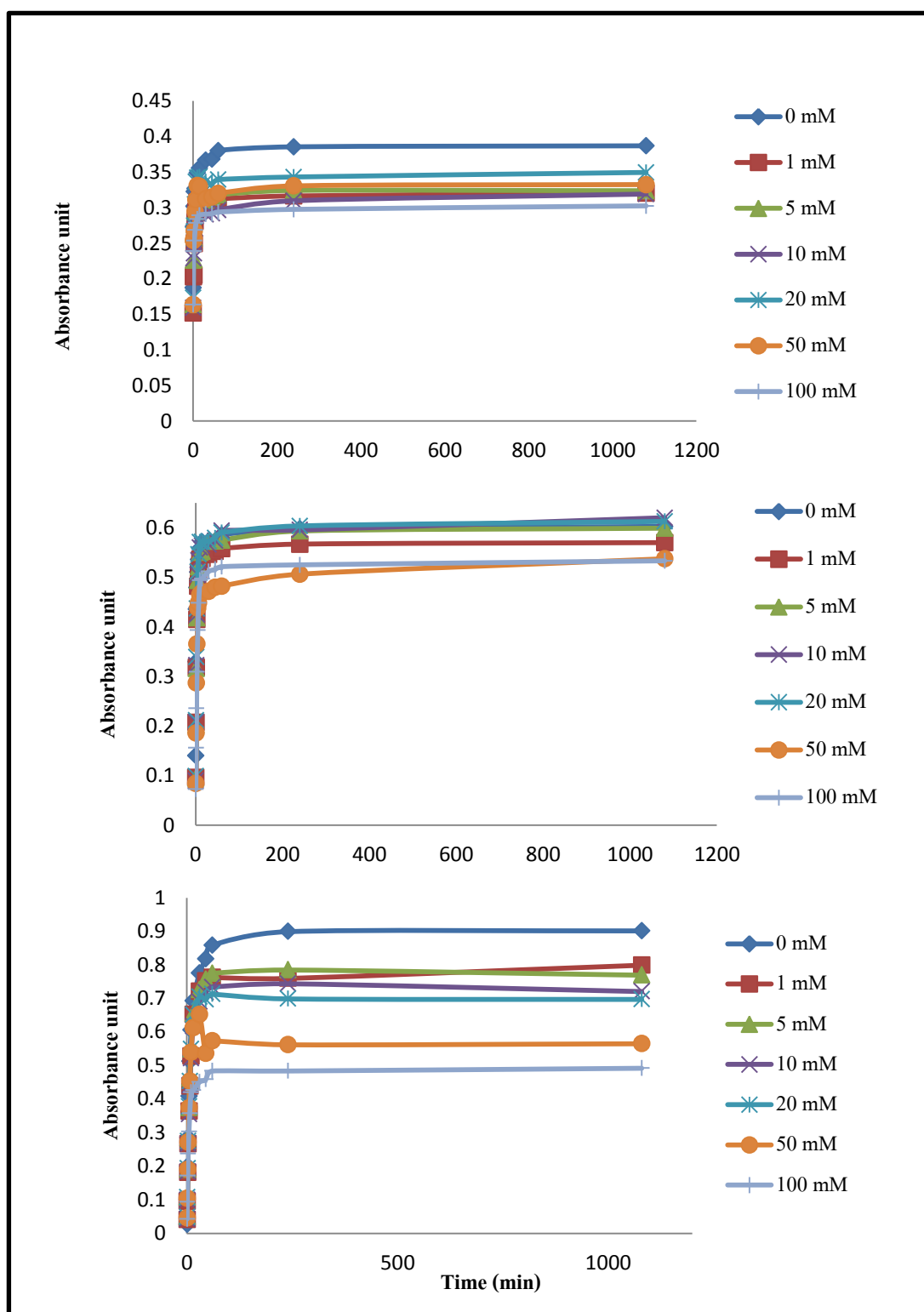


Figure 4.12 The kinetic adsorption of (a) SNP-FA 1:5, (b) SNP-FA 1:1 and (c) SNP-FA 1:0.1 on the substrate when varied concentration of salt from 0 to 100 mM.

For SNP-PSSMA, it was found that adding salt promoted monolayer adsorption of SNP-PSSMA. In the highest capping agent could be added salt more than 1M, it had still increased the absorbance value of film as shown in figure 4.13 and 4.14. The result was the same in medium and low capping agent, the maximum of absorbance value was shown when adding salt 50 mM. However when added salt 100 mM, for medium capping agent shown the absorbance value slightly decrease. This different to low capping agent which the absorbance value was highly decrease after adding salt 100 mM. When compared to no adding salt, SNP-PSSMA 0.1:1 was highly adsorbed and shown brown color in monolayer thin film. This oppositely to SNP-PSSMA 1:1 and SNP-PSSMA 0.1:1 was less adsorbed on the substrate and shown slightly yellow thin film. Therefore SNP-PSSMA which was high stability but low adsorption could be improved adsorption property by adding salt.

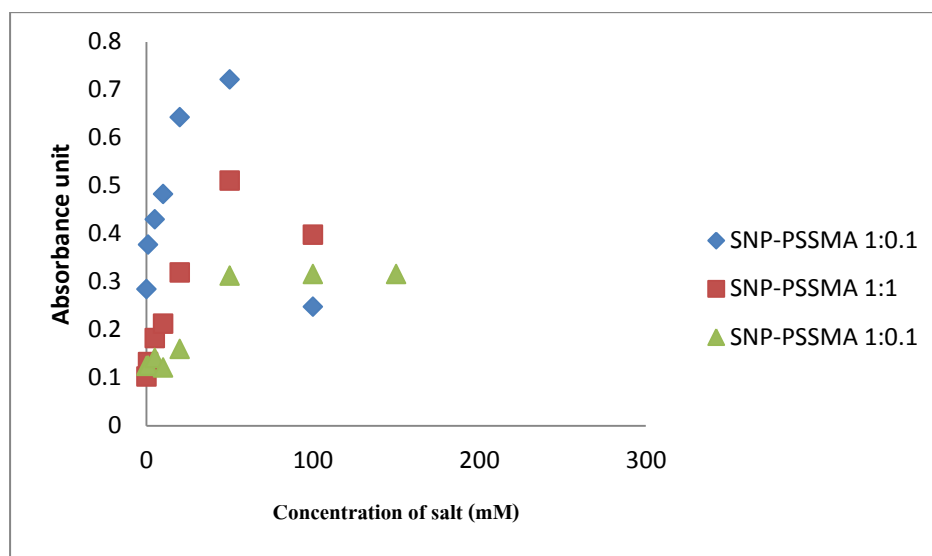


Figure 4.13 The plot of maximum absorbance value of SNP-PSSMA 1:5, SNP-PSSMA 1:1 and SNP-PSSMA 1:0.1 as a function of concentration of salt at 18 hour

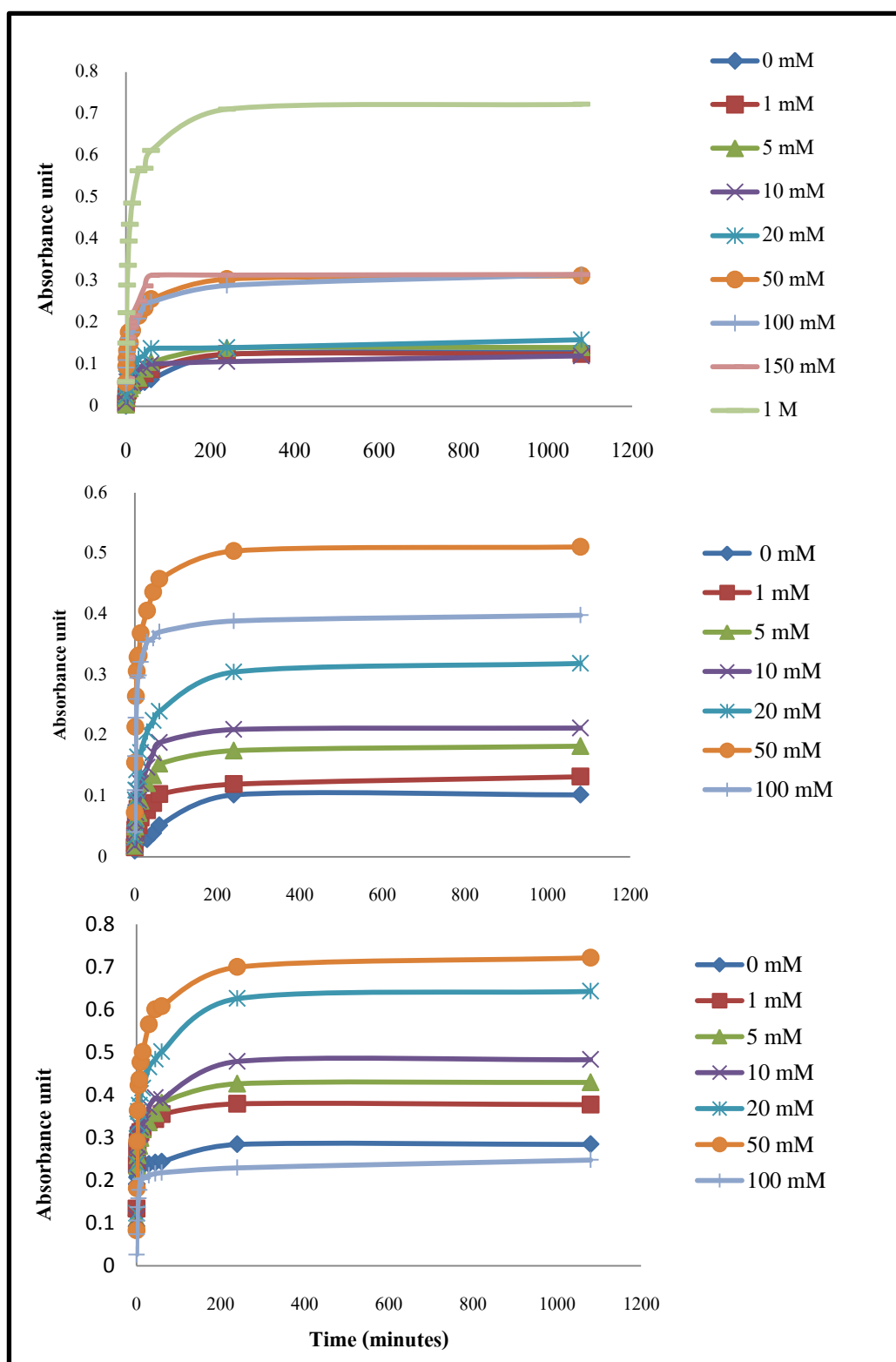


Figure 4.14 The kinetic adsorption of (a) SNP-PSSMA 1:5, (b) SNP-PSSMA 1:1 and (c) SNP-PSSMA 1:0.1 on the substrate when varied concentration of salt from 0 to 100 mM.

In no adding salt condition of SNP-AL, monolayer film was metallic color and high absorbance value in the lowest capping agent. While in medium and high capping agent were yellow color film and low absorbance value. Adding salt used to promote adsorption property of SNP-AL. In figure 4.15 showed the maximum absorbance peak value of SNP when added salt in various concentrations. In high capping agent could added salt until 20mM, after that the absorbance was decrease and solution precipitated. These result was due to high charge surface of high capping agent protect the particles from aggregation when salt neutralized charge surface. For medium capping could added salt until 10 mM and at 20 mM the absorbance was clearly decrease. While low capping agent could be added salt until 5 mM and the absorbance value would slightly decrease in 10 mM of salt. After that it was slightly in monolayer adsorption cause from precipitate of SNP-AL. This was shown that high capping agent was more stability than medium and low capping agent, it could be added more concentraiton of salt for developing in adsorption more than low capping agent. Figure 4.16 showed the kinetic adsorption of SNP-PSSMA when increase concentration of salt

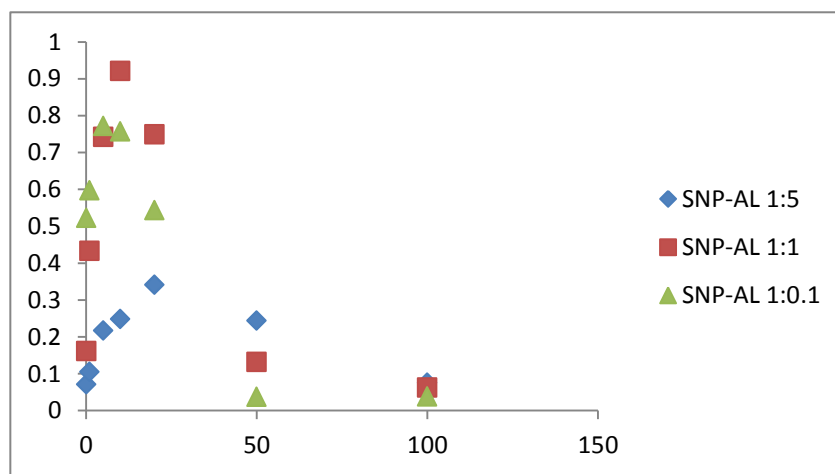


Figure 4.15 The plot of maximum absorbance value of SNP-AL 1:5, SNP-AL 1:1 and SNP-AL 1:0.1 as a function of concentration of salt at 18 hour.

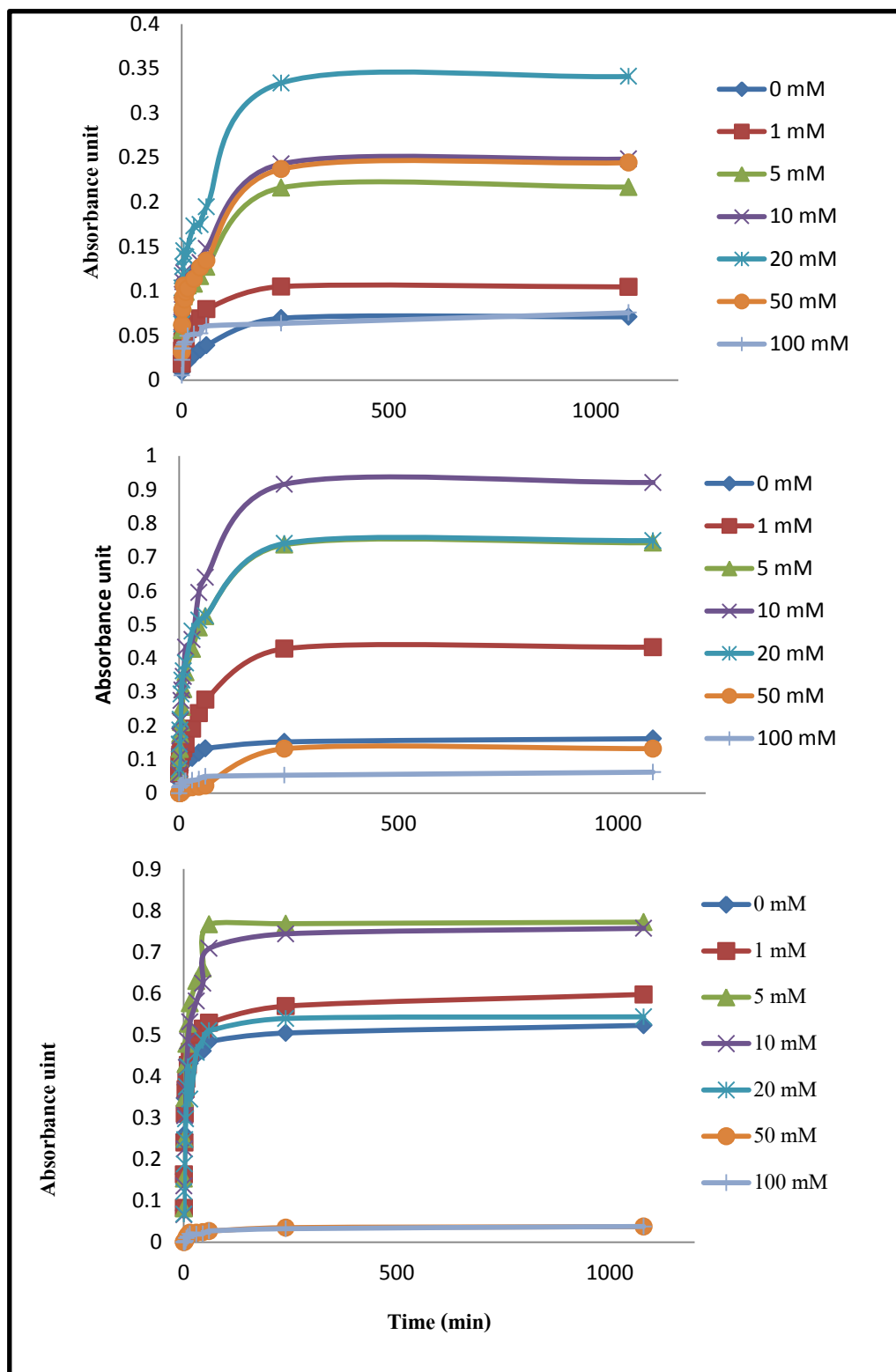


Figure 4.16 The kinetic adsorption of (a) SNP-AL 1:5, (b) SNP-AL 1:1 and (c) SNP-AL 1:0.1 on the substrate when varied concentration of salt from 0 to 100 mM

For the effect of concentration of salt to monolayer adsorption, it was summarized that salt was used to improve the adsorption of SNP-PSSMA and SNP-AL. SNP-PSSMA could be added salt more than SNP-AL, whereas salt could not improve the adsorption of SNP-FA. Therefore SNP-PSSMA was the highest stability and SNP-FA was the lowest stability. Moreover SNP which contained high capping agent was higher stable than low capping agent.

4.3.1.3 Effect of dilution to monolayer adsorption

Cost benefit of chemical agent using in silver nanoparticles preparation process was expensive if it was mentioned for industrial field. So study the adsorption of SNP which was diluted with distilled water 2, 10 and 100 time was necessary to develop SNP using in industry. In this work all SNP were diluted and studied the monolayer adsorption by measuring the plasmon absorbance peak overnight and results were shown in figure 4.17-4.19. It can be observed that dilution 2 time lead to slightly decrease in the absorbance value. But when dilution 10 times was decrease half in absorbance value and could not adsorbed on the substrate when diluted 100 time.

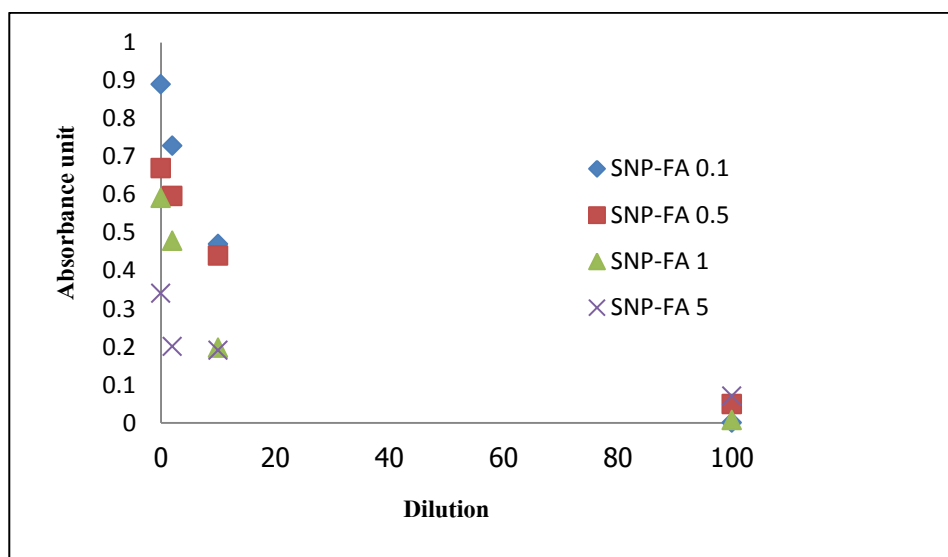


Figure4. 17 The plasmon absorbance of SNP-FA monolayer adsorption when was diluted 2,10 and 100 times.

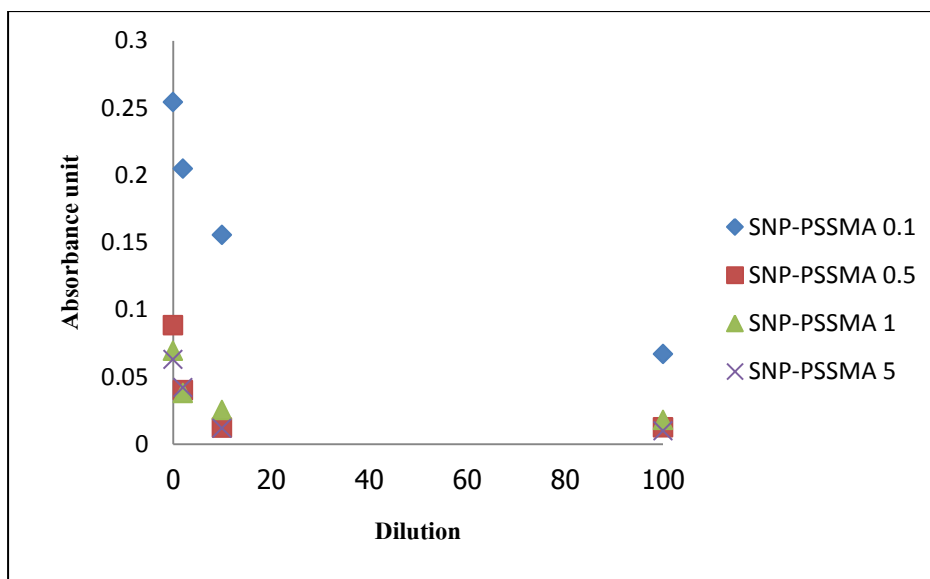


Figure 4.18 The plasmon absorbance of SNP-PSSMA monolayer adsorption when was diluted 2,10 and 100 times.

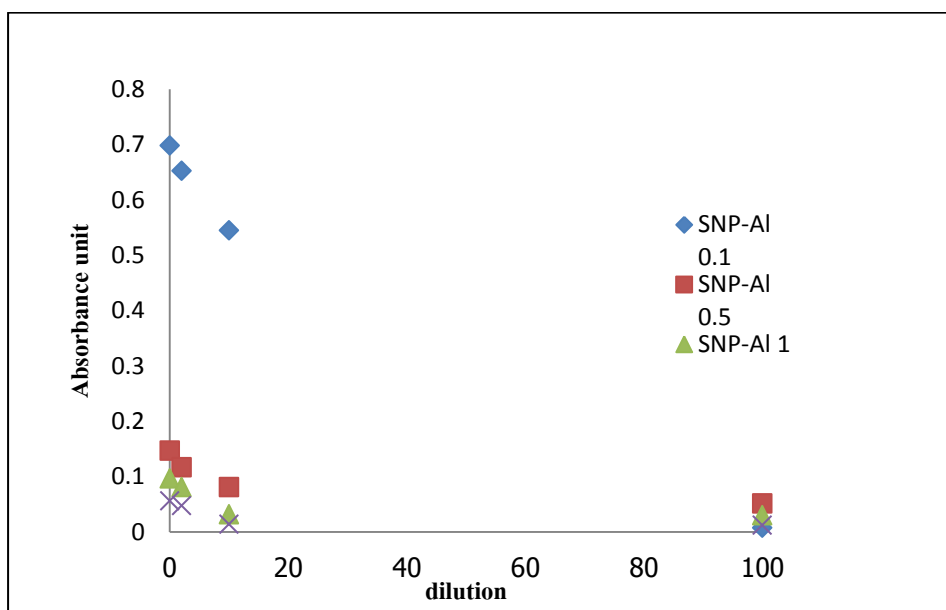


Figure 4.19 The plasmon absorbance of SNP-AL monolayer adsorption when was diluted 2,10 and 100 times.

4.3.2 Polyelectrolytes multilayer thin film (PEM)

4.3.2.1 PEM on glass slide

PDADMAC was used as cationic polyelectrolyte and SNP was used as anionic polyelectrolyte. These PDADMAC and SNP was performed layer-by-layer via PEM technique until 20 layers were formed. In this section studied parameters which influenced to multilayer formation including type, concentration of capping agent and number of layer.

4.3.2.1.1 Effect of type of capping agent

In figure 4.20 showed the effect of type of capping agent to multilayer thin film formation. All conditions of SNP-FA could be formed thin film thicker than SNP-AL and SNP-PSSMA when analyzed in the absorbance peak. According to SNP-AL was formed thin film thicker than SNP-PSSMA except 0.1 mM of AL which thinner than 0.1 mM of PSSMA. Only 0.1 mM of SNP-PSSMA could performed a thicker thin film but in other concentration was exactly performed thin film. It could be observed that high capping of SNP-FA was not found the competition effect from excess of capping agent. it was due to FA was a small molecule. When stick on the PDADMAC layer, it could be pull out from layer by PDADMAC which was strong polyelectrolytes and mix with the PDADMAC solution. From this reason, their absorbance was not different when increase the concentration of FA. When compare to SNP-AL and SNP-PSSMA, there are different in absorbance when increase the concentration of capping due to the competition effect from excess. AL and PSSMA was the polymer which contained high molecular weight, So they was strong and PDADMAC could not pull them from the layer. Therefore they still large impact in competition effect.

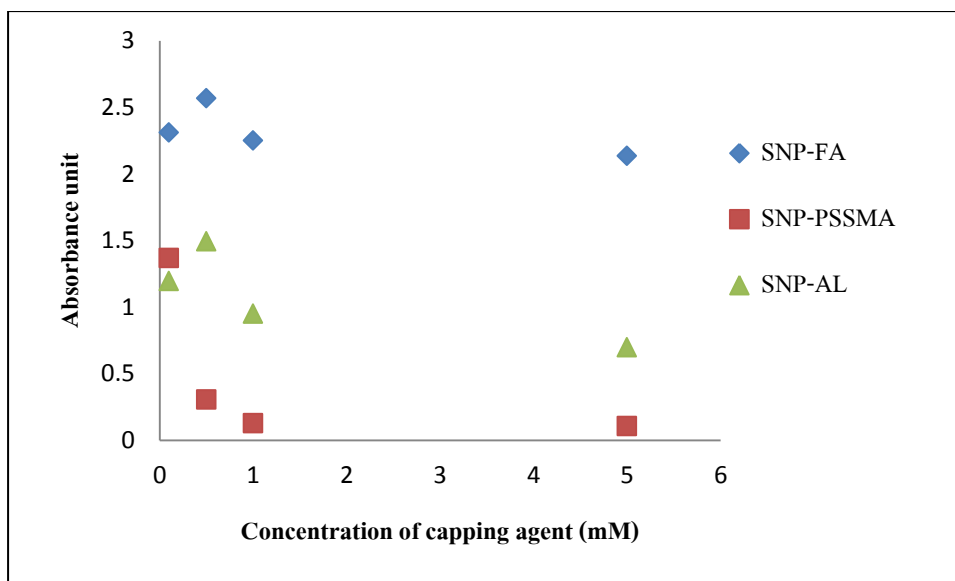


Figure 4.20 The plasmon absorbance peak of SNP/PDADMAC multilayer thin film at 20 layers. Each of SNP was varied the concentration of capping agent (0.1, 0.5, 1 and 5 mM).

4.3.2.1.2 Effect of number of layer

When considering the thickness as a function of the number of layer, increasing the number of layer, the thickness is increase which correspond to the experiment of Stephan T. et al [55] show formation of polyelectrolyte multilayer thin film with PSS/PDADMAC. They found that when increased the number of these polyelectrolytes leading to increase in the absorbance value measure by UV-vis spectroscopy. In this work, polyelectrolytes multilayer technique could construct the thin film on a various substrates. Both anionic and cationic polyelectrolytes were self-assembled layer by layer on the substrate until the desired number of layer was formed. Herein, PDADMAC used as cationic polyelectrolytes was built sequentially with anionic silver nanoparticles. Layer-by-layer thin film was continued until 20 layers and measured the absorbance value every 4 layers. As expected, the absorbance of film was high value due to the number of layer increased when characterized with UV-Vis spectroscopy. A plot of the UV-Vis absorbance values at lambda max when increasing number of layers is shown in figure 4.21-4.23. For SNP-FA, we found that the absorbance value was highly performed at 0.5 mM of folic acid.

This was due to the low negative charge and less in excess of folic acid. When nanoparticles contact to one another, the localized surface plasmon resonance is decrease due to coupling occurs between nanoparticles. So the typical yellow absorbance of the nanoparticles is replaced by a shiny metallic[92]. Oppositely higher folic concentration contained high surface charge and excess of folic acid would less adsorb on the substrate due to high repulsive interaction between particles. So it can be observed that the film display metallic all conditions except the highest capping agent which was dark brown color which was exhibited in figure 4.20.

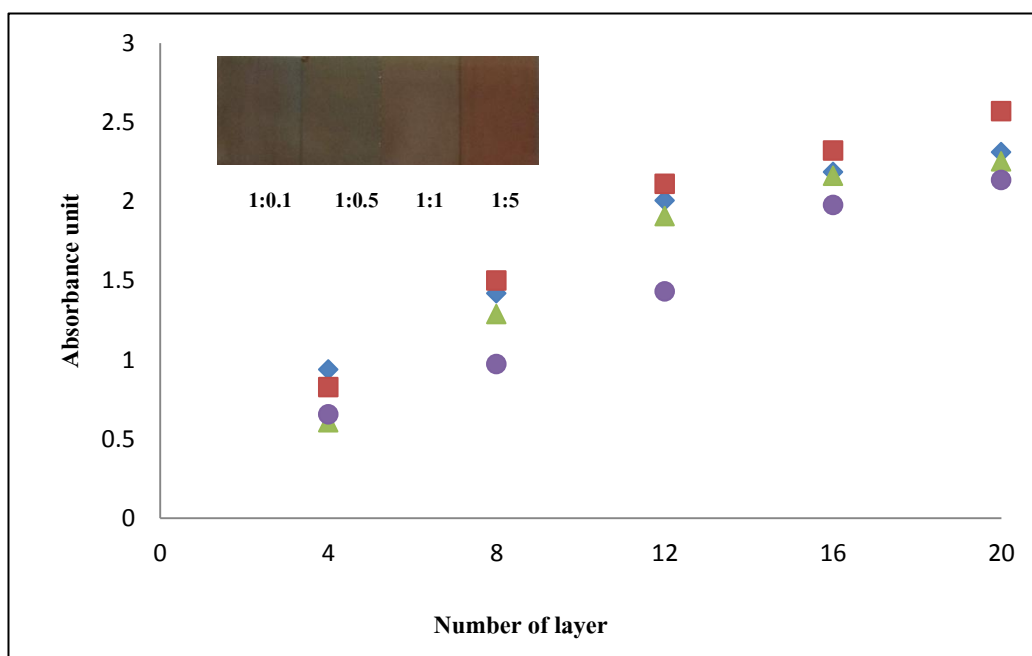


Figure 4.21 UV-Vis absorbance values of PDADMAC and SNP-FA multilayer thin film on glass slides as a function of the number of layers of silver nanoparticles deposited. The nanoparticles were prepared with various concentrations of sodium alginate (0.1 mM= ◆, 0.5 mM= ■, 1 mM= ▲, 5 mM= ●) and the different color of PDAD-MAC/SNP-FA film at 20 layers.

Polyelectrolytes multilayer thin film was formed between PDADMAC used as cationic polyelectrolyte and SNP used as anionic polyelectrolytes.. For layer-by-layer of

PDADMAC/SNP-FA (all concentrations), the plasmon absorbance band at maximum value every 4 layers deposition was analyzed as shown in figure 4.24. It was found that the absorbance value was increase when increasing the number of layer. For PDADMAC/SNP-PSSMA and PDADMAC/SNP-AL multilayer were as previous result, the lambda max of Plasmon absorbance value was increased when increasing the number of layer. In PDADMAC/SNP-PSSMA had different clearly between high and low capping agent. Low capping agent was performed in closed packing of particles due to low surface charge and excess. The optical property of film in this condition was shown in strong brown color with the highest absorbance at 20 layers.

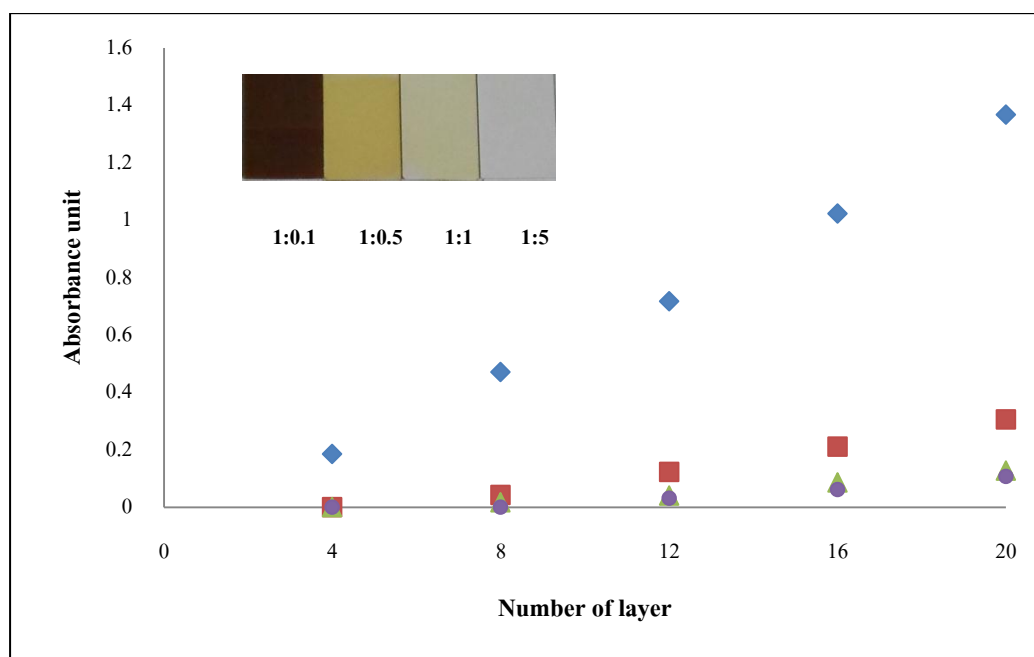


Figure 4.22 UV-Vis absorbance values of PDADMAC and SNP-PSSMA multilayer thin film on glass slides as a function of the number of layers of silver nanoparticles deposited. The nanoparticles were prepared with various concentrations of sodium alginate (0.1 mM= ◆, 0.5 mM= ■, 1 mM= ▲, 5 mM= ●) and the different color of PDAD-MAC/SNP-PSSMA film at 20 layers.

Different to higher capping agent which was form with high surface charge and excess was self-assemble on the substrate with a sparse packing of particles. Because of high repulsive interaction between particles was result to form a thinner film. Therefor in 0.5, 1 and 5 mM of PSSMA was performed slightly yellowish film with a low absorbance value as shown in figure 4.22.

In PDADMAC/SNP-AL, the pattern of this multilayer thin film is similar to PDADMAC/ SNP-FA. The lambda max of absorbance value of 0.5 mM of alginate was the highest at 20 layers as a result of low surface charge and excess of alginate. Although the pattern was similar but the Plasmon absorbance value between high and low capping was clearly difference. The absorbance value of low capping agent was too low when compared to low capping agent of SNP-FA. The performance of multilayer thin film of SNP-AL was shown in figure 4.23. In close packing form of low alginate was shown in shiny and metallic film which was difference to high alginate with a slightly yellowish film.

It can be concluded that difference in type of capping agent would perform in a various color and pattern of particles packing. Otherwise increasing the number of layer leading to increase the absorbance value was the same.

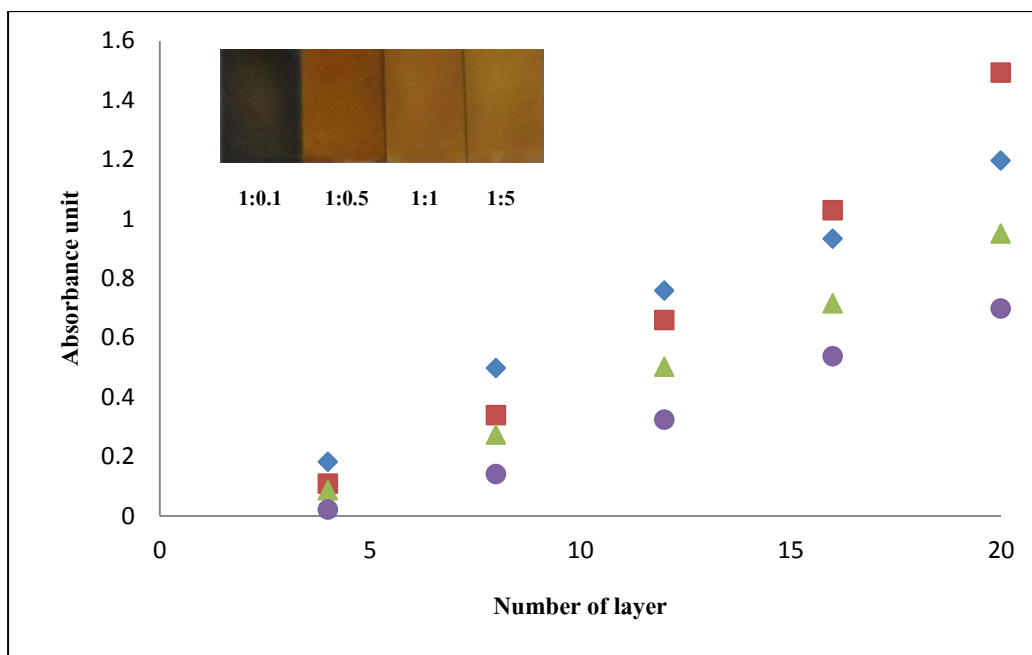


Figure 4.23 UV-Vis absorbance values of PDADMAC and SNP-AL multilayer thin film on glass slides as a function of the number of layers of silver nanoparticles deposited. The nanoparticles were prepared with various concentrations of sodium alginate (0.1 mM= ◆, 0.5 mM=■, 1 mM=▲, 5 mM=●) and the different color of PDAD-MAC/SNP-FAfilm at 20 layers.

4.3.2.2 PEM on suture material

PDADMAC which posses a positive charge and the SNP having negative charge polyelectrolyte could form layer-by-layer via polyelectrolyte multilayer method (PEM). The polyelectrolyte multilayer thin film can be formed on various substrates including silicon wafer, glass slide, metal and fiber [38, 93]. Beside studied polyelectrolyte multilayer thin film on glass slide, in this work The commonly thin film were polyamide suture material. Suture are material used to closed the wound and promote wound healing can be modified to decrease t inflammation and delivering drug to the wound area by PEM. Here, PDADMAC/SNP films were formed using the layer-by-layer method on suture material, and the parameter that influenced film formation was studied.



Figure 4.24 PEM of PDADMAC and SNP coated on polyamide suture material. (a) PDADMAC/SNP-FA 20 layers, (b) PDADMAC/SNP-PSSMA 20 layers and (c) PDADMAC/SNP-AL 20 layers.

4.3.2.2.1 Effect of type and concentration of capping agent

PDADMAC/SNP built on the suture material displayed various strikingly different color of film as shown in figure 4.24. The results on the fiber are similar to the PEM on glass slide. PDADMAC/SNPFA films appear shiny and metallic for all concentration of capping agent except in 5 mM of folic acid which displayed brown color film. In PDADMAC/SNP-PSSMA was had a dark brown color film in 0.1 mM. Different to higher capping agent was performed in slightly yellowish color. In PDADMAC/SNP-AL showed metallic film in 0.1 mM and yellowish

film in higher capping agent. Then these PEM films were analyzed by scanning electron microscopy(SEM).

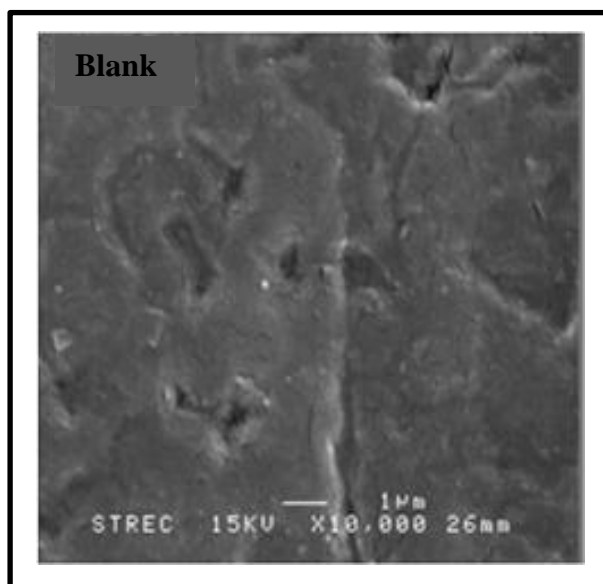


Figure 4.25 SEM image of polyamide suture material with no SNP coated on the surface

For PDADMAC/SNP-FA, it was found that the particles could be clearly observed. SNP was close packed in low capping agent and less packed in high capping agent as shown in figure 4.26. This confirms the result from the PDADMC /SNP-FA on glass slide which the film was close packed particles in low capping agent due to low surface charge and was also less packed due to high surface charge and excess of folic acid. For high capping agent when compared to PDADMAC/SNP-PSSMA (figure 4.27), it can be observed that the surface formed a smooth film better than PDADMAC/SNP-FA. The film was close packed and dense in 0.1 mM of PSSMA and thin and very smooth in high capping agent. PDADMAC/SNP-PSSMA film could not observe the particles clearly and in high capping agent had still observed the morphology of polyamide surface of suture material which was shown in figure 4.25. The surface of polyamide suture material was some loops and pores, moreover could not see the particles on the surface.

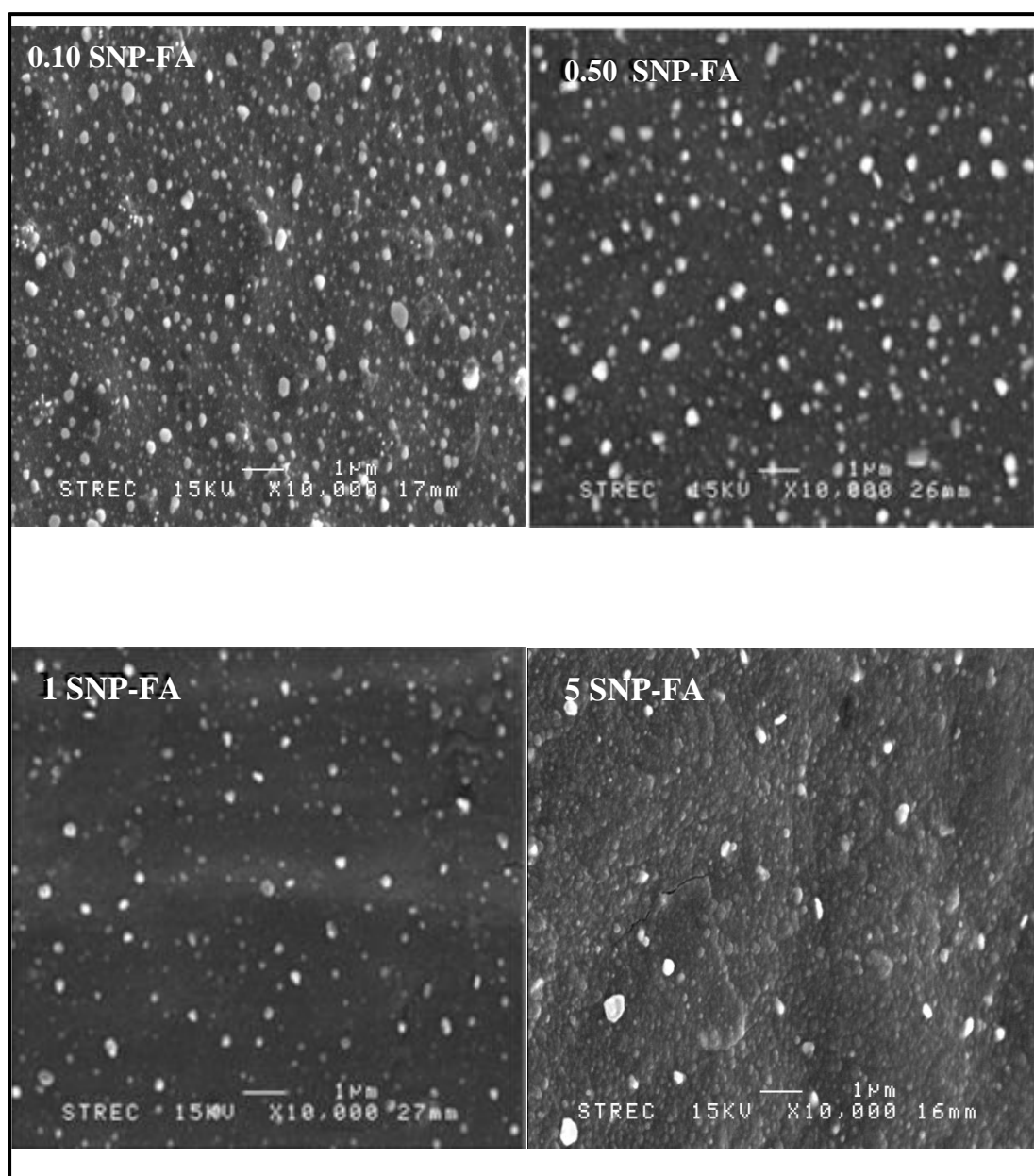


Figure 4.26 SEM image of PDADMAC/SNP-FA was coated layer-by-layer on suture material with a various concentration of folic acid (0.1, 0.5, 1 and 5mM)

For PDADMAC/AL multilayer thin film, SEM image was similar to PDADMAC/SNP-PSSMA, however in 1mM of alginate was more dense and close packed than PDADMAC/SNP-PSSMA. In higher capping agent was smooth and less packed as PDADMAC/SNP-PSSMA which was exhibited in figure 4.28.

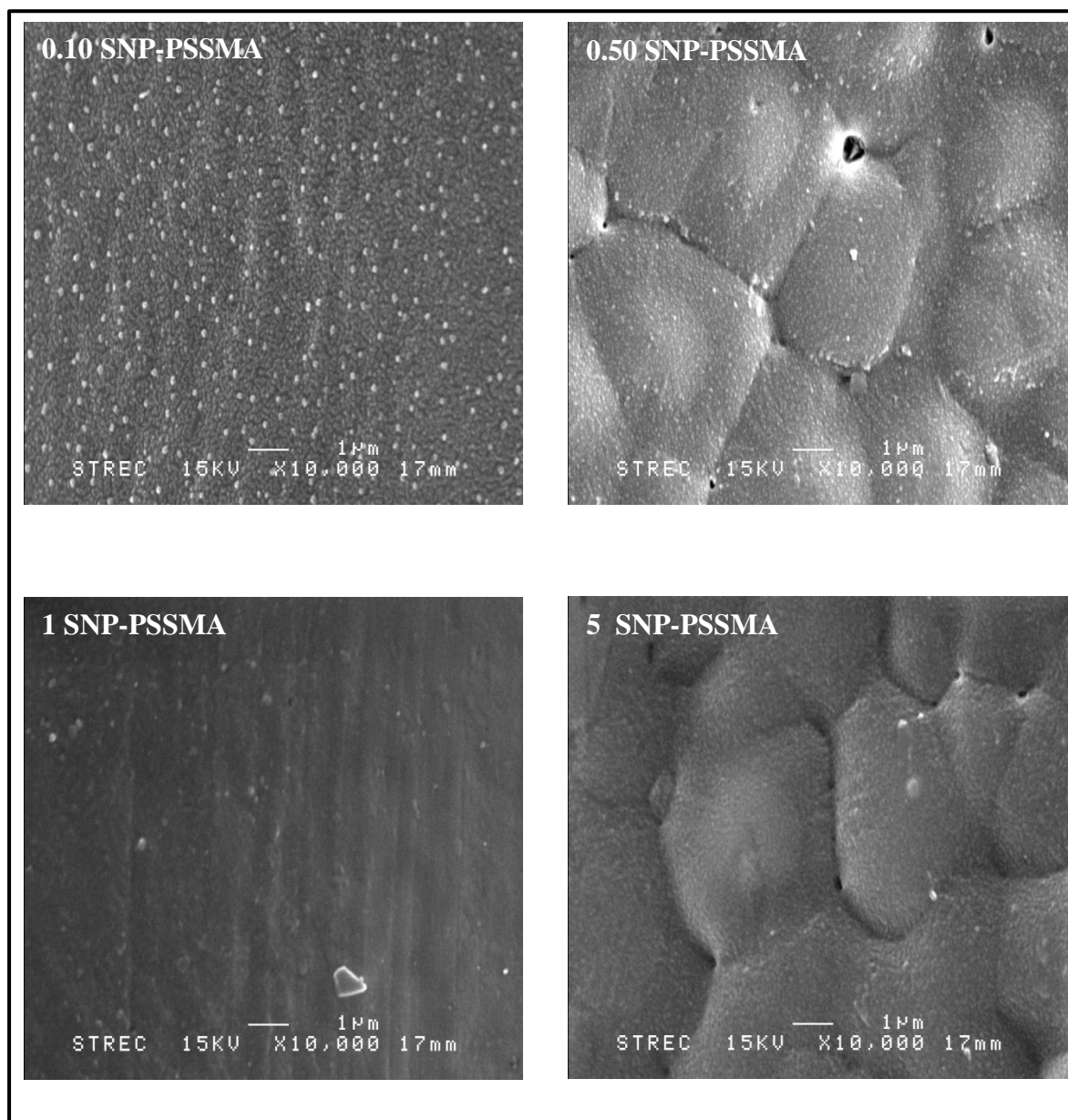


Figure 4.27 SEM image of PDADMAC/SNP-PSSMA was coated layer-by-layer on suture material with a various concentration of folic acid (0.1, 0.5, 1 and 5mM)

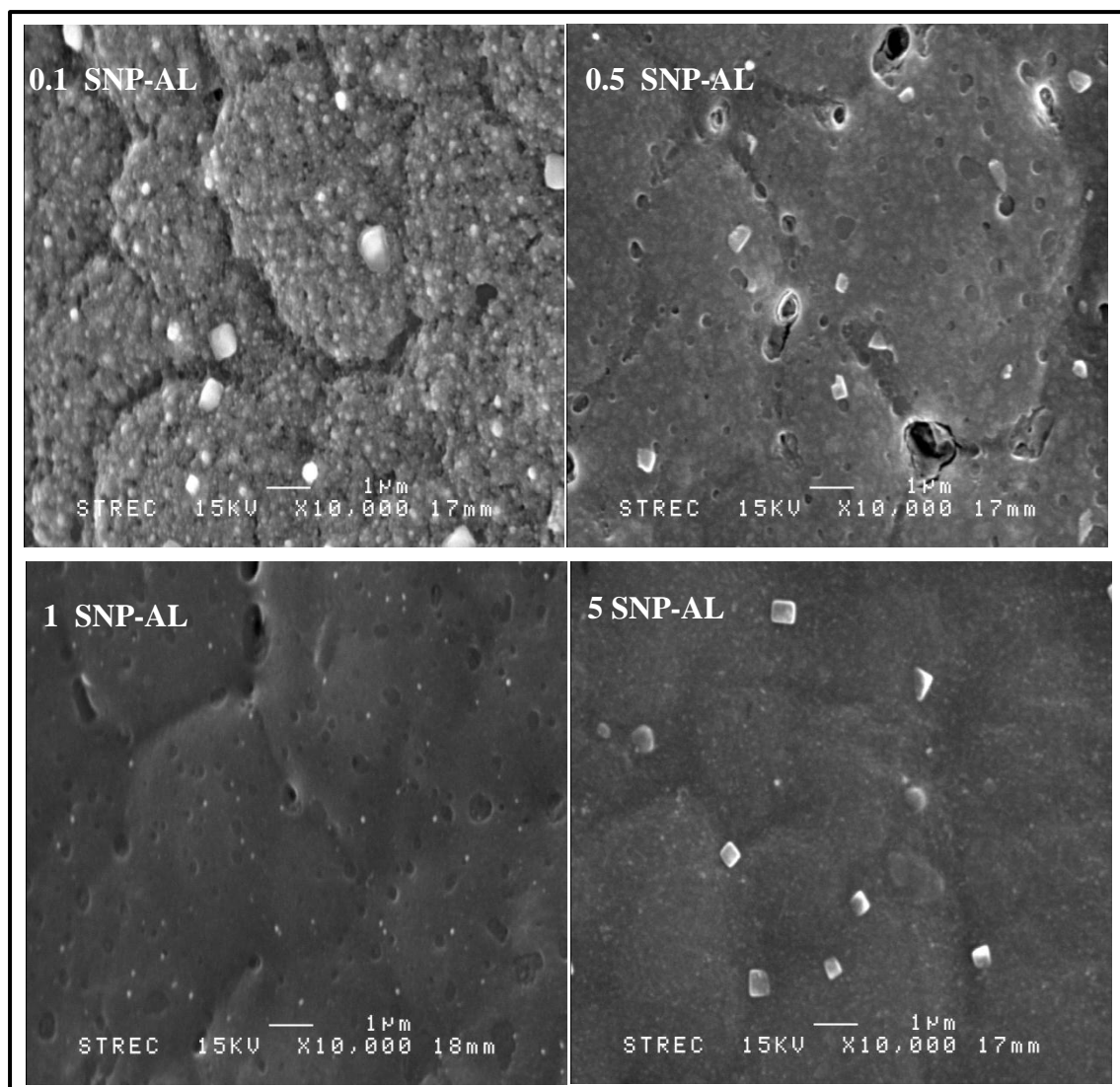


Figure4. 28 SEM image of PDADMAC/SNP-AL was coated layer-by-layer on suture material with a various concentration of folic acid (0.1, 0.5, 1 and 5mM)

It can be summarized that the multilayer thin film between PDADMAC and SNP could be performed by PEM method on surgical suture. A different in type of capping agent was shown in a various pattern of these film. SNP-FA made the film denser and close packed than other SNP, oppositely SNP-PSSMA made the film smoother. Moreover the concentration of capping agent also effect to morphology of thin film. In low capping agent was performed densely and close packed different to high capping agent that was smoother.

4.3.2.2.2 Effect of high temperature to PEM on suture material (at 121 °C)

In this section, the stability of PDADMAC and SNP film on suture material to high temperature (121°C) was studied. It was due to before closing the wound, suture material have to sterile and usually use autoclave at 121°C. Therefore the effect of temperature (121 °C) to PDADMAC/SNP film on suture material was mentioned. When suture material was sterile by autoclave 121°C, the SEM image of them was different to non-autoclave suture material.

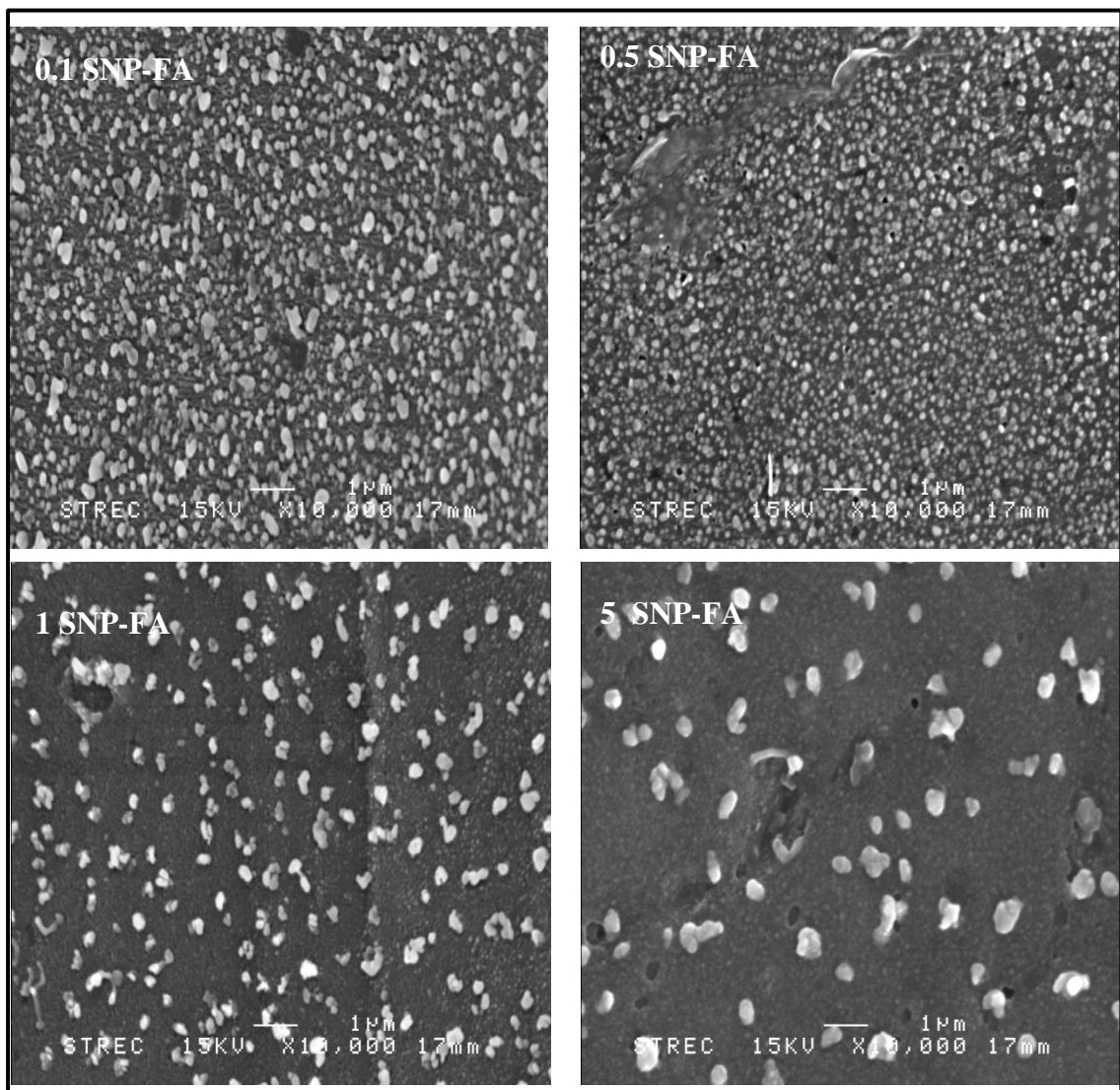


Figure 4.29 SEM image of PDADMAC/SNP-FA film with a various concentration of capping agent was coated on suture material followed by autoclave at 121 °C

For PDADMAC/SNP-FA image by SEM, all condition had still observed particles which different to SNP-AL and SNP-PSSMA. In low capping agent particles was denser and smaller than high capping agent. The SEM image of SNP-FA film after autoclave was shown in figure 4.29.

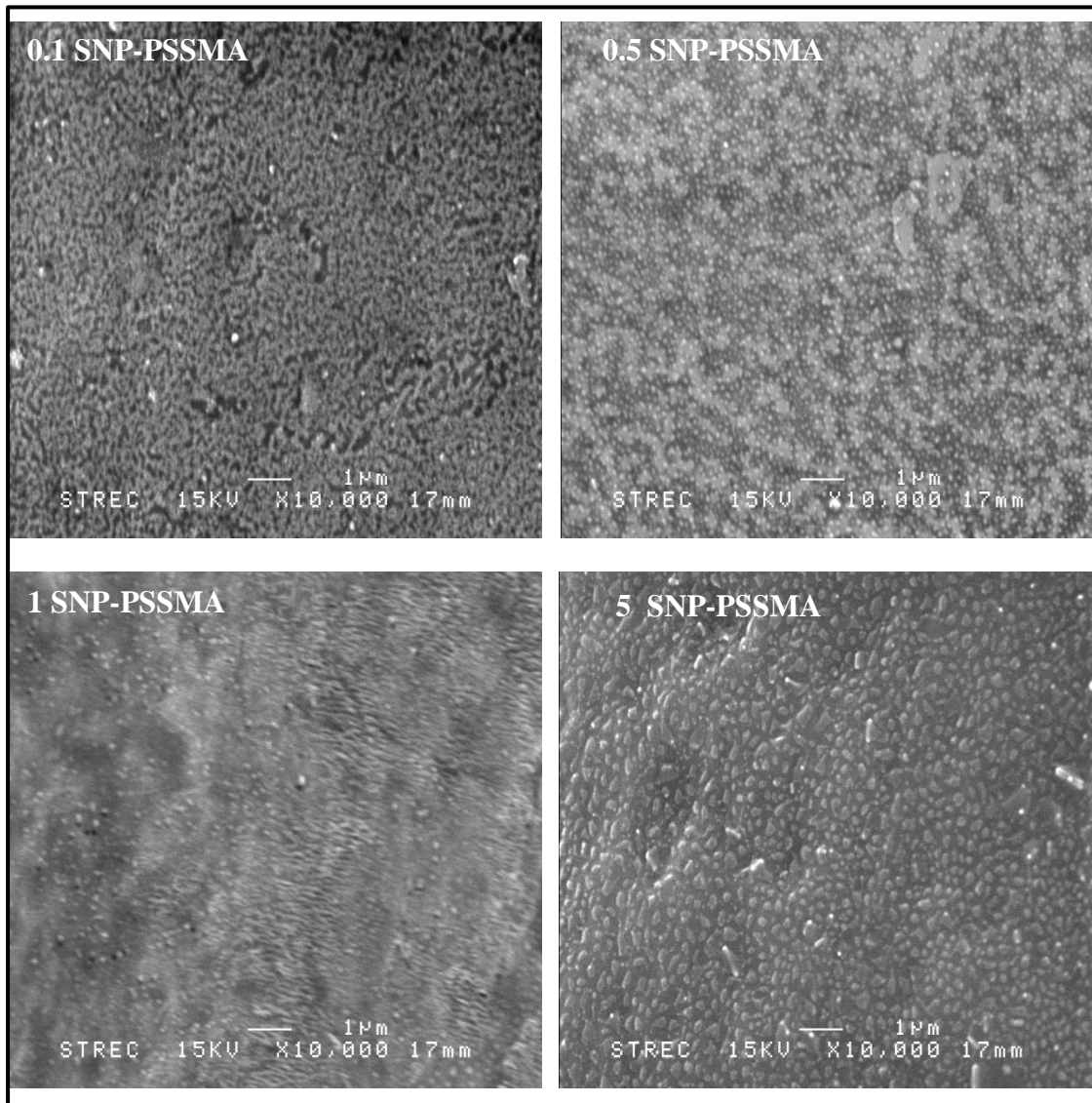


Figure 4.30 SEM image of PDADMAC/SNP-PSSMA film with a various concentration of capping agent was coated on suture material follow by autoclave at 121 °C

For PDADMAC/SNP-PSSMA image by SEM which could observed in figure 4.30 was found that all condition could not found the particles on surface. We could observe only the

aggregated film or the island film spread on the surface. This was exactly different surface from non- autoclave suture.

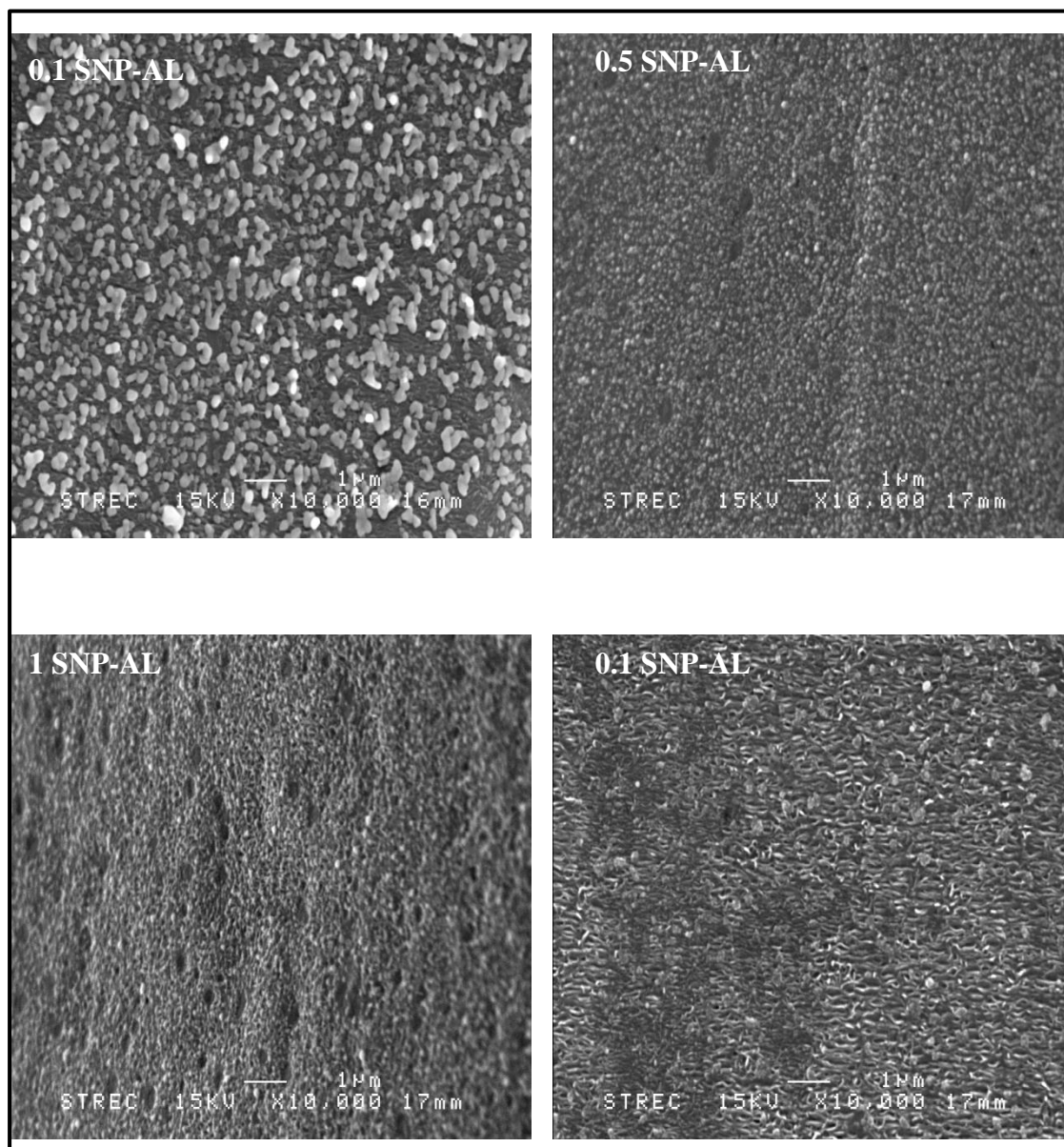


Figure 4.31 SEM image of PDADMAC/SNP-AL film with a various concentration of capping agent was coated on suture material followed by autoclave at 121 °C

In PDADMAC/SNP-AL image by SEM in figure 4.31 was found that only 0.1 mM of alginate had still observed the particles clearly. However particles were bigger and more

aggregated than non- autoclave suture. For other concentration of capping agent could not be noticed particles and could observed the cracked line and shrink of film.

When analyzed only physical surface, It could be assumed that SNP-FA film was tolerant to high temperature more than other SNP. So it was suggested that PDADMAC/SNP-FA coated on suture material could be sterile by autoclave. But for PDADMAC/SNP-AL and PSSMA should sterile by different technique such as alcohol.

4.4 Silver ion leaching from PEM

Normally, silver ion could anticancer and antibacterial. When PADAMAC/SNP film were dipped in to solution, silver ion was released into this solution. The effect of concentration of capping agent, time and pH value had influence to concentration of silver ion leaching to this solution. In this part, the concentration of silver ion leaching from PDADMAC/SNP film was investigated via 3 methods including UV-vis spectrophotometer, AFM and AAS. PDADMAC/SNP film coated on glass slide would be analyzed in film desorption by UV-vis spectrophotometer and measure their thickness via AFM. For PDADMAC/SNP film coated on suture material would be investigated the concentration of silver ion leaching by AAS.

4.4.1. Silver ion leaching from PEM coated on glass slide

PEM between PDADMAC/SNP film which was formed on glass slide 20 layers was studied the silver ion leaching from thin film in acetic-acetate buffer(pH 5.5) and phosphate buffer (pH 7.4) by UV-vis spectroscopy. The plasmon absorbance value of the film was recorded after dipping the thin films in the buffer solutions at 1, 3, 7, 14, 21 and 28 days. In this work, the ability of capping agent to protect SNP from buffer solution was studied. The different in capping agent would different effect in pattern of SNP leaching from thin film also. Moreover, the pattern of SNP leaching from thin film would different between pH 5.5 and pH 7.4 solutions because the the capping agent could change in charge when change pH value. Normally, in high pH value it

have more negative charge than low pH. For the effect of concentration of capping agent, the absorbance value of PDADMAC/SNP-FA 0.1 mM film was the lowest value. When increased the concentration of capping agent, the absorbance value of film was increased except 1mM of SNP-FA which shown the highest absorbance value. Figure 4.32 was shown the absorbance of film when dipped in buffer solution pH 5.5 and pH 7.4 as a function of time. The percent of degradable of film was calculated by using this equation;

$$\% \text{ of film degradable} = A-B/A*100$$

A = the absorbance value of PDADMAC/SNP 20 layers

B = the absorbance value of PDADMAC/SNP when dipped in buffer solution 28 days

After calculated percent of film degradable, it was found that 0.1 mM of SNP-FA film was higher degradable than higher capping agent. But the lowest degradable was 1 mM of SNP-FA. This result was similar in pH 5.5 and pH 7.4 as show in table 4.2. Percent of film degradable of SNP-FA was correspond to the absorbance value of film when dipped in buffer solution. When considered in effect of pH dependence, SNP-FA multilayer thin films all concentration of folic acid were degradable in pH 5.5 more than pH 7.4 [94]except 0.1mM. of SNP-FA that was degradable in pH 5.5 less than pH 7.4 about 3.35 %. This result was due to the functional group of folic acid contained COOH group. The pKa of folic acid was 4.65, 6.75 and 9. In this work used pH 5.5 and 7.4, it meant that SNP-FA in pH 5.5 was low negative charge than pH 7.4. So electrostatic force between PDADMAC and SNP-FA was decreased in pH 5.5 and promoted the degradable of film.

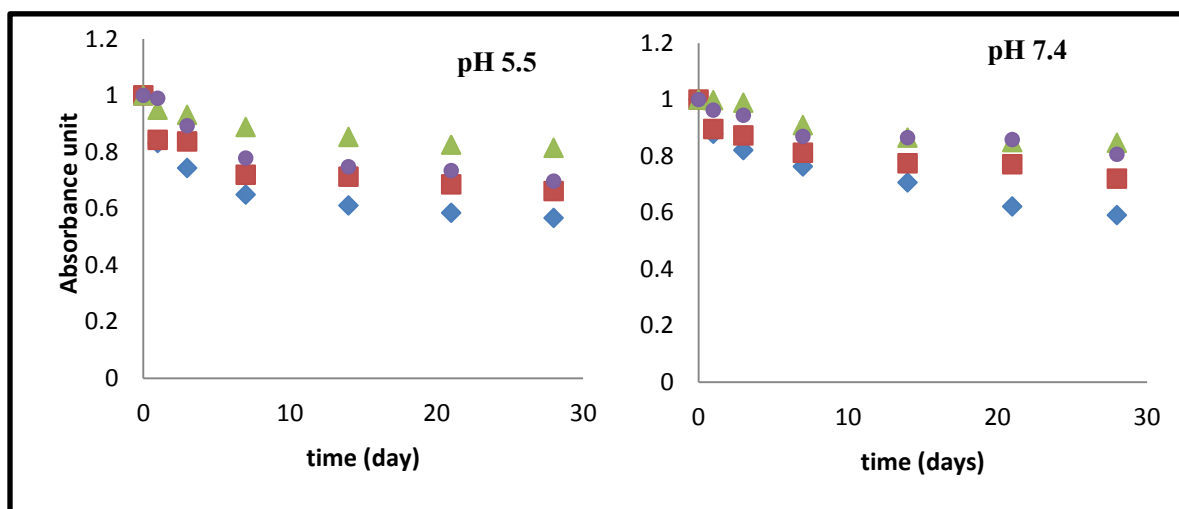


Figure 4.32 the plot of the absorbance value of PDADMAC/SNP-FA as a function of time when dipped in buffer solution pH 5.5 and 7.4(0.1 mM= ◆, 0.5 mM= ■, 1 mM= ▲, 5 mM= ●)

When dipped PDADMAC/SNP-PSSMA film in buffer solution and measured the absorbance peak until 28 days, it was found that 0.1 SNP-PSSMA illustrated the highest absorbance value and trend of curve was nearly constant. While higher capping agent presented the lower absorbance value and curve was higher slope than the lowest capping agent as displayed in figure 4.33. this results was correspond to percent of film degradable in table 4.2, percent of degradable of 0.1 mM of PSSMA was the lowest. It was increased when concentration of PSSMA was increased by the highest percent of degradable was 1 mM of PSSMA. Considering in effect of pH dependence, SNP-PSSMA film was degradable in pH 5.5 more than pH 7.4. It was indicated that buffer solution pH 5.5 had more effect to PSSMA. pKa of PSSMA was 2.9 and 8.8 [14]. It meant that PSSMA in high pH was deprotonated solution, opposite that in lower pH it became protonated. So dipping SNP-PSSMA in pH5.5 should degradable more than pH 7.4 because it change into more positive charge and could not stabilized SNP. However 0.1 mM of PSSMA which dipped in pH 5.5 had still decreased in absorbance value more than in pH 7.4. This result was also similar to PDADMAC/SNP-FA film.

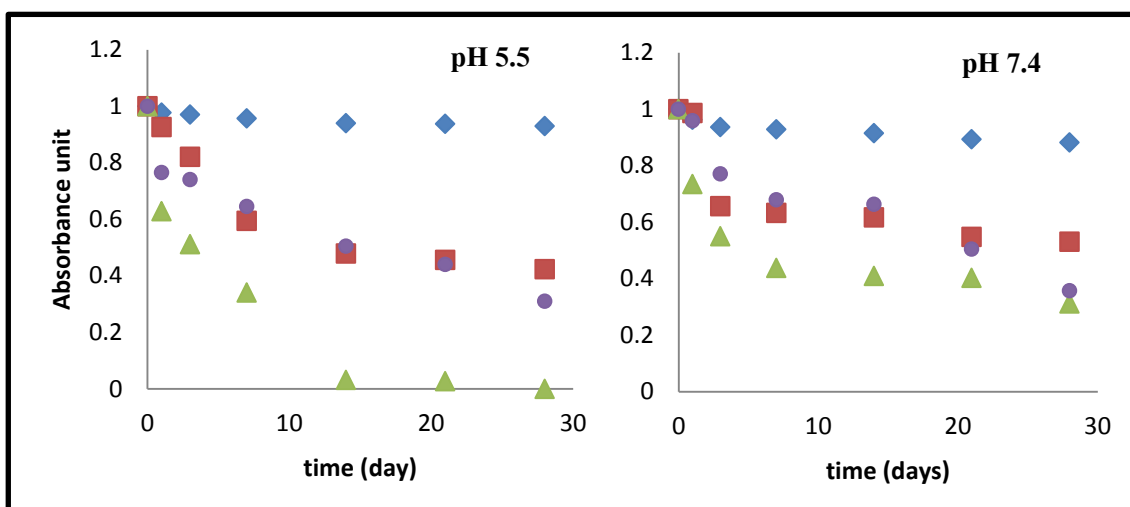


Figure 4.33 the plot of the absorbance value of PDADMAC/SNP-PSSMA as a function of time when dipped in buffer solution pH 5.5 and 7.4 (0.1 mM= ◆, 0.5 mM= ■, 1 mM= ▲, 5 mM= ●)

PDADMAC/SNP-AL films were studied effect of concentration of capping agent to degradable of film when dipped in buffer solution and effect of pH dependence. In concentration of capping agent dependence, the absorbance value was analyzed every 1, 3, 7, 14, 21, and 28 days. The results was exhibited that 0.5 mM of SNP-AL shown the lowest in absorbance value, then in higher capping agent presented higher absorbance value both in pH 5.5 and 7.4. for 0.1 mM of SNP-AL presented the highest absorbance value in pH 5.5 and almost highest in pH 7.4. it was confirmed that in 0.1 mM of SNP all capping agent displayed the highest absorbance which was stable film in both pH condition as shown in figure 4.33. This result was according to percent of film degradable, the highest percent of film degradable was 0.5 SNP-AL. Then it was decreased in higher capping agent except 0.1 mM of SNP-AL which was still low in percentage. When considered to effect of pH dependence, it was different to SNP-FA and SNP-PSSMA which more degradable in pH 5.5. The degradable of SNP-AL film was high in pH 7.4 due to pKa value of alginic acid 3.45. So alginic acid had already negative charge at pH 5.5 and 7.4. The structure of alginic acid contained hydroxyl and carboxylic group which was deprotonated at high pH value.

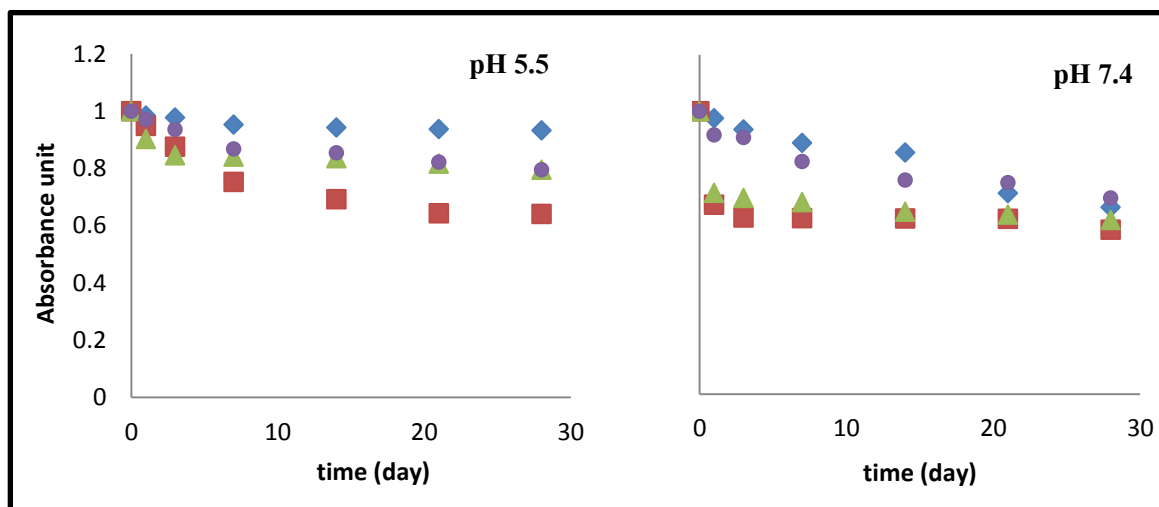


Figure 4.34 The plot of the absorbance value of PDADMAC/SNP-AL as a function of time when dipped in buffer solution pH 5.5 and 7.4 (0.1 mM= \blacklozenge , 0.5 mM= \blacksquare , 1 mM= \blacktriangle , 5 mM= \bullet)

Table 4.2 The percent of film degradable from the glass slide after releasing in buffer pH 5.5 and 7.4 at 28 day

SNP solution	pH 5.5		pH 7.4	
	% of release	% of release	% of release	% of release
	UV-vis	AFM	UV-vis	AFM
SNP-FA 1:0.1	43.34	49.46	46.69	40.83
SNP-FA 1:0.5	33.85	51.68	31.29	43.59
SNP-FA 1:1	18.59	32.38	15.40	28.30
SNP-FA 1:5	30.35	42.44	20.20	21.88
SNP-PSSMA 1:0.1	7.01	22.91	11.77	14.07
SNP-PSSMA 1:0.5	57.72	68.62	46.88	50.40
SNP-PSSMA 1:1	100	93.14	68.75	58.99
SNP-PSSMA 1:5	69	30.42	64.29	64.29
SNP-AL 1:0.1	6.74	32.44	33.94	53.07
SNP-AL 1:0.5	35.87	27.45	41.92	38.89
SNP-AL 1:1	20.5	18.80	38.52	30.38
SNP-AL 1:5	20.44	10.44	30.66	38.24

4.4.1.2 Thickness of PEM film before and after release measure by AFM

In this section, the thickness of PDADMAC/SNP films was measured by AFM including the original film and film which dipped in pH 5.5 and 7.4 at 28 days. This thickness was used to compared to the absorbance values of these film and calculated into percent of film degradable.

After PDADMAC/SNP film all capping agent were dipped in buffer solution for 28 days, these samples was also measured their thickness by AFM. Thickness of these films compared between original film and film which dipped in pH 5.5 and 7.4 were shown in table 4.3. According to a previous result, thickness of the original film was thicker than film dipped in pH 5.5 and 7.4. in SNP-FA film, concentration of capping agent effected to thickness of film after degradable. In low capping agent was the lowest thickness, in higher capping agent thickness was increased until maximum thickness at 1 mM of SNP-FA and decreased again in 5 mM SNP-FA both in pH 5.5 and 7.4. when calculated percent of film degradable had some different to percent release which calculated from UV-vis spectroscopy.

4.4.2 Silver ion leaching from PEM coated on suture material(AAS)

Because of silver ion leaching from PDADMAC/SNP film cannot analyzed by UV-Vis spectrophotometer and AFM, so in this experiment was used AAS to measured concentration of silver ion. This technique could be measure the quantity of silver ion which release from suture material.

Table 4.3 the thickness of SNP multilayer thin film was measured by AFM analysis. Compare between multilayer thin film of PDADMAC/SNP 20 layer, PDADMAC/SNP 20 layer released in buffer pH 5.5 for 28 day and PDADMAC/SNP 20 layer released in buffer pH 7.4 for 28 day

SNP solution	Origin	PH 5.5	pH 7.4
	Thickness (nm)	Thickness (nm)	thickness (nm)
SNP-FA 1:0.1	73.72 ± 1.97	37.26 ± 2.56	43.62 ± 2.16
SNP-FA 1:0.5	97.02 ± 3.83	46.88 ± 1.95	54.73 ± 1.91
SNP-FA 1:1	141.72 ± 3.54	95.83 ± 1.34	101.62 ± 1.02
SNP-FA 1:5	80.93 ± 1.99	46.58 ± 0.92	63.22 ± 2.04
SNP-PSSMA 1:0.1	61.01 ± 2.84	47.03 ± 6.78	52.42 ± 1.63
SNP-PSSMA 1:0.5	46.05 ± 1.01	14.45 ± 0.57	22.84 ± 2.11
SNP-PSSMA 1:1	38.63 ± 1.10	2.65 ± 1.33	15.84 ± 1.70
SNP-PSSMA 1:5	23.08 ± 0.56	16.06 ± 1.48	19.77 ± 0.52
SNP-AL 1:0.1	96.68 ± 2.81	65.32 ± 4.22	45.37 ± 3.05
SNP-AL 1:0.5	75.99 ± 0.64	55.13 ± 3.52	46.44 ± 1.27
SNP-AL 1:1	61.38 ± 1.53	49.84 ± 1.68	42.73 ± 1.44
SNP-AL 1:5	53.09 ± 2.22	47.55 ± 1.85	32.79 ± 0.93

In this section the amount of silver ion was coated on suture material before dipped in buffer solution was investigated. Coated suture materials all conditions were dipped in high concentration of nitric acid 5 minutes. Then suture materials were change into white color which was meant that SNP had released already. After that these solutions were filtered and analyzed concentration of silver ion by atomic absorption spectroscopy. This result showed that SNP-AL and SNP-PSSMA were similar result. In low capping agent was contained high concentration of silver ion with decreasing in high capping agent. This was due to ability of SNP that could arrange on the surface of substrate. Generally, low capping of SNP was coated with low negative charge polyelectrolytes result in close packing particles and contained high concentration of SNP.

Oppositely, high capping of SNP was contained low concentration of silver ion due to high negative charge on SNP leading to less packing. So it contained low concentration of SNP which was shown in table 4.4. For SNP-FA, their surface charge was different trend from SNP-AL and SNP-PSSMA by the highest capping of SNP was low negative charge. And in the lowest capping was high negative charge, so it was result in opposite trend of SNP-AL and SNP-PSSMA.

PDADMAC/SNP all conditions were coated layer by layer on the surface of polyamide suture material 20 layers. 2 meters in length of coated suture material were dipped in buffer solution both pH 5.5 and 7.4 for studying the leaching of silver ion from suture material. This section we mentioned in type of capping agent, concentration of capping agent and pH value effected to concentration of silver ion leaching from suture material. Atomic adsorption spectrophotometer(AAS) used to investigated the concentration of silver ion when release in buffer 1, 3, 7, 14, 21 and 28 days. For SNP-FA, both concentration of capping agent and pH condition had impacted to silver ion leaching from suture material. The highest capping agent concentration (5 mM) could release higher concentration of silver ion to the buffer solution. When time was increased affected to increase the concentration of silver ion too. By the highest capping agent shown higher slope than lower capping agent consider from the plot of concentration of silver ion and time as shown in figure 4.34. Oppositely in the lowest capping agent displayed nearly constant line in this graph. This result was correspond to zeta potential value that shown less value in high capping agent, it was not stable and would promoted more leaching of silver ion from film. When contrast to low capping agent that contained high zeta potential, it meant that it was more stable and would difficult to silver ion leaching from film.

Table 4.4 The concentration of silver ion was coated on suture material in different in type and capping concentration.

condition	Concentration of silver ion
	($\mu\text{g/ml}$)
SNP-AI 1:0.1	507.2
SNP-AI 1:0.5	213.6
SNP-AI 1:1	124
SNP-AI 1:5	113.6
SNP-PSSMA 1:0.1	125.6
SNP-PSSMA 1:0.5	30.4
SNP-PSSMA 1:1	28
SNP-PSSMA 1:5	17.6
SNP-FA 1:0.1	329.6
SNP-FA 1:0.5	418.4
SNP-FA 1:1	436
SNP-FA 1:5	424.8

When discussed the effect of pH condition to silver ion leaching from film, it was found that silver ion could release in pH 5.5 more than pH 7.4. Due to the functional group of folic acid which was carboxylic group was more negative charge in high pH and low charge in lower pH. So in pH 5.5, negatively charge was low and could not protect around silver nanoparticles then silver ion would leaching from film. In higher pH, the negatively charge was still high so it could protect silver ion leaching from film.

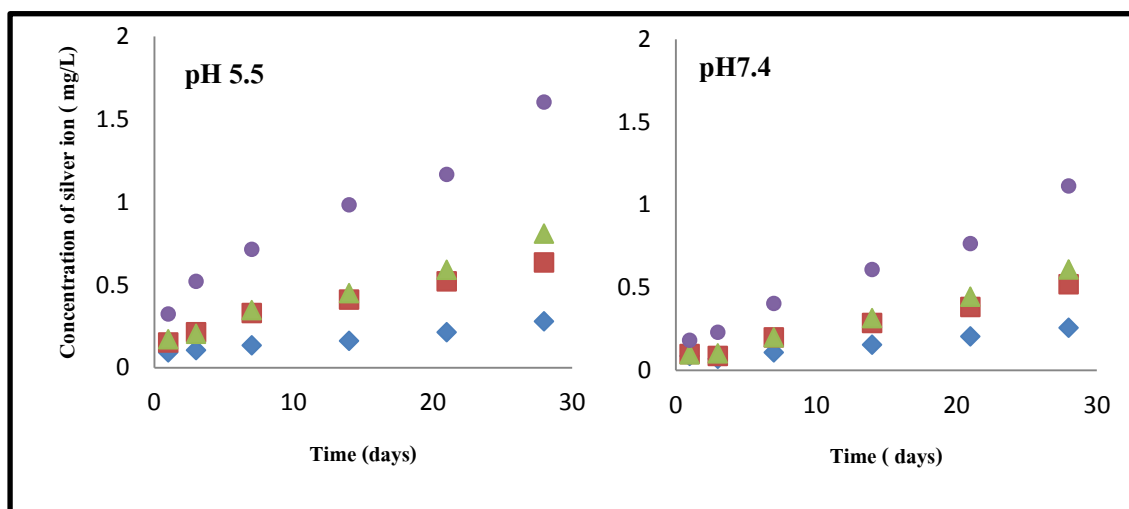


Figure 4.35 The plot of the concentration of silver ion released from PDADMAC/SNP-FA which coated on suture material as a function of time when dipped in buffer solution pH 5.5 and 7.4 (0.1 mM=◆, 0.5 mM=■, 1 mM=▲, 5 mM=●)

When calculate percent of release, it was the same trend of concentration of silver ion leaching in the previous result. The highest capping agent exhibited in high percent of release and oppositely in low capping agent, this percent of silver ion release of SNP-FA was shown in figure 4.35. It was meant that concentration of SNP on suture material was corresponding to concentration of silver ion release from suture material.

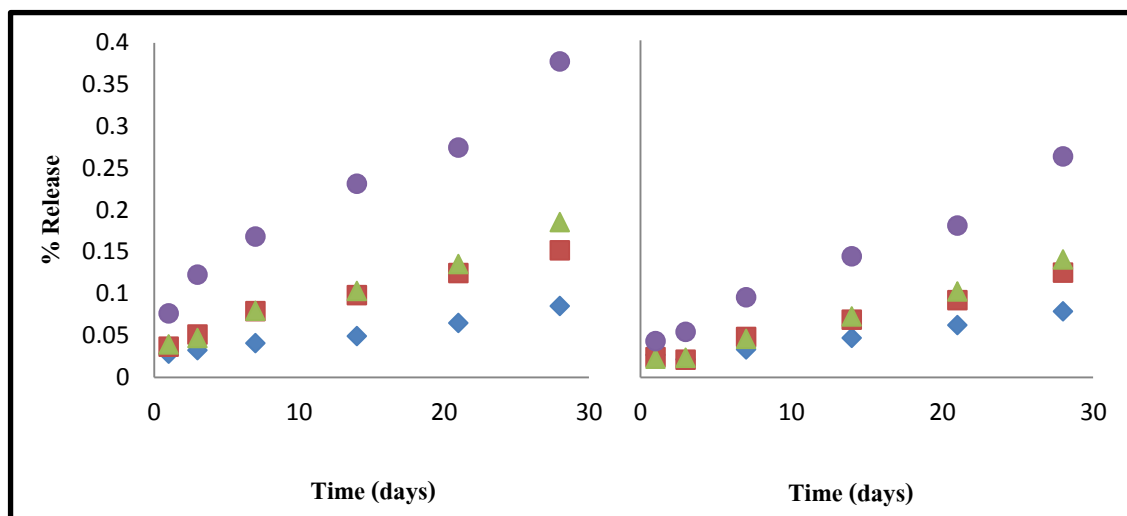


Figure 4.36 The percent of silver ion release form PDADMAC/SNP-FA film on suture material after dipped in buffer solution until 28 days (0.1 mM= ◆, 0.5 mM= ■, 1 mM= ▲, 5 mM= ●)

In figure 4.36 illustrated the plot of concentration of silver ion which leaching from PDADMAC/SNP-PSSMA film as a function of time. When analyzed in concentration of capping agent effect, the lowest capping agent (0.1mM) could be released from suture material more than high capping agent. When time was increased, the concentration of silver ion was increased also. In the highest capping agent (5mM) could be released less than 0.01 mg/L and was not different when time was increased until 28 days. The imprecise data was shown in 0.5 and 1 mM of capping agent which the trend of silver ion leaching from film was unclear in pH 5.5 condition. However, concentration of capping agent had still impact to silver ion leaching in pH 7.4 condition by more leaching in low capping agent and less leaching in higher capping agent sequentially.

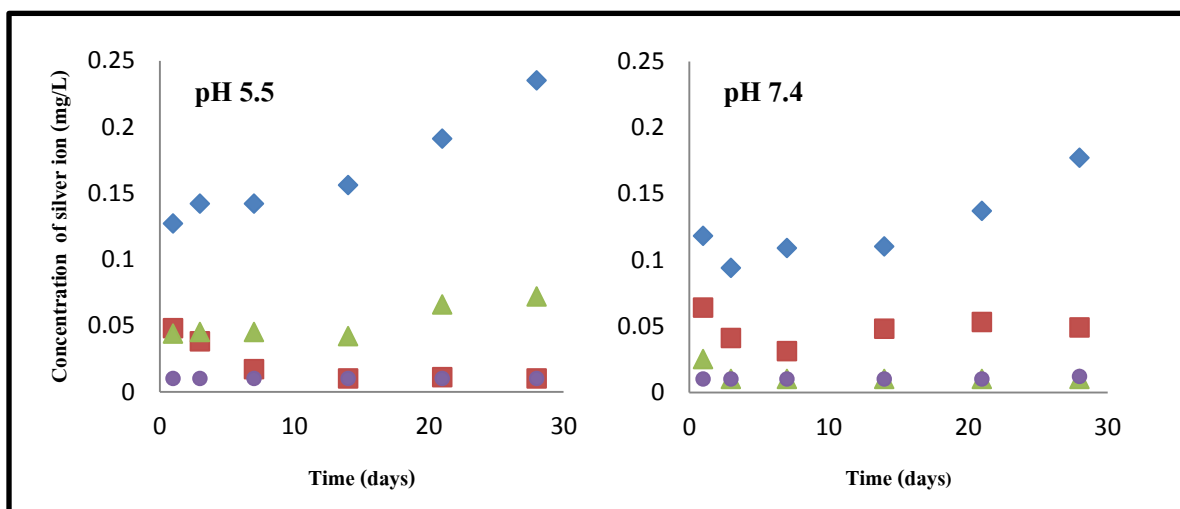


Figure 4.37 The plot of the concentration of silver ion released from PDADMAC/SNP-PSSMA which coated on suture material as a function of time when dipped in buffer solution pH 5.5 and 7.4 (0.1 mM= ◆, 0.5 mM= ■, 1 mM= ▲, 5 mM= ●)

For the effect of pH condition to PDADMAC/SNP-PSSMA was shown in figure 4.37, it could be compared in 0.1 mM PSSMA that was released in pH 5.5 more than pH 7.4 differentially. But it was no different in 5mM PSSMA. This result was caused from changing in charge surface of capping agent (carboxylic group) in different pH condition. PSSMA was weak polyelectrolyte which the surface charge was more negatively in high pH condition and less in low pH condition. For 0.5 and 1 mM PSSMA could not describe clearly because 1 mM of PSSMA was more leaching than 0.5 mM in pH 5.5 and oppositely result in pH 7.4.

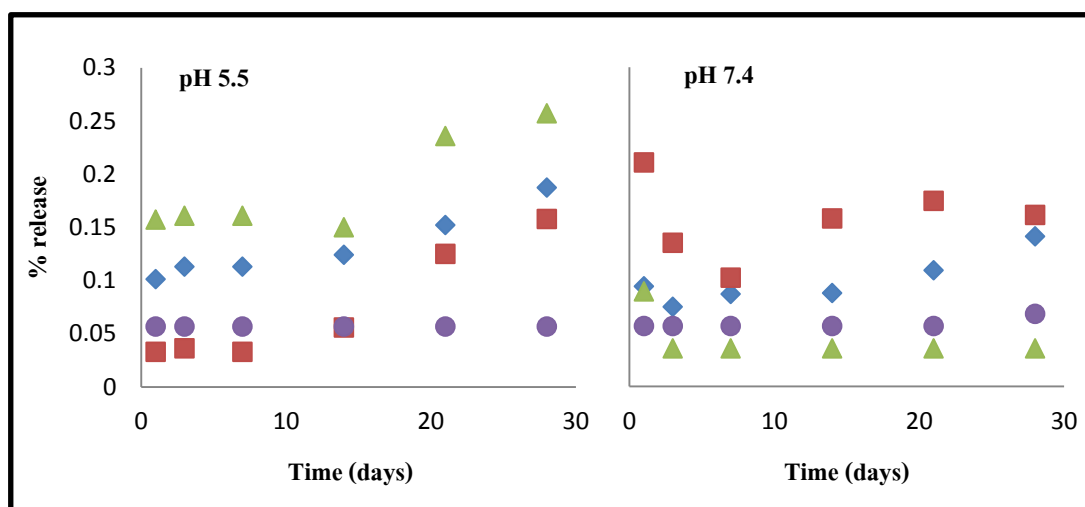


Figure 4.38 The percent of silver ion release form PDADMAC/SNP-PSSMA film on suture material after dipped in buffer solution until 28 days (0.1 mM= \blacklozenge , 0.5 mM= \blacksquare , 1 mM= \blacktriangle , 5 mM= \bullet)

When compare to percent of release, it was not correspond between concentration of SNP on suture material and concentration of silver ion leaching. For pH 5.5, in 1 mM capping of SNP was leaching silver ion from film less than low capping agent, but concentration of SNP on suture material was less also. So when calculate in percent of release, it showed high in percent of release. We could explain that it was almost leaching of SNP all but this concentration of silver ion leaching was still less than low capping agent. For other conditions were the same trend of previous result. For pH 7.4, 0.5 mM capping agent showed the percent of release more than 0.1 mM capping, this could explain like the previous result. When compared percent of silver ion release between pH 5.5 and 7.4, it was found that silver ion could release in pH 5.5 more than pH 7.4 in 0.1 and 0.5 mM of capping agent. In 1 and 5 mM of capping was the same trend. The figure of percent of silver ion leaching form PDADMAC/SNP-PSSMA was shown in figure 4.38

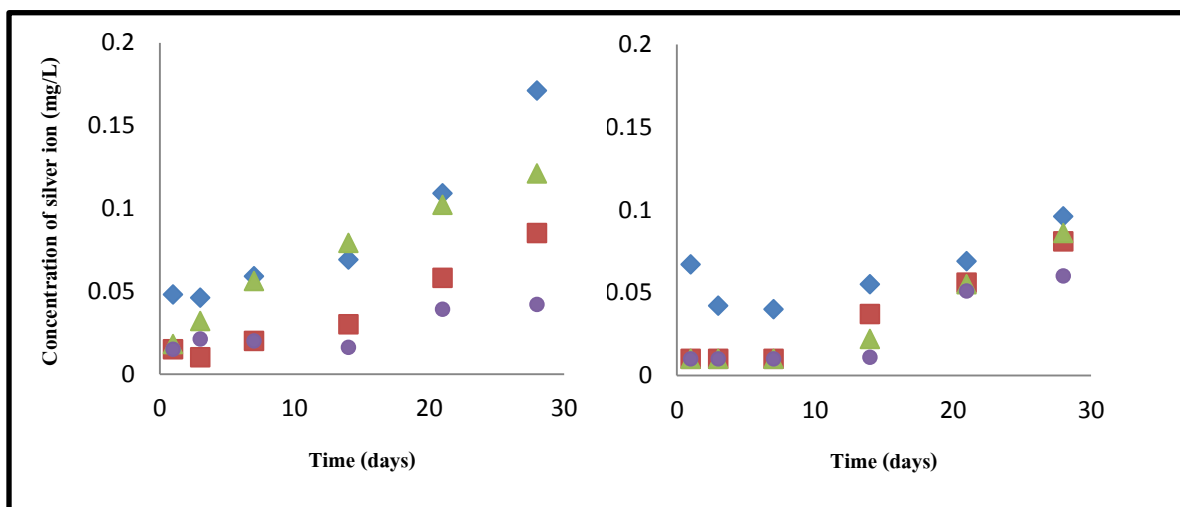


Figure 4.39 The plot of the concentration of silver ion released from PDADMAC/SNP-AL which coated on suture material as a function of time when dipped in buffer solution pH 5.5 and 7.4 (0.1 mM= ◆, 0.5 mM= ■, 1 mM= ▲, 5 mM= ●)

For PDADMAC/SNP-AL film, it was concluded that concentration of capping agent have influenced to silver ion leaching from film. The result was similar to above, silver ion released in 0.1 mM of alginate more than higher capping agent both in pH 5.5 and 7.4 condition. In early time, the leaching was slightly increased and rapidly in finally. When compare between pH 5.5 and 7.4, it was found that silver ion could release in pH 5.5 more than pH 7.4 except in 5 mM of alginate which higher leaching in pH 7.4. the figure which was described the part was shown in figure 4.38

Considering the effect of type of stabilizing agent, all conditions of PDADMAC/SNP-FA film were the highest leaching of concentration of silver ion. In 0.1 mM of PSSMA and alginate, it was shown that PSSMA could release more than Alginate but less than in higher capping agent. It could be observed that most of PDADMAC/SNP film was released in pH 5.5 more than pH 7.4. we could expect that these silver nanoparticles were toxic to cancer cell (pH around 5.5 to 6.5) more than healthy cell (pH 7.4)

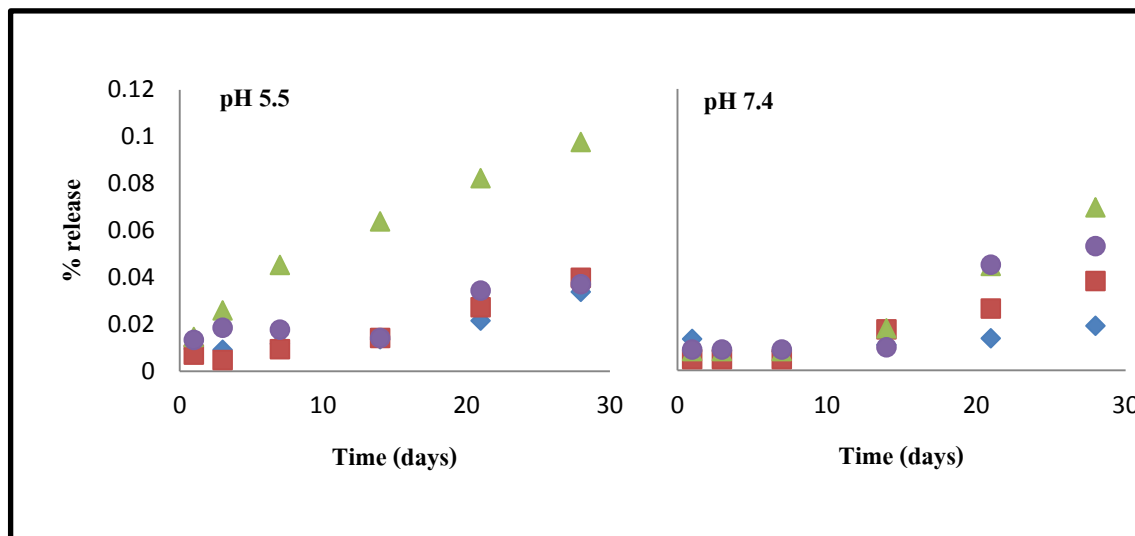


Figure 4.40 The percent of silver ion release form PDADMAC/SNP-AL film on suture material after dipped in buffer solution 28 days (0.1 mM= ◆, 0.5 mM= ■, 1 mM= ▲, 5 mM= ●)

Percent of silver ion leaching from PDADMAC/SNP-AL was shown in figure 4.40. trend of this result was different to concentration of silver ion leaching from suture material due to the same reason to result of SNP-PSSMA. In 0.1 mM SNP could release silver ion more than low capping agent but the total concentration of SNP before release was high, when calculate into percent of release was less than high capping agent. this result was corresponding to SNP-PSSMA.

This result was quite different to a previous experiment which studied in degradable of PDADMAC/SNP film on glass slide. However the pattern of leaching from suture material was compatibility to effect of capping agent and pH condition and had trend which could be described contrast to from glass slide which was not clear.

4.5 Anticancer and antibacterial testing

4.5.1 Anticancer test

Cancer is the major cause of mortality worldwide. Generally, cancer cell is irregular shape, rapidly growth and destruction in normal cell. There are two mechanisms of anticancer agents which could disrupt cancer cell. First, silver nanoparticles will interfere normal cellular

function and cell membrane leading to induce apoptosis signaling gene of cell and programmed cell death[19, 20]. Second, silver nanoparticles have influence to mitochondria in cell by inhibiting mitochondrial respiration chain. Then ATP level will be decreased and increase reactive oxygen species(ROS) in cell leading to cancer cell death[19, 21]. Silver nanoparticles are internalized in to cell by three pathways that are fluid- phase endocytosis, phagocytosis and receptor mediated endocytosis. Normally silver nanoparticles have limited access to the cell by endocytosis, so surface modified with ligand was developed to efficiently internalized to target cell via receptor mediated endocytosis pathway [11, 24, 95]. In this section, we mentioned the toxicity of SNP to cancer cell. The factor of type and concentration of capping agent toxic to cancer cell were studied, especially folic acid which was high affinity to folate receptor usually found surface of cancer cell. It was hypothesized that SNP-FA could toxic to cancer cell more than SNP-AL and PSSMA. In this work studied the effect of SNP to BT474(invasive ductal breast carcinoma), MCF-7 (Human breast adenocarcinoma), Jurkat cell (leukemia cell which the cancer of white blood cell), Chargo(lung carcinoma) and Wi38(normal fibroblast of lung)

4.5.1.1 Effect of SNP to BT474

Silver nanoparticles (SNP-FA, SNP-PSSMA and SNP-Al) were tested cytotoxicity with BT474 cell by MTT assays. Both SNP-Al and SNP-PSSMA could not against cancer cell, Even with the increased concentration of capping agents as show the inhibitory concentration 50(IC₅₀) more than 53.5 µg/ml in table 4.5. SNP-FA could inhibit BT474 cell in higher concentration of capping agent (1 and 5 mM). It was found that 1mM of capping agent obtained IC₅₀ around 12.1 µg/ml. In 5 mM of capping agent, IC₅₀ value was decrease to 9.6 µg/ml. This anticancer propertiy of SNP-FA was caused from the properties of FA which specific targeted to folate receptor on the surface of cancer cell. Therefore SNP-FA was more specific attachment to the surface of BT474 cell than other SNP. Normally, silver nanoparticles have limited access to the cell by the endocytosis pathway, so surface modified with folic acid was developed to efficiently internalize to target cell

via receptor mediated endocytosis pathway as show in figure 5 [96, 97]. When analyzed in the IC_{50} value, we could control this value by tuning the concentration of capping agent. Increasing the concentration of FA, IC_{50} value was decreased , it meant that in higher capping agent is more toxicity to BT474 cell.

Table 4.5 Cytotoxicity of SNP to breast cancer cell (BT474)

condition	IC 50 BT474(ug/ml)
SNP-A1 1:0.1	>53.5
SNP-A1 1:0.5	>53.5
SNP-A1 1:1	>53.5
SNP-A1 1:5	>53.5
SNP-PSSMA 1:0.1	>53.5
SNP-PSSMA 1:0.5	>53.5
SNP-PSSMA 1:1	>53.5
SNP-PSSMA 1:5	>53.5
SNP-FA 1:0.1	>53.5
SNP-FA 1:0.5	>53.5
SNP-FA 1:1	12.1 ± 3.96
SNP-FA 1:5	9.6 ± 0.47
DI water	>53.5
Alginic acid 5 mM	>53.5
PssMA 5 mM	>53.5
Folic acid 5 mM	>53.5

4.5.1.2 Effect of SNP to MCF-7

As the result above, we found that only SNP-FA solution could toxic to BT474. So this section it was studied in SNP-FA and only 0.1 SNP-PSSMa (as compared data). Viability of Vero(African green monkey kidney fibroblast) and MCF -7 (Human breast adenocarcinoma) cell was investigated in a different concentration of SNP-FA by MTT assays. SNP-FA could reduce the viability of both Vero and MCF-7, especially in the MCF-7 cell. Follow as table 4.6 was shown the inhibitory concentration 50(IC_{50}) of SNP-FA which effect to Vero and MCF-7 cell. It was concluded that the IC_{50} value of MCF-7cell was significant lower than Vero cell almost all conditions. It meant that SNP-FA exhibited the efficiency to reduce the MCF-7 cell more than Vero cell[98]. This result was caused from the properties of FA which specific targeted to folate receptor on the surface of cancer cell. This effect was different to the normal cell which rarely found the folate receptor on the surface. Therefore SNP-FA was more specific attachment to the surface of MCF-7 cell than Vero cell. Normally, silver nanoparticles have limited access to the cell by the endocytosis pathway, so surface modified with folic acid was developed to efficiently internalize to target cell via receptor mediated endocytosis pathway as show in figure 5 [96, 97]. When analyzed in the IC_{50} value, we could control this value by tuning the concentration of capping agent. Increasing the concentration of FA, IC_{50} value was decrease due to membrane of both Vero and MCF-7 provide the negative charge whereas the surface charge of SNP-FA show the negative charge also. It meant that there was high degree of repulsion between SNP-FA and cell membrane which formed the electrostatic barrier lead to limit the cell-particles interaction and reduce their toxicity. In low negative zeta potential of SNP-FA was reduce the electrostatic barrier which promoted the cell-particles interaction and increased their toxicity to cancer cell[99]. When compare to silver nanoparticles capped with PSSMA which no specific to folate receptor on the surface of cancer cell, the IC_{50} of SNP-PSS-MA is higher than SNP-FA in low capping agent both in Vero and MCF-7. It was shown that SNP-FA is more specific to cancer

cell than SNP-PSSMA. This result was confirmed the specific targeted to cancer cell property of SNP-FA.

Table 4.6 Cytotoxicity of SNP to breast cancer cell (MCF-7)

Condition (mM)	IC₅₀ (µg/ml)	IC₅₀ (µg/ml)
	Vero (African green monkey kidney fibroblast)	MCF-7 (Human breast adenocarcinoma) cell
SNP-FA 1:0.05	>84.435	>84.435
SNP-FA 1:0.1	79.276 ± 1.90	76.946 ± 2.33
SNP-FA 1:0.5	42.248 ± 0.73	25.243 ± 3.35
SNP-FA 1:1	26.997 ± 1.67	17.738 ± 0.08
SNP-FA 1:5	26.379 ± 0.84	16.205 ± 0.1
SNP-CoPss 1:0.1	>84.435	50.745 ± 4.33

4.5.1.3 Effect of SNP to Jurkat cell

Jurkat cell is the cancer of white blood cell or leukemia. Normally, Jurkat cell contained folate receptor[104], so it was hypothesized that SNP-FA was toxic to Jurkat cell more than SNP-AL and SNP-PSSMA. This part was study the cytotoxicity of SNP to Jurkat cell via MTT assay. It was found that SNP all type of capping agent were toxic to this cell which was shown in table 4.6. For SNP-AL, in high capping agent was toxic to cell more than low capping agent. The result of their IC₅₀ value showed less value in 5 mM of AL and high value in 0.1 mM of AL. It meant that higher capping agent was more toxic to Jurkat cell. This result was different to SNP-PSSMA which was more toxic in lower capping agent, but the cytotoxicity was low when increase concentration of capping agent except 5 mM of PSSMA that similar to 0.1 mM of PSSMA. This trend was corresponding to SNP-FA which was more toxic to Jurkat cell in low

capping agent and 5mM of FA. For DI water, AL, FA and PSSMA was no toxic to jurkat cell. This could be confirmed that this capping agent was affected to jurkat cell and the toxicity of SNP was due to ability of silver ion releasing from SNP and SNP. It was corresponding to previous hypothesis, IC 50 of SNP-FA was less than SNP-AL and SNP-PSSMA. This was due to Jurkat cell had folate receptor with high affinity to FA which used to modify surface of SNP. When SNP-FA attached to folate receptor, it was entrapped to cancer cell via folate receptor mediated endocytosis pathway and cancer cell death. This was promoted ability of SNP-FA to anticancer. For SNP-AL and SNP-PSSMA, they could reduce Jurkat cell by direct effect of SNP and did not special channel. Finally, it could be concluded that all SNP was toxic to jurkat cell depend on concentration and type of capping agent. So this result was different to other cell which SNP-FA was only toxic to MCF-7, BT474, Chago cell and Wi 38.

Table 4.7 Cytotoxicity of SNP to Jurkat cell

condition	IC 50 Jurkat (ug/ml)
SNP-AI 1:0.1	42.90 ± 4.90
SNP-AI 1:0.5	21.95 ± 2.07
SNP-AI 1:1	18.82 ± 2.54
SNP-AI 1:5	13.11 ± 0.95
SNP-PSSMA 1:0.1	17.68 ± 1.05
SNP-PSSMA 1:0.5	27.24 ± 3.78
SNP-PSSMA 1:1	38.54 ± 1.52
SNP-PSSMA 1:5	19.81 ± 1.50
SNP-FA 1:0.1	11.65 ± 3.45
SNP-FA 1:0.5	13.29 ± 3.13
SNP-FA 1:1	21.27 ± 2.12
SNP-FA 1:5	14.41 ± 2.37
DI water	>53.5
Alginic acid 5 mM	>53.5
PssMA 5 mM	>53.5
Folic acid 5 mM	>53.5

4.5.1.4 Cytotoxicity of SNP to Chago cell (lung undifferentiated human) and WI-38VA-13 subline 2RA (fibroblast human lung cell)

This section was studied the cytotoxic of SNP in all capping agent to Chago cell (lung undifferentiated human) derived from a bronchogenic carcinoma[105] and WI-38VA-13 subline 2RA (fibroblast human lung cell). It was expected that these SNP was toxic to Chago cell which was the cancer cell of lung and non-toxic to WI-38 which was normal cell lung. Because of in WI-38 did not have receptor for SNP such as folate receptor. MTT assay was used to analyze in this part. The result was shown in figure 4.8 that SNP-PSSMA and SNP-AL all concentration of capping agent and all dilution was no toxic to WI-38 and Chago cell. IC50 value was more than 53.5 $\mu\text{g/ml}$ all conditions of SNP-PSSMA and SNP-AL. it was interesting that in SNP-FA all conditions were no toxic to both Chago cell and WI-38 cell except 5 mM of FA that toxic to Chago cell at 43.31 $\mu\text{g/ml}$. this data was similar to the effect of SNP-FA to BT474 that in high capping agent of SNP-FA was toxic to cancer cell. This was due to SNP-FA was modified surface with FA which was high affinity to folate receptor on surface of cancer cell. WI-38 was the normal cell lung which was folate receptor, so SNP-FA was no toxic to them. Oppositely, Chago which was cancer cell was contain folate receptor on their surface, therefore SNP-FA could toxic to them especially in high concentration of FA. High FA was increase binding side of SNP-FA to surface of cancer cell. For SNP-PSSMA and SNP-AL, PSSMA and AL which coated around surface of SNP could not bind to specific receptor on Chago and WI-38, so in the same concentration of SNP was no toxic to both cells. We could be applied this result to medical filed for treatment in cancer disease.

Table 4.8 Cytotoxicity of SNP to Chago cell (lung undifferentiated human) and WI-38VA-13 subline 2RA (fibroblast human lung cell)

condition	IC 50 Chago (ug/ml)	IC 50 WI-38 (ug/ml)
SNP-A1 1:0.1	>53.5	>53.5
SNP-A1 1:0.5	>53.5	>53.5
SNP-A1 1:1	>53.5	>53.5
SNP-A1 1:5	>53.5	>53.5
SNP-PSSMA 1:0.1	>53.5	>53.5
SNP-PSSMA 1:0.5	>53.5	>53.5
SNP-PSSMA 1:1	>53.5	>53.5
SNP-PSSMA 1:5	>53.5	>53.5
SNP-FA 1:0.1	>53.5	>53.5
SNP-FA 1:0.5	>53.5	>53.5
SNP-FA 1:1	>53.5	>53.5
SNP-FA 1:5	43.31 ± 2.90	>53.5
DI water	>53.5	>53.5
Alginate acid 5 mM	>53.5	>53.5
PssMA 5 mM	>53.5	>53.5
Folic acid 5 mM	>53.5	>53.5

We could explain that SNP can be improved for more specific targeting to cancer cell by developing the pharmacokinetics, pharmacodynamics and active intercellular delivery[22]. All of these characteristics depend on size and surface including the targeting ligand. In this work, SNP was improved the active intercellular delivery via controlling size and concentration of the targeting ligand on the surface. First, the size of nanoparticles should be less than 100 nm, it was increase the potential to access into cancer cell[22]. This is consistent with the size of SNP-FA which is less than 10 nm, it increases the ability of SNP-FA to access into cancer cell. Second, tuning the concentration of folic acid which is the targeting ligand is improve this SNP-FA for anticancer also. Two parameters that used to tuning the attachment to target cell are the affinity and density of targeting ligand[22]. It is well known that folic acid has high affinity to folate receptor which usually presence on the surface of cancer cell including BT474. Thus modified surface of SNP with folic acid certainly promote anticancer property on SNP-FA. In addition, when increase concentration of folic acid, the ability to against cancer cell was improved as show the IC_{50} value of 5 mM of folic acid. It meant that the density of folic acid which coated on the SNP-FA was increased leading to promote the ability of their anticancer property. This result was confirmed the specific targeted to cancer cell property and anticancer property of SNP-FA. For the pure folic acid, alginate acid and PSSMA in 5 mM could not anticancer as showing the IC_{50} value more than 53.5 $\mu\text{g/ml}$. this result was the same with distilled water which could not anticancer also. This data confirmed that all capping agents could not against cancer cell, therefore folic acid was used to target to surface of cancer cell only not effect to inhibited cancer cell.

4.5.2 Antibacterial test

The well-known properties of SNP were antibacterial agent which could modify to use in many commercial products. In this work, the effect of concentration and type of capping agent to antibacterial property was studied. SNP at 5.35 $\mu\text{g/ml}$ all conditions were cultured with

staphylococcus aureus (*S. aureus*) and Escherichia coli (*E. coli*) 1 hours. And then they were cultured on plate agar 24 hours. Colony of bacteria were counted and calculated. The result was shown in table 4.9.

Table 4.9 Antibacterial test to Staphylococcus aureus (*S. aureus*) and Escherichia coli (*E. coli*)

condition	% Reduction	
	Staphylococcus aureus	Escherichia coli
SNP-A1 1:0.1	38.88	68.75
SNP-A1 1:0.5	27.77	99.99
SNP-A1 1:1	11.11	99.99
SNP-A1 1:5	30.55	99.99
SNP-PSSMA 1:0.1	38.88	99.99
SNP-PSSMA 1:0.5	99.99	99.99
SNP-PSSMA 1:1	27.77	99.99
SNP-PSSMA 1:5	38.88	99.99
SNP-FA 1:0.1	41.66	99.99
SNP-FA 1:0.5	88.88	99.99
SNP-FA 1:1	90.00	99.99
SNP-FA 1:5	30.55	99.99
DI water	-	-
Alginate acid 5 mM	27.77	-
PssMA 5 mM	30.55	18.75
Folic acid 5 mM	30.55	6.25

From this result, it could be found that SNP-AL, SNP-PSSMA and SNP-FA which contained a various concentration of capping agent could reduce *E. coli* nearly 100 %. It meant that the concentration and type of capping agent did not have effect to antibacterial activity of *E. coli*. For *S. aureus*, all conditions of SNP could reduce *S. aureus* less than *E. coli* in the same condition. The concentrations of capping agents have low effect to antibacterial activity. It could found that in SNP-AL, low capping agent have percent of reduction more than high capping agent, but it was not clear in 5mM AL of SNP which had percent of reduction more than 1 and 0.5 mM of AL. this might be from toxicity of AL 5 mM to *S. aureus* which their percent of reduction was around 27.77 %. FOR SNP-PSSMA, their percent of reduction was no trend when increased concentration of capping agent. However in 0.5 mM of PSSMA could reduce *S. aureus* nearly 100%. Oppositely in SNP-FA, low capping agents have percent of reduction less than high capping agent and decrease in 5 mM of FA. When consider in type of capping agent, it was found that SNP-AL was low potential to reduce *S. aureus* than SNP-FA and SNP-PSSMA.

The different structure between Gram positive bacteria such as *S. aureus* and Gram negative bacteria such as *E. coli* is structure of cell wall or cell membrane. For *E. coli* is consist of protein, lipid and lipopolysaccharides (LPS) which was protect them from many agents. For *S. aureus* does not consist of LPS. Moreover there are difference in thickness of peptidoglycan layer, in Gram positive bacteria contain 30 nm and lack of outer membrane but in Gram negative bacteria is around 2-3 nm between cytoplasm membrane and outer membrane.

Generally, the mechanism of antibacterial agent is different between silver ion and silver nanoparticles. SNP could destroy bacterial cell by 3 ways. First, SNP which their size is around 1-10 nm could bind to cell wall and change their function such as respiratory function. Second, it can pass to bacterial cell and damage sulphur and phosphorus compound like DNA. Third, it can release silver ion which contain antibacterial property[106]. For silver nanoparticles which usually coated with negative charge agent, it could not attach to cell wall of bacteria because

repulsive force from negative charge of cell wall and SNP. But SNP can interact with building elements of bacterial membrane resulting in structure change, degradation and cell death. From this reason and peptidoglycan of Gram negative bacteria was thinner, so SNP was toxic to Gram negative bacteria more than Gram positive bacteria. Silver ion contain positive charge, therefore it can attach to cell wall of bacteria by electrostatic attraction. Then it can antibacterial by 2 ways, first it could destroy and made structure change in cell membrane by the formation of small electron-dense granules formed by silver ion. Finally cell death. Second, It interacts with thiol groups of vital enzymes and inactivates them, finally cell death[106]. It was concluded that silver ion is more toxic to Gram positive bacteria than Gram negative bacteria. In this section, SNP was expose to *S. aureus* and *E. coli* 1hr, so SNP could release silver ion incomplete. This solution was contained SNP more than silver ion. Therefore all conditions of SNP was toxic to *E. coli* than *S. aureus* due to SNP property.

CHAPTER V

CONCLUSIONS

Silver nanoparticles(SNP) with a various type of capping including FA, PSSMA and AL could be synthesized and varied concentration of capping agent 0.1, 0.5, 1 and 5 mM. Adding salt could promote the monolayer adsorption on the substrate by decreasing the repulsive interaction between particles. It was found that SNP-PSSMA was added salt more concentration than SNP-AL and SNP-FA sequentially. This point could be increased potential of modified surface of material. SNP/PDADMAC was coated layer by layer on a various of substrates such as glass slide and polyamide suture material. It was found that low capping agent was generated densely film with high absorbance value, oppositely high capping agent was performed less packing film with a lower absorbance value. Then the pattern of silver ion leaching and film desorption of coated glass slide and suture material was studied by dipping this thin film in buffer solution pH 7.4 and 5.5. It was shown that silver ion could leach from PEM in pH 5.5 more than pH 7.4. So it was meant that this SNP multilayer thin film could release silver ion in cancer cell more than healthy cell. This was corresponding to desorb of film from glass slide which was more desorption in pH 5.5 than pH 7.4. from this result it could be applied to control release of drug or agent to target cell.

For anticancer activity, it was found that SNP-AL and SNP-PSSMA was not toxic to both cancer cell (BT474, Chargo cell) and healthy cell(Wi-38). However, SNP-FA at high concentration of FA toxic to cancer cell, but it could not toxic to Wi-38 cell. All condition of SNP were toxic to Jurkat cell depend on concentration of capping agent. From this result it could be applied the SNP to treated in cancer disease because it was toxic to only cancer cell not to healthy cell. It was relieve side effect of chemical which used in chemotherapy treatment for patient. For antibacterial property of SNP, it was found that SNP-AL, SNP-PSSMA and SNP-FA could reduce E. coli nearly 100 %. It was different to S. aureus which SNP was toxic less than E. coli

and depend on the concentration of capping agent. It was modified this SNP to use as antibacterial agent by selecting the agent follow their efficacy.

From this work, these SNP which were prepared with a different capping agent such as AL (natural agent), PSSMA (synthetic agent) and FA (vitamin that contain high affinity to folate receptor) was contained a various properties follow by their capping agent. Therefore we can developed them to use in medical field such as SNP-FA was suitable to use as anticancer agent due to it was specific binding the folate receptor which is on the cancer cell and not toxic to healthy cell. Although SNP-AL and SNP-PSSMA was toxic only Jurkat cell, but their antibacterial agent was potential. So SNP-AL was promoted to use as antibacterial agent especially for medical field because AL was natural and biocompatible. SNP-PSSMA should be used as antibacterial agent in equipment because it was synthetic agent.

References

- [1] Kholoud, M.M., Abou El-Nour, A.E., Abdulrhman, A.W., and Ammar, R.A.A. Synthesis and applications of silver nanoparticles. Arabian Journal of Chemistry 3(2010):135–40.
- [2] Zhu, S.L. and Zhou, W. Optical Properties and Immunoassay Applications of Noble Metal Nanoparticles. J Nanomater (2010):-.
- [3] Porter, R., Kabil, A., Forstern, C., Slevin, C., Kouwenberg, K., Szymanski, M. and et al. A Novel, Generic, Electroanalytical Immunoassay Format Utilising Silver Nano-Particles as a Bio-Label. J Immunoass Immunoch 30(2009):428-40.
- [4] Sun, H., Choy, T.S., Zhu, D.R., Yam, W.C., Fung, Y.S. Nano-silver-modified PQC/DNA biosensor for detecting E. coli in environmental water. Biosens Bioelectron 24(2009):1405-10.
- [5] Pradeep, T., Anshup. Noble metal nanoparticles for water purification: A critical review. Thin Solid Films 517(2009):6441-78.
- [6] Simpson, J.L., Bailey, L.B., Pietrzik, K., Shane, B., Holzgreve, W. Micronutrients and women of reproductive potential: required dietary intake and consequences of dietary deficiency or excess. Part I - Folate, Vitamin B12, Vitamin B6. Journal of Maternal-Fetal & Neonatal Medicine 23(2010):1323-43.
- [7] Asadishad, B., Vossoughi, M. and Alemzadeh, I. Folate-Receptor-Targeted Delivery of Doxorubicin Using Polyethylene Glycol-Functionalized Gold Nanoparticles. Industrial & Engineering Chemistry Research 49(2010):1959-63.
- [8] Dixit, V., Van den, B.J., Sherman, D.M., Thompson, D.H., Andres, R.P. Synthesis and grafting of thioctic acid-PEG-folate conjugates onto Au nanoparticles for selective targeting of folate receptor-positive tumor cells. Bioconjugate chemistry. 17(2006):603-609.
- [9] Zhang, Z.W., Jia, J., Lai, Y.Q., Ma, Y.Y., Weng, J., Sun, L.P., Conjugating folic acid to gold nanoparticles through glutathione for targeting and detecting cancer cells. Bioorganic & Medicinal Chemistry 18(2010):5528-5534.
- [10] Leamon, C.P., Low, P.S. Folate-mediated targeting: from diagnostics to drug and gene delivery. Drug Discovery Today 6(2001):44-51.

- [11] Liong, M., Lu, J., Kovoichich, M., Xia, T., Ruehm, S.G., Nel, A.E. and et al. Multifunctional inorganic nanoparticles for imaging, targeting, and drug delivery. ACS Nano 2(2008):889-896.
- [12] Jeon, C., Park, J.Y., Yoo, Y.J. Characteristics of metal removal using carboxylated alginic acid. Water research 36(2002):1814-1824.
- [13] Ji-Sheng, Y.Y-JX. and Wen, H. Research progress on chemical modification of alginate: A review. Carbohydrate polymers 84(2011):33-9.
- [14] Gong, X., Han, L., Yue, Y., Gao, J. and Gao, C. Influence of assembly pH on compression and Ag nanoparticle synthesis of polyelectrolyte multilayers. Journal of colloid and interface science 355(2011):368-373.
- [15] Tjipto, E., Quinn, J.F. and Caruso, F. Assembly of multilayer films from polyelectrolytes containing weak and strong acid moieties. Langmuir : the ACS journal of surfaces and colloids 21(2005):8785-92.
- [16] Elvira, T.J. and Frank, C. Layer-by-Layer Assembly of Weak-Strong Copolymer Polyelectrolytes: A Route to Morphological Control of Thin Films. Journal of Polymer Science: Part A: Polymer Chemistry 45(2007):4341-51.
- [17] Hui-Yu, D.Y-YX., Bao-Ku, Z., Xiu-Zhen, W., Fu, L. and Zhen-Yu, C. Polyelectrolyte membranes prepared by dynamic self-assembly of poly (4-styrenesulfonic acid-co-maleic acid) sodium salt (PSSMA) for nanofiltration (I). Journal of membrane science 323(2008):125-133.
- [18] Sriram, M.I., Kanth, S.B., Kalishwaralal, K. and Gurunathan, S. Antitumor activity of silver nanoparticles in Dalton's lymphoma ascites tumor model. Int J Nanomedicine 5(2010):753-762.
- [19] Pallab, S.A.C. and Siddhartha S.G. Induction of Apoptosis in Cancer Cells at Low Silver Nanoparticle Concentrations using Chitosan Nanocarrier. ACS Appl Mater Interfaces 3(2011):218-228.
- [20] P. Gopinatha, S.K.G., Pallab, S., Anumita, P. and Arun Chattopadhyayb, S.S.G. Signaling gene cascade in silver nanoparticle induced apoptosis. Colloids and Surfaces B: Biointerfaces 77(2010):240-245.

- [21] Cla'udio Se'rgio, C.J., Juliana, F.D., Cinara, L.G., Gislaine, T.R., Emilio, L.S., Marcos, M. S.P. In vitro effects of silver nanoparticles on the mitochondrial respiratory chain. Mol Cell Biochem 342(2010):51-56.
- [22] Mark, E., Davis, Z. Nanoparticle therapeutics:an emerging treatment modality for cancer. NATURE REVIEWS drug discovery 7(2008):771-782.
- [23] Hu-Lieskovan, S., Heidel, J.D., Bartlett, D.W., Davis, M.E., Triche, T.J. Sequence-specific knockdown of EWS-FLI1 by targeted, nonviral delivery of small interfering RNA inhibits tumor growth in a murine model of metastatic Ewing's sarcoma. Cancer research 65(2005):8984-8992.
- [24] Dhar, S., Liu, Z., Thomale, J., Dai, H.J., Lippard, S.J. Targeted single-wall carbon nanotube-mediated Pt(IV) prodrug delivery using folate as a homing device. Journal of the American Chemical Society 130(2008):11467-11476.
- [25] Xia, W., Low, P.S. Folate-targeted therapies for cancer. Journal of medicinal chemistry 53(2010):6811-6824.
- [26] Shakeri-Zadeh, A., Ghasemifard, M., Mansoor, G.A. Structural and optical characterization of folate-conjugated gold-nanoparticles. Physica E 42(2010):1272-1280.
- [27] Saad, M., Garbuzenko, O.B., Ber, E., Chandna, P., Khandare, J.J., Pozharov, V.P. and et al. Receptor targeted polymers, dendrimers, liposomes: which nanocarrier is the most efficient for tumor-specific treatment and imaging? Journal of controlled release : official journal of the Controlled Release Society 13(2008):107-114.
- [28] Banerjee, M., Mallick, S., Paul, A., Chattopadhyay, A., Ghosh, S.S. Heightened reactive oxygen species generation in the antimicrobial activity of a three component iodinated chitosan-silver nanoparticle composite. Langmuir : the ACS journal of surfaces and colloids 26(2010):5901-5908.
- [29] Feng, Z.X.W., Yuyue, C. and Hong, L. Application of Silver Nanoparticles to Cotton Fabric as an Antibacterial Textile Finish. Fibers and Polymers 10(2009):-.
- [30] Jain, P. and Pradeep, T. Potential of silver nanoparticle-coated polyurethane foam as an antibacterial water filter. Biotechnology and bioengineering 90(2005):59-63.

- [31] Sukdeb, P.Y. and Joon, M.S. Does the Antibacterial Activity of Silver Nanoparticles Depend on the Shape of the Nanoparticle? A Study of the Gram-Negative Bacterium *Escherichia coli*. Applied and environmental microbiology 73(2007):1712-1720.
- [32] Panacek, A, Kvitek, L., Prucek, R., Kolar, M., Vecerova, R., Pizurova, N. and et al. Silver colloid nanoparticles: synthesis, characterization, and their antibacterial activity. The journal of physical chemistry B 110(2006):16248-16253.
- [33] Siddhartha, S.T.B., Arnab, R., Gajendra, S., Ramachandrarao, P. and Debabrata, D. Characterization of enhanced antibacterial effects of novel silver nanoparticles. Nanotechnology. 18(2007):1-9.
- [34] Han, X., Kasahara, N. and Kan, Y.W. Ligand-directed retroviral targeting of human breast cancer cells. Proceedings of the National Academy of Sciences of the United States of America 92(1995):9747-9751.
- [35] Sudimack, J. and Lee, R.J. Targeted drug delivery via the folate receptor. Advanced drug delivery reviews 41(2000):147-162.
- [36] Liu, L. and et al. An electrochemical method to detect folate receptor positive tumor cell. Electrochemistry Communications 9(2007):2547-2550.
- [37] Ramos, A.P., Doro, F.G., Tfouni, E., Goncalves, R.R. and Zaniquelli, M.E.D. Surface modification of metals by calcium carbonate thin films on a layer-by-layer polyelectrolyte matrix. Thin Solid Films 516(2008):3256-3262.
- [38] Boddohi, S., Killingsworth, C.E. and Kipper, M.J. Polyelectrolyte multilayer assembly as a function of pH and ionic strength using the polysaccharides chitosan and heparin. Biomacromolecules 9(2008):2021-2028.
- [39] Shen, L. and Hu, N. Electrostatic adsorption of heme proteins alternated with polyamidoamine dendrimers for layer-by-layer assembly of electroactive films. Biomacromolecules 6(2005):1475-1483.
- [40] Basel, F.A. Structure and mechanism of formation of polyelectrolyte multilayers. Polymer 47(2006):3674-3680.
- [41] Wang, L., Chen, D.D. and Sunt, J.Q. Layer-by-Layer Deposition of Polymeric Microgel Films on Surgical Sutures for Loading and Release of Ibuprofen. Langmuir 25(2009):7990-7994.

- [42] Gomez-Alonso, A., Garcia-Criado, F.J., Parreno-Manchado, F.C., Garcia-Sanchez, J.E., Garcia-Sanchez, E., Parreno-Manchado, A. and et al. Study of the efficacy of Coated VICRYL Plus Antibacterial suture (coated Polyglactin 910 suture with Triclosan) in two animal models of general surgery. *J Infect* 54(2007):82-88.
- [43] Zhukovsky, V. Bioactive surgical sutures. *AUTEX Research Journal* 3(2003):41-45.
- [44] Shibuya, T.Y., Kim, S., Nguyen, K., Do, J., McLaren, C.E., Li, K.T. and et al. Bioactive suture: a novel immunotherapy for head and neck cancer. *Clin Cancer Res* 10(2004):7088-7099.
- [45] Blaker, J.J., Nazhat, S.N. and Boccaccini, A.R. Development and characterisation of silver-doped bioactive glass-coated sutures for tissue engineering and wound healing applications. *Biomaterials* 25(2004):1319-1329.
- [46] Mingmalairak, C., Ungbhakorn, P. and Paocharoen, V. Efficacy of antimicrobial coating suture coated polyglactin 910 with triclosan (Vicryl plus) compared with polyglactin 910 (Vicryl) in reduced surgical site infection of appendicitis, double blind randomized control trial, preliminary safety report. *J Med Assoc Thai* 92(2009):770-775.
- [47] Zhou, J., Romero, G., Rojas, E., Ma, L., Moya, S. and Gao, C.Y. Layer by layer chitosan/alginate coatings on poly(lactide-co-glycolide) nanoparticles for antifouling protection and Folic acid binding to achieve selective cell targeting. *J Colloid Interf Sci* 345(2010):241-247.
- [48] Dautzenberg, H.J.W., Kotz, J., Philipp, B., Seidel, C. and Stscherbina, D. Polyelectrolytes Formation, Characterization and application. 1994.
- [49] Yoo, D., Shiratori, S.S. and Rubner, M.F. Controlling bilayer composition and surface wettability of sequentially adsorbed multilayers of weak polyelectrolytes. *Macromolecules* 31(1998):4309-4318.
- [50] Potisatityuenyong, A., Tumcharern, G., Dubas, S.T. and Sukwattanasinitt, M. Layer-by-layer assembly of intact polydiacetylene vesicles with retained chromic properties. *Journal of colloid and interface science* 304(2006):45-51.
- [51] Clark, S.L.M.M. and Hammond, P.T. Ionic effects of sodium chloride on the templated deposition of polyelectrolytes using layer-by-layer ionic assembly. *Macromolecules* 30(1997):7237-7244.

- [52] Decher, G.S.J. Multilayer thin films. Wiley-VCH Verlag GmbH & Co. KGaA 2002.
- [53] G, A. An effective modelling approach to estimate nonlinear bending behavior of cantilever type conducting polymer actuators. Sensor and Actuators B 141(2009):248-292.
- [54] Limsavarn, L., Sritaveesinsub, V. and Dubas, S.T. Polyelectrolyte assisted silver nanoparticles synthesis and thin film formation. Material letter 61(2007):3048-3051.
- [55] Dubas, S.T. and Schlenoff, J.B. Factors controlling the growth of polyelectrolyte multilayers. Abstracts of Papers of the American Chemical Society 219(2000):U532-U.
- [56] Andelman, D.J.J. Polyelectrolyte adsorption. Comptes Rendus De L Academic Des Sciences Serie Iv Physique Astrophysique 1(2000):1153-1162.
- [57] Pereira da, S., Gomes, J.F., Rank, A., Kronenberger, A., Fritz, J., Winterhalter, M. and Ramaye, Y. Polyelectrolyte-coated unilamellar nanometer-sized magnetic liposomes. Langmuir : the ACS journal of surfaces and colloids 25(2009):6793-6799.
- [58] Schlenoff, J.B., Dubas, S.T and Farhat, T. Sprayed polyelectrolyte multilayers. Langmuir 16(2000):9968-9969.
- [59] Mabrook, M.F.P.C., Jombert, A.S., Zeze, D.A. and Petty, M.C. The morphology, electrical conductivity and vapour sensing ability of inkjet-printed thin films of single-wall carbon nanotubes. Carbon. 47(2009):752-757.
- [60] Dubas, S.T., Farhat, T.R. and Schlenoff, J.B. Multiple membranes from "true" polyelectrolyte multilayers. Journal of the American Chemical Society 123(2001):5368-5369.
- [61] Tan, H.L., M, M., Pan, G.Q. and Van Patten, P.G. Temperature dependence of polyelectrolyte multilayer assembly. Langmuir : the ACS journal of surfaces and colloids 19(2003):9311-9314.
- [62] Kaur, P., Yue, H., Wu, M., Liu, M., Treece, J., Waldeck, D.H. and et al. Solvation and aggregation of polyphenylethynylene based anionic polyelectrolytes in dilute solutions. The journal of physical chemistry B 111(2007):8589-8596.
- [63] Antipov, A.A.S.G. and Mohwald, H. Influence of ionic strength on the polyelectrolyte multilayers' permeability. Langmuir : the ACS journal of surfaces and colloids 19(2003):2444-2448.

- [64] Antipov, A.A.S.G. Polyelectrolyte multilayer capsules as vehicles with tunable permeability. Advances in colloid and interface science 111(2004):49-61.
- [65] Mansouri, S., Winnik, F.M. and Tabrizian, M. Modulating the release kinetics through the control of the permeability of the layer-by-layer assembly: a review. Expert opinion on drug delivery 6(2009):585-597.
- [66] Ye, S., Wang, C., Liu, X., Tong, Z., Ren, B. and Zeng, F. New loading process and release properties of insulin from polysaccharide microcapsules fabricated through layer-by-layer assembly. Journal of controlled release : official journal of the Controlled Release Society 112(2006):79-87.
- [67] Dubas, S.T. and S, J. Swelling and Smoothing of polyelectrolyte multilayers by salt. . Langmuir : the ACS journal of surfaces and colloids 17(2001):7725-7727.
- [68] Burke, S.E. and Barrett, C.J. Swelling behavior of hyaluronic acid/polyallylamine hydrochloride multilayer films. Biomacromolecules 6(2005):1419-1428.
- [69] Kozlovskaya, V.K.E, Mansfield, M.L. and Sukhishvili, S.A. Poly(methacrylic acid) hydrogel films and capsules: response to pH and ionic strength, and encapsulation of macromolecules. Chemistry of Materials 18(2006):328-336.
- [70] Lu, H. and Hu, N. Salt-induced swelling and electrochemical property change of hyaluronic acid/myoglobin multilayer films. The journal of physical chemistry B 111(2007):1984-1993.
- [71] Dubas, S.T. and S, J. Polyelectrolyte multilayers containing a weak polyacid: construction and deconstruction. Macromolecules 34(2001):3736-3740.
- [72] Burke, S.E. and B, C. pH-dependent loading and release behavior of small hydrophilic molecules in weak polyelectrolyte multilayer films. Macromolecules 37(2004):5375-5384.
- [73] Sukhorukov, G.B.F.A., Brumen, M. and Mohwald, H. Physical Chemistry of Encapsulation and Release. Physical chemistry chemical physics 6(2004):4078-4089.
- [74] Lee, D.N.A., Kunz, A.L., Rubner, M.F. and Cohen, R.E. pH-induced hysteretic gating of track-etched polycarbonate membranes: swelling/deswelling behavior of polyelectrolyte multilayers in confined geometry. Journal of the American chemical society 128(2006):8521-8529.

- [75] Wang, C., Ye, S., Dai, L., Liu, X. and Tong, Z. Enhanced resistance of polyelectrolyte multilayer microcapsules to pepsin erosion and release properties of encapsulated indomethacin. Biomacromolecules 8(2007):1739-1744.
- [76] Ren, K., Ji, J. and Shen, J. Construction and enzymatic degradation of multilayered poly-L-lysine/DNA films. Biomaterials 27(2006):1152-1159.
- [77] Wood, K.C., Boedicker, J.Q., Lynn, D.M. and Hammond, P.T. Tunable drug release from hydrolytically degradable layer-by-layer thin films. Langmuir : the ACS journal of surfaces and colloids 21(2005):1603-1609.
- [78] Wood, K.C.C.H., Batten, R.D., Lynn, D.M. and Hammond, P.T. Controlling interlayer diffusion to achieve sustained, multiagent delivery from layer-by-layer thin films. Proceedings of the National Academy of Sciences of the United States of America 103(2006):10207-10212.
- [79] Zhao, Q. and Li, B. pH-controlled drug loading and release from biodegradable microcapsules. Nanomedicine : nanotechnology, biology, and medicine 4(2008):302-310.
- [80] Ahamed, M., Karns, M., Goodson, M., Rowe, J., Hussain, S.M., Schlager, J.J. and et al. DNA damage response to different surface chemistry of silver nanoparticles in mammalian cells. Toxicology and applied pharmacology 233(2008):404-410.
- [81] Liu, W., Wu, Y., Wang, C., Li, H.C., Wang, T., Liao, C.Y. and et al. Impact of silver nanoparticles on human cells: effect of particle size. Nanotoxicology 4(2010):319-330.
- [82] Jorgensen, J.H. and Ferraro, M.J. Antimicrobial susceptibility testing: a review of general principles and contemporary practices. Clinical infectious diseases : an official publication of the Infectious Diseases Society of America 49(2009):1749-1755.
- [83] Boccaccini, A.R., Stamboulis, A.G., Rashid, A. and Roether, J.A. Composite surgical sutures with bioactive glass coating. Journal of biomedical materials research Part B, Applied biomaterials 67(2003):618-626.
- [84] Z, F. A New Conception of Bouguer-Lambert-Beer's Law. Anal Chem 297(1979):419.
- [85] Liu, J. and Hurt, R.H. Ion release kinetics and particle persistence in aqueous nano-silver colloids. Environmental science & technology 44(2010):2169-2175.

- [86] Keiji, T.A.T. and Tisato, K. Film Thickness Dependence of the Surface Structure of Immiscible Polystyrene/Poly(methyl methacrylate) Blends. Macromolecules 29(1996):3232-3239.
- [87] Christopher, M.H.N.S., Paul, W. and Martha, L.M. A comparison of atomic force microscopy (AFM) and dynamic light scattering (DLS) methods to characterize nanoparticle size distributions. Journal of nanoparticle research : an interdisciplinary forum for nanoscale science and technology 10(2008):89-96.
- [88] Martı́nez-Castan˜o'n NNo-Mn, G.A., Martı́nez-Gutierrez, F., Martı́nez-Mendoza, J.R., Facundo, R. Synthesis and antibacterial activity of silver nanoparticles with different sizes. Journal of nanoparticle research : an interdisciplinary forum for nanoscale science and technology 10(2008):1343-1348.
- [89] Sadowskiihm, Z., Grochowalska, B., Polowczyk, I. and Kozlec, T. Synthesis of silver nanoparticles using microorganisms. Materials Science-Poland 26(2008):419-424.
- [90] Etienne, Y., Lasfargues, W.G.C. and Ernest, S.R. Isolation of From Solid Two Human Tumor Epithelial Breast Carcinomas 1,2 Cell Lines. Journal of the National Cancer Institute. 61(1978):967-978.
- [91] Dubas, S.T., Wacharanad, S. and Potiyaraj, P. Tuning of the antimicrobial activity of surgical sutures coated with silver nanoparticles. Colloids and Surfaces A: Physicochem Eng Aspects 308(2011):25-28
- [92] Teng, H.F.M. and Limin, Q. Facile Synthesis and One-Dimensional Assembly of Cyclodextrin-Capped Gold Nanoparticles and Their Applications in Catalysis and Surface-Enhanced Raman Scattering. J Phys Chem 113(2009):13636-13642.
- [93] Bhumkar, D.R., Joshi, H.M., Sastry, M. and Pokharkar, V.B. Chitosan reduced gold nanoparticles as novel carriers for transmucosal delivery of insulin. Pharm Res 24(2007):1415-1426.
- [94] El Badawy, A.M., Luxton, T.P., Silva, R.G., Scheckel, K.G., Suidan, M.T. and Tolaymat, T.M. Impact of environmental conditions (pH, ionic strength, and electrolyte type) on the surface charge and aggregation of silver nanoparticles suspensions. Environmental science & technology 44(2010):1260-1266.

- [95] Dubas, S.T. and S, J. Factors controlling the growth of polyelectrolyte multilayers. Abstracts of Papers of the American Chemical Society 219(2000):U532-U.
- [96] Dubas, S.T., Wacharanad, S., Potiyaraj, P. Tuning of the antimicrobial activity of surgical sutures coated with silver nanoparticles. Colloid Surf A-Physicochem Eng Asp. 308(2011):25-28
- [97] Ramos, A.P., Doro, F.G., Tfouni, E., Goncalves, R.R. and Zaniquelli, M.E.D. Surface modification of metals by calcium carbonate thin films on a layer-by-layer polyelectrolyte matrix. Thin Solid Films 2008:516.
- [98] Zhang, T., Yan, H., Peng, M., Wang, L., Ding, H. and Fang, Z. Construction of flame retardant nanocoating on ramie fabric via layer-by-layer assembly of carbon nanotube and ammonium polyphosphate. Nanoscale 5(2013):3013-3021.
- [99] Dixit, V., Van den Bossche, J., Sherman, D.M., Thompson, D.H. and Andres, R.P. Synthesis and grafting of thioctic acid-PEG-folate conjugates onto Au nanoparticles for selective targeting of folate receptor-positive tumor cells. Bioconjugate Chem 17(2006):603-609.
- [100] Marano, F., Hussain, S., Rodrigues-Lima, F., Baeza-Squiban, A. and Boland, S. Nanoparticles: molecular targets and cell signalling. Archives of toxicology 85(2011):733-741.
- [101] Krpetic, Z., Porta, F., Caneva, E., Dal Santo, V. and Scari, G. Phagocytosis of biocompatible gold nanoparticles. Langmuir 26(2010):14799-14805.
- [102] Shahbazzadeh, D.A.H., Motalebi, A.A., Anvar, A.A., Moaddab, S., Asadi, T., Shokrgozar, M.A. and Rahman-Nya, J. In vitro effect of Nanosilver toxicity on fibroblast and mesenchymal stem cell lines. Iranian Journal of Fisheries Sciences 3(2011):487-496.
- [103] El Badawy, A.M., Silva, R.G., Morris, B., Scheckel, K.G., Suidan, M.T. and Tolaymat, T.M. Surface charge-dependent toxicity of silver nanoparticles. Environmental science & technology 45(2011):283-287.
- [104] Graham, S., Andrew, J.R., Ning, C., Luk, H.V., James, L.R. and Paul, B. Folate Receptor Alpha and Caveolae Are Not Required for Ebola Virus Glycoprotein-Mediated Viral Infection. Journal of Virology 77(2003):13433-13438.

- [105] David, T.W.W., Jennifer, A.H. and Debajit, K.B. Mechanism of Induction of Human Chorionic Gonadotropin in Lung Tumor Cells in Culture. The Journal of Biological Chemistry 259(1984):10738-10744.
- [106] Mritunjai, S., Shingini, S., S, P. and I, S.G. Nanotechnology in Medicine and Antibacterial effect of Silver nanoparticles. Digest Journal of Nanomaterials and Biostructures 3(2008):115 - 122.

APPENDIX

A. SCHOLARSHIPS

- 2012-2013 The 90 th Anniversary of Chulalongkorn university Fund
 (Ratchadaphiseksomphot Endowment Fund)
 Graduate School, Chulalongkorn University
- 2011 Conference Grant for Ph.D. Student
 Graduate School, Chulalongkorn University
- 2013 Conference Grant for Ph.D. Student
 Nanoscience and Technology program

B. LIST OF CONFERENCES (Oral Presentation)

1. **2013 3rd International Conference on Key Engineering Materials (ICKEM 2013)**

at Grand borneo hotel, Kota kinabalu, Malesia on 8-9 March 2013

Title “Tunable Silver Leaching From Polyelectrolyte Multilayers Thin Films”

C. LIST OF CONFERENCES (Poster presentation)

1. **ICMAT2011 International Conference on Materials for Advance Technologies**

at Suntec , Singapore on 26 June – 1 July 2011

Title “Tunning of the Antimicrobial Activity of Surgical Sutures Coated with Silver Nanoparticles”

D. LIST OF PUBLICATIONS

1. **Wacharanad S.**, Dubas S.T. Tunable Silver Leaching From Polyelectrolyte Multilayers Thin Films. Advance Material Research. 2013;701 **Accepted**
2. Dubas S.T., **Wacharanad S.**, Potiyaraj P. Tuning of the antimicrobial activity of surgical sutures coated with silver nanoparticles. Colloids and Surfaces A: Physicochemical and Engineering Aspects. 2011; 380: 25-28

Study the surface charge of silver nanoparticles

After preparation, silver nanoparticles capped with FA, PSSMA and AL were analyzed their surface charge by zeta potential. As expected, SNP-PSSMA and SNP-AL had high surface charge when increased concentration of capping agent due to the carboxylic group which showed the negatively charge was increased follow by concentration of capping agent[100]. The data which illustrated the surface charge of all condition of SNP was showed in this table

Table: The zeta potential of silver nanoparticles capped with FA, PSSMA and AL

Conditions	Zeta potential (mV)
SNP-FA 1:0.1	-39.1
SNP-FA 1:0.5	-32.53
SNP-FA 1:1	-30.9
SNP-FA 1:5	-16.97

It was oppositely in SNP-FA, in high capping agent contained very low negative charge (-17 mV) and high negatively charge in lower capping which around -39.1 mV in 0.1 mM of FA. Although this result had not been clearly explained, it could hypothesize that it was increased cation of electrolyte in the system. Due to folic acid were dissolved in phosphate buffer first and adjusted pH to pH 9 with NaOH. This buffer would increase cation such as Na^+ in the solution and had a significant decreased on the zeta potential of SNP-FA. The complexation between cation (Na^+ ion) and carboxyl groups on the surface of SNP-FA was potentially increased charge screening. This effect is the main reason for the reduction of charge surface and agglomeration.[101, 102].

VITAE**PERSONAL DATA**

Name : Sirorat Wacharanad
Nationality : Thai
Date of Birth : August 21, 1980
E-mail : Sirorat.W@student.chula.ac.th

EDUCATION

1999-2006 **Doctor of dental surgery**

Faculty of Dentistry, Naresuan University, Phitsanulok, Thailand

2008-2013 **Doctor of Philosophy**

Doctor of Philosophy Program in Nanoscience and Technology,
Graduate School, Chulalongkorn University, Bangkok, Thailand

Major: Nanoscience and Technology

Thesis title: Targeted and Controlled Release of Ag⁺ from Silver Nanoparticles by Polyelectrolyte Multilayers and Folic acid Surface Modification for Cancer Therapy

PUBLICATIONS IN THIS DISSERTATION

1. **Wacharanad S.,** Dubas S.T. Tunable Silver Leaching From Polyelectrolyte Multilayers Thin Films. Advance Material Research. 2013;701
2. Dubas S.T., **Wacharanad S.,** Potiyaraj P. Tuning of the antimicrobial activity of surgical sutures coated with silver nanoparticles. Colloids and Surfaces A: Physicochemical and Engineering Aspects. 2011; 380: 25-28